AD-A119 700 CHARLES STARK DRAPER LAB INC CAMBRIDGE MA F/G 17/7
LOW ALTITUDE NAVIGATION AUGMENTATION SYSTEM.(U)
DEC 81 D A KOSO F33615-80-C-1209
UNCLASSIFIED CSDL-R-1526 AFWAL-TR-81-1222 NL

1 2

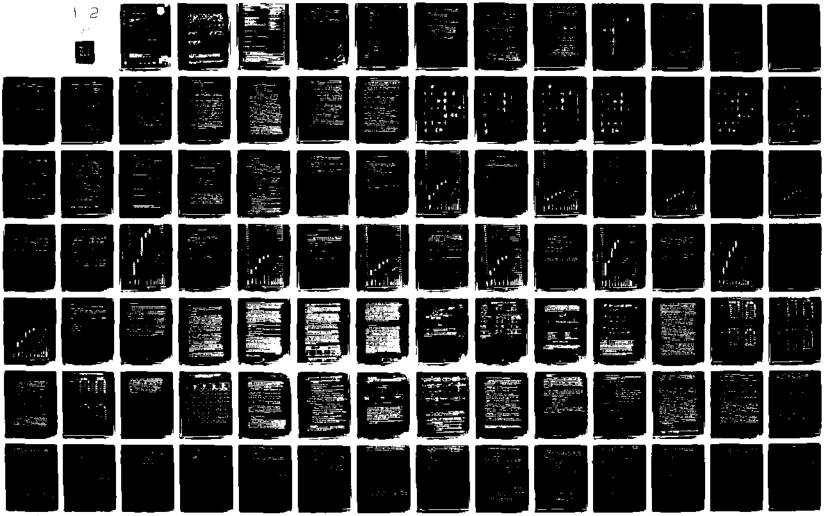

AD A119700

AFWAL-TR-81-1222

LOW ALTITUDE NAVIGATION AUGMENTATION SYSTEM

THE CHARLES STARK DRAPER LABORATORY, INC.
555 TECHNOLOGY SQUARE
CAMBRIDGE, MA 02139

DECEMBER 1981

FINAL REPORT FOR PERIOD: SEPTEMBER 1980 - AUGUST 1981

Approved for public release; distribution unlimited.

AVIONICS LABORATORY
AIR FORCE WRIGHT AERONAUTICAL LABORATORIES
AIR FORCE SYSTEMS COMMAND
WRIGHT-PATTERSON AIR FORCE BASE, OHIO 45433

NOTICE

When Government drawings, specifications, or other data are used for any purpose other than in connection with a definitely related Government procurement operation, the United States Government thereby incurs no responsibility nor any obligation whatsoever; and the fact that the government may have formulated, furnished, or in any way supplied the said drawings, specifications, or other data, is not to be regarded by implication or otherwise as in any manner licensing the holder or any other person or corporation, or conveying any rights or permission to manufacture use, or sell any patented invention that may in any way be related thereto.

This report has been reviewed by the Office of Public Affairs (ASD/PA) and is releasable to National Technical Information Service (NTIS). At NTIS, it will be available to the general public, including foreign nations.

This technical report has been reviewed and is approved for publication.

James E. Barnes

JAMES E. BARNES
Project Engineer

Ronald L. Ringo

RONALD L. RINGO
Chief, Reference Systems Branch
System Avionics Division

FOR THE COMMANDER

Frank A. Scarpino

FRANK A. SCARPINO, Acting Chief
System Avionics Division
Avionics Laboratory

"If your address has changed, if you wish to be removed from our mailing list, or if the addressee is no longer employed by your organization please notify AFWAL/AAAN-3, WPAFB OH 45433 to help us maintain a current mailing list."

Copies of this report should not be returned unless return is required by security considerations, contractual obligations, or notice on a specific document.

1. [illegible]-81-1222

2. AD-A119 700

4. LOW ALTITUDE NAVIGATION
[illegible] SYSTEM

5. [illegible]
[illegible]/81

6. [illegible]

7. [illegible]

D. Alexander Koso

8. F33615-80-C-1209

9. The Charles Stark Draper Laboratory, Inc.
555 Technology Sq.
Cambridge, MA 02139

10. 6095 15 25

11. Avionics Laboratory
Air Force Wright Aeronautical Laboratories
Wright-Patterson Air Force Base, Ohio 45433

12. [illegible] 1981

13. 115

14. [illegible]

15. UNCLASSIFIED

15a. [illegible]

16. [illegible]

Approved for public release; distribution unlimited.

17. [illegible]

18. [illegible]

19. [illegible]

navigation, electronic map, displays, simulation

20. [illegible]

The C.S. Draper Laboratory has been developing technology needed for naviga-tion and piloting of aircraft operating at low altitude.

Under Air Force Contract No. [illegible] a plan for the [illegible] Low Altitude Navigation [illegible] System was [illegible].

This simulation will be used for an evaluation of the [illegible] experienced in low altitude aircraft operations.

DD [illegible] 1473 [illegible]

Acknowledgement

The work reported was performed under contract no. F33615-[illegible] by the Charles Stark Draper Laboratory, 555 Technology Sq., Cambridge, MA 02139.

The contract monitors were Mr. W. Shephard and Mr. J. Barnes AFWAL/AAAN. Their support and guidance is greatly appreciated.

The concept for the Low Altitude Navigation Augmentation system was developed by Mr. S. Joel Premselaar. Mr. Roy Nurse, Mr. John Fuchaska, Dr. Howard Musoff, and Mr. Dale Landis contributed the technical data.

Table of Contents

1.0 Introduction

The ever-increasing defense threat encountered by [illegible] aircraft has made low-altitude operations in various [illegible] scenarios necessary.

The Low Altitude Navigation Augmentation Concept provides the pilot with an electronic map display on the aircraft's HUD, so that head down operations (looking at maps or moving map displays) are not required.

In addition to the display concept, bearing measurements to known landmarks can be utilized to update the navigation system and also to estimate errors between the navigation system coordinate frame and the map coordinate frame.

The concept for the LANA was developed by CSDL under IRAD funding to determine the lowest performance INS usable in the LANA configuration. The simulation configuration described in this plan, however, utilizes higher performance equipment; since the higher performance equipment will be procured for the F-16 and A-10 aircraft.

In this report, a plan is developed to simulate the LANA concept on an Air Force simulator. The simulation will be used to verify both system performance and pilot work load under realistic flight conditions.

2.0 The [illegible] Concept

2.1 [illegible]

The [illegible] utilizes [illegible] [illegible] [illegible]

[illegible]

since the system is [illegible] [illegible] [illegible]

altitude, map data is presented in perspective [illegible] the aircraft's

HUD.

2.2 Comparison to Existing Systems

In a conventional navigation system with a map display as

used for example in the A-7 aircraft, the navigation (whether

inertial or doppler & [illegible]) [illegible] the map display. [illegible]

[illegible] compares his location as seen [illegible] [illegible]

the map display based on the [illegible] [illegible].

This approach has two major [illegible] in this type of

implementation:

Heads down viewing of the display is [illegible].

The area seen from the cockpit is [illegible] large so that

a map comparison can be made.

2.3 Operational Description

In a single seat aircraft, operating at 100 to [illegible] altitude,

heads down operation is not possible and generally the objects

seen through the cockpit are objects of [illegible] [illegible] and

not the maplike planar view seen from higher altitudes (and dis-

played on conventional maps).

To overcome these difficulties, the [illegible] [illegible] [illegible]

electronic map (utilizing the [illegible] digital [illegible] [illegible] [illegible]

an essential [illegible] of the map in a [illegible] [illegible] [illegible]

aircraft HUD. Then if there are no navigation [illegible] [illegible]

within the navigation and [illegible] [illegible] [illegible] [illegible]

and the real world [illegible] [illegible] [illegible] [illegible] [illegible]

Differences between the display and the real world provide the pilot with an indication of navigation data quality.

To reduce the need for manual map updating, the pilot uses a helmet mounted sight to measure bearings to landmarks (or way points). These bearing measurements are utilized to update the aircraft navigator and thus to reduce the discrepancy between the map display and the real world.

2.4 Hardware Description

The system consists of six major components:

A Navigator.

The baseline is the F-16 SKN 2416 navigator. Other inertial systems or Radio Navigators or Doppler systems can also be utilized. (A model for an MLS navigator is also available.)

The DMAC elevation and cultural features data base of the aircraft operating area.

The Display Generator, which selects the relevant data from the data base, transforms this data HUD coordinates and selects the relevant features for HUD presentation.

The HUD where the pilot compares the three-dimensional map presentation and the real world.

The Helmet Sight used to measure bearings to selected landmarks to update the aircraft navigation information.

The Data Processor used to mix navigator, data base and helmet sight information to provide a best estimate of position and heading for the display generator.

A block diagram of this concept is shown in Figure 2.1. For purposes of simulation, this model has been broken down into further parts. These are discussed in Section [illegible].

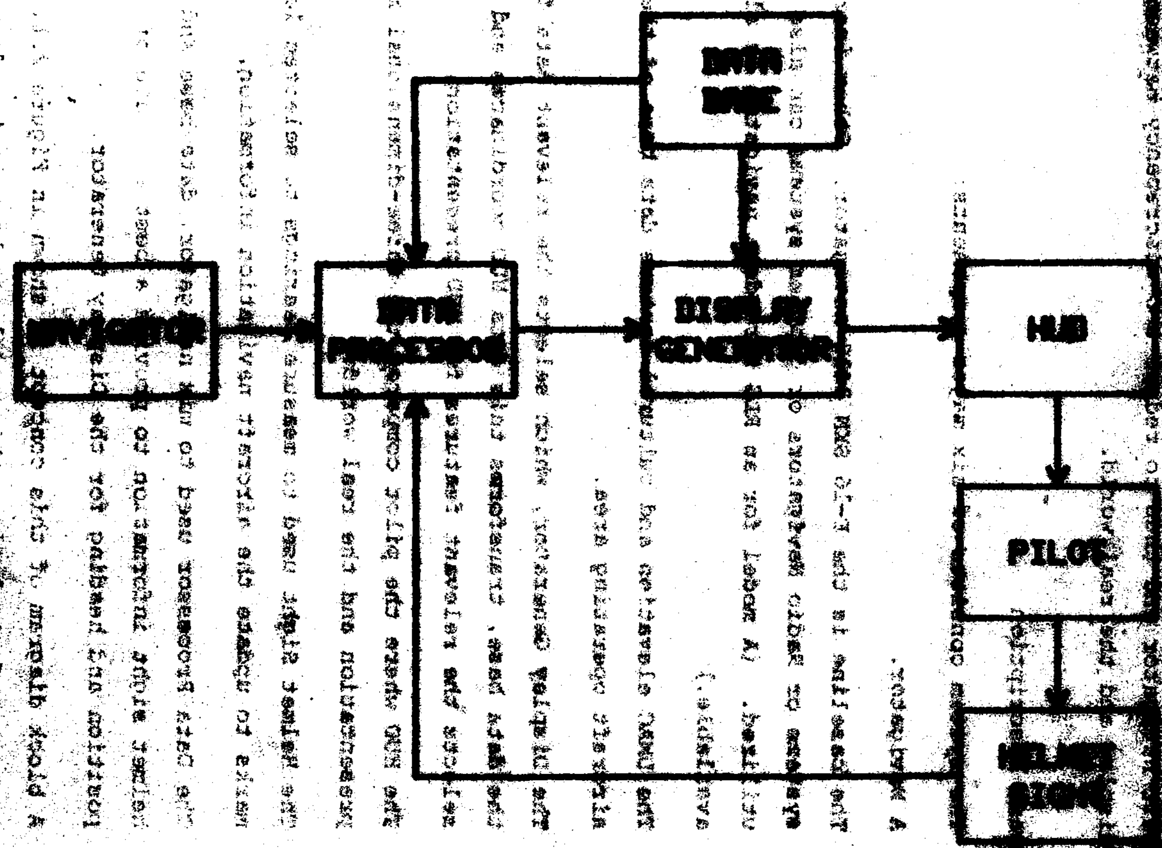

Figure 2.1. LAMA Concept

3.0 Error Models

3.1 Inertial Navigator

The original premise of [illegible] was to use the lowest performance navigator possible. However, since tactical aircraft will utilise higher quality navigators, performance characteristics of the SKN 2416 or of a strapdown system based on the Bell XI accelerometer and Honeywell GG 1328 should be utilised in the baseline simulation.

3.2 Map Errors

The making of maps (including the development of the digital data) is a very manpower intensive process. Error models could be generated based on various areas of the world and based on the time when these surveys were completed.

However, in discussion with DMAC the following model was devised:

1) Bias between the coordinate system used by the INS and the map segment.

2) Random errors in the location of individual points on the map segment. These errors are correlated; relative errors depend on the distance between points.

3) There is no correlation of errors between map segments. Not all segment boundaries are known.

4) Maps contain point errors; especially in the cultural data base. New features may not exist in the data base; features are located in wrong positions; some features have been physically removed from the world but not from the data base.

These error sources will have to be introduced into the DMA like data base of the simulation system.

3.6 Summary

The display on the HUD is inaccurate due to

1) Differences between the map and inertial coordinate frame and errors in the map

2) Errors in the position and heading output of the inertial navigator and errors in the aircraft altitude readout

The update system is inaccurate due to

1) Errors between the inertial and HUD coordinate frame

2) Errors in the pointing system

3.7 Recommended Error Model Values for the LANA Components

GYRO ERROR MODEL TERMS
FOR TACTICAL AIRCRAFT GIMBALLED IMU

Error Designation	Error Type	Numerical Value (1σ)
Bias Drift Uncertainty	Random Constant	0.004°/h
Bias Drift Randomness	1st-Order Markov	0.0067°/h T = 20 min
g-Sensitive IA Drift	Random Constant	0.005°/h/g
g^2-Sensitive Drift (Specific Forces along IA and SA)	Random Constant	$0.005^\circ/h/g^2$

Note: Gyro type: gyroflex

ACCELEROMETER ERROR MODEL TERMS

FOR TACTICAL AIRCRAFT [illegible] IMU

Error Designation	Error Type	Numerical Value (1σ)
Bias Drift Uncertainty	Random Constant	50μg
Bias Randomness	Random Walk	Negligibly Small (Numerical Value Not Available)
Scale-Factor Uncertainty	Random Constant	500ppm
Scale-Factor Asymmetry	Random Constant	50ppm
Scale-Factor Nonlinearity	Random Constant	Negligibly Small ($5\mu g/g^2$)
IA Nonorthogonality	Random Constant	0.2mrad

Note: Accelerometer type: Pendulous

GYRO ERROR MODEL TERMS FOR STRAPDOWN IMU

Error Designation	Error Type	Numerical Value (1σ)
Bias Drift Uncertainty	Random Constant	$0.02°/h$
Bias Drift Randomness	Random Walk in Drift Angle	$0.01°/\sqrt{h}$
Scale-Factor Uncertainty	Random Constant	1ppm
Scale-Factor Asymmetry	Random Constant	1ppm
Scale-Factor Nonlinearity	Random Constant	5×10^{-3} ppm/°/s
IA Nonorthogonality/ Alignment Stability	Random Constant	1sec
Quantization	—	3.15sec/pulse

Notes: (1) Gyro type: Ring Laser, Honeywell GG1328

ACCELEROMETER ERROR MODEL TERMS FOR [illegible]

Error Designation	Error Type	Numerical Value (1σ)
Bias Uncertainty	Random Constant	30μg
Bias Randomness	Random Walk	Negligibly Small (Numerical Value Not Available)
Scale-Factor Uncertainty	Random Constant	50ppm
Scale-Factor Nonlinearity	Random Constant	$1\mu g/g^2$
IA Nonorthogonality	Random Constant	0.05mrad

Map Error Model

Location Error	100 meter rms
	5000 meter correlation distance
	Zero correlation in transition between map segments

Helmet Sight Error Model

Bias Error	.25 degree rms
	30 minute correlation time
Random	.1 degree rms
	random constant

Attitude System Error Model

Bias Error	.25 degree rms
	30 minute correlation time

Gravity Error Model

Deflection	10 arc sec
	50 KM correlation distance

4.0 Facility Requirements

4.1 Introduction:

At all facilities, the visual simulation consists of three parts.

1) A display of the "real world" as seen from the cockpit of the aircraft
2) A display of the HUD presentation of the real world
3) The HMS reticle projected on the "real world."

4.2 Projection System Considerations

Since it is extremely difficult to match the distortions of the three optical systems, it is recommended that the HUD display and HMS reticle (cross hair) be mixed electronically in the projection system video, so that distortions introduced in the projection system affect all displays equally.

4.3 Accuracy Requirements

The modeling in the simulation is based on the following principle in both the display (HUD) simulation and in the measurement (HMS) system simulation:

Errors in the computed parameters are added to the "true" values to move the HUD display relative to the "real world" and measurement errors are added to the HMS reticle location (as defined in the video) to develop the bearing angle errors.

Thus errors in the simulation hardware have to be smaller than errors expected in the LAMA implementation.

4.4 **Display Chain Errors**

These errors will introduce misregistration between the HUD and real world display.

The major contributors are:

Aircraft Location

Aircraft Heading

Aircraft Attitude (Roll, Pitch, Yaw)

The simulation hardware contribution to these errors should be small compared to the expected accuracy of the [illegible] navigation performance.

Two sets of numbers need to be considered: relatively long flights between two points, such that any errors between the points are uncorrelated, and relative navigation in a local area. For long flights expected system position uncertainty is approximately 100 meters. For 5KM visibility to landmarks, angular errors are 20 millirad. Thus for long distance navigation:

Location of the aircraft in the "real world" model needs to be known to approximately 20 meters.

Heading of the aircraft in the "real world" and attitude of the aircraft in the "real world" need to be known to approximately 4 millirad or .25 degrees.

If the location is degraded to approximately 100 meters or if the angular errors degrade to 1 degree, simulation errors will control the performance of the [illegible] system.

Local navigation (for offset aimpoint bombing for example) has not been considered in the simulation modeling up to this point. Correlation of errors within the navigation system will have to be modeled with considerably greater accuracy if large improvements in relative navigation accuracy are to be achieved.

5.0 Simulator Facility Site Survey

The simulation facilities included in the survey were:

Williams Air Force Base

AFWAL Facilities in Bldg. 620

Flight Control Development Laboratory Facilities

C.S. Draper Laboratory Facilities

The Williams AFB simulators are not typical operational training simulators. They are in fact, moving base research simulators that are presently configured with an F-15 and an F-16 cockpit. A 150° vertical and 300° azimuthal outside (computer generated) scene is provided for each cockpit.

The Williams AFB simulators employ obsolescent G.E. computers with Singer-Link software to generate an outside scene, and SEL 32-75 computers for platform operations. A 2 x 2 mile target area is the only scene utilizing the digital DMA landmass systems (DLMS) data base. This data base will have to be considerably expanded to accommodate the LANA requirements. However, with the additional data base the Williams AFB facilities remain a viable option for simulating a total Low Altitude Navigation Augmentation (LANA) System. Scheduling for work and demonstrations does not appear to be an issue; in fact, the personnel were receptive to conducting experimental operations at Williams AFB facilities. The Williams AFB facilities will undergo a modernization and expansion program which, when completed in 2 1/2 years hence, may enable them to accommodate the full scale simulation of the LANA System.

A meeting with AFWAL/FI personnel and a tour through their simulation facilities in Building 620, WPAFB, indicated that at least three options to conduct [illegible] demonstrations are available. These options include a [illegible] tied to the F-111 [illegible] cockpit, the F-15 cockpit, or the F-16 [illegible] (which is scheduled to be configured into a quasi-cockpit in the

[illegible] Another option is the F-15 cockpit [illegible] figured for a real-world display and a third option [illegible] the F-16 in a similar fashion.

The negative aspect of the terrain belt is that a data base does not exist for it and, although [illegible] has been charged with the task of providing such a data base, the timeline is uncertain. In addition, both the F-15 and the F-16 are, at this time, limited in the size of the outside scene that can be [illegible] modeled.

The C.S. Draper facility can also be used for the LAMA simulation. A considerable software effort will be required to produce a useable LAMA simulator at this facility. After this investment it will do no more than the F-15 simulator in Building 620 except that simulator time scheduling at the Draper facility will offer no problem.

The Flight Control Development Laboratory has a 13.5 x 37.5 mile terrain board with a TV probe and several cockpit configurations. The topographical (DMA type) data base is now available. A cultural (DMA type) data base will be developed for the board starting in CY1981. The board can be "overflown" several times in both directions to provide the required flight times.

An extensive hybrid computing facility is available at the laboratory. Upgrading of the computational facility is now in process. Accuracy of the TV probe system is close enough to the LAMA requirement to make use of this facility feasible.

The laboratory staff has shown considerable interest in the LAMA concept and is interested in supporting the simulation program.

Based on the survey, the Flight Control Development Laboratory has been used as the baseline for the detailed simulation development plan.

6.0 Simulation Development Plan

A block diagram of the full [illegible] simulation is shown in Figure 6.1. The TV camera (probe) position will be utilized as the "real world" position within the system. The probe attitude will be utilized as the true aircraft heading and true aircraft attitude.

Based on the aircraft attitude and force inputs to the INS, errors will be generated and added to the camera position as the INS introduced navigation errors.

Similarly attitude errors will be added to the camera attitude to generate the HUD LOS errors.

However, due to the complexity of the simulation, it is recommended that the simulation be developed in steps. Using this approach, the majority of the coding can be done off line. Thus, debugging of the code and running time of the various modules can be calculated while the simulator is used for the support of other programs. Figure 6.2 represents the first step in the simulation.

First a representative flight path will be flown across the terrain board and recorded for further use. This flight path will be utilized as the baseline for simulation development.

A HUD presentation of the flight path can now be developed off line utilizing software developed at CSDL or modifications of software developed under the Air Force's electronic map program.

Differences between the HUD and visual display should only be due to errors within the data base. These errors can then be removed or additional errors can be added to make the data base "more realistic."

The next recommended configuration is shown in Figure 6.3. This configuration will be used to gather pointing error statistics from the simulated Helmet Mounted Sight. The data will be utilized in the HMS error model used in the complete simulation.

Figure 6.4 shows addition of the INU, altitude, and data base error models. The errors should be noticeable as displacements between the visual display and the HUD. It is recommended that these errors be added sequentially and that each model be evaluated separately.

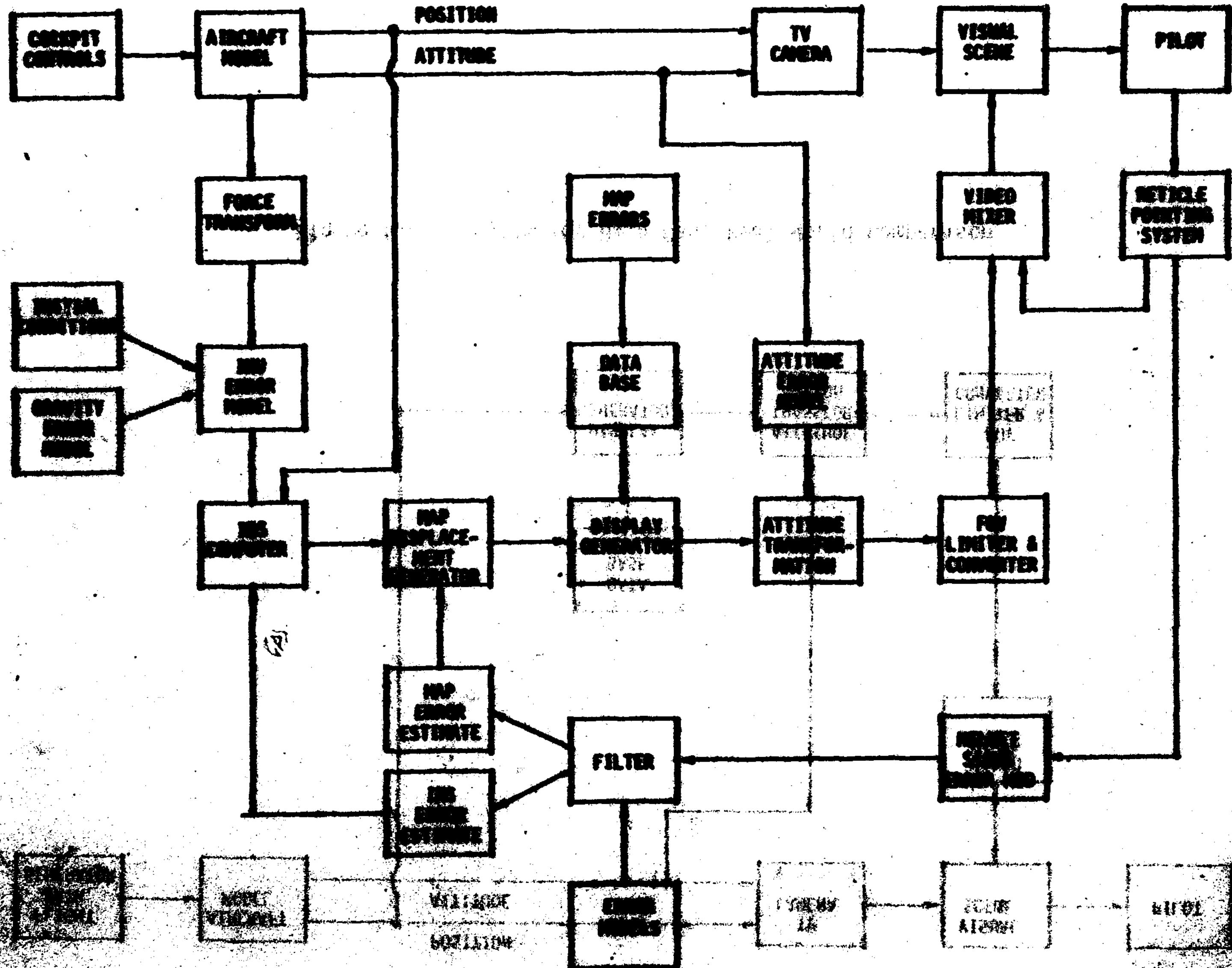

Figure 6.1. Block Diagram of Complete Simulation

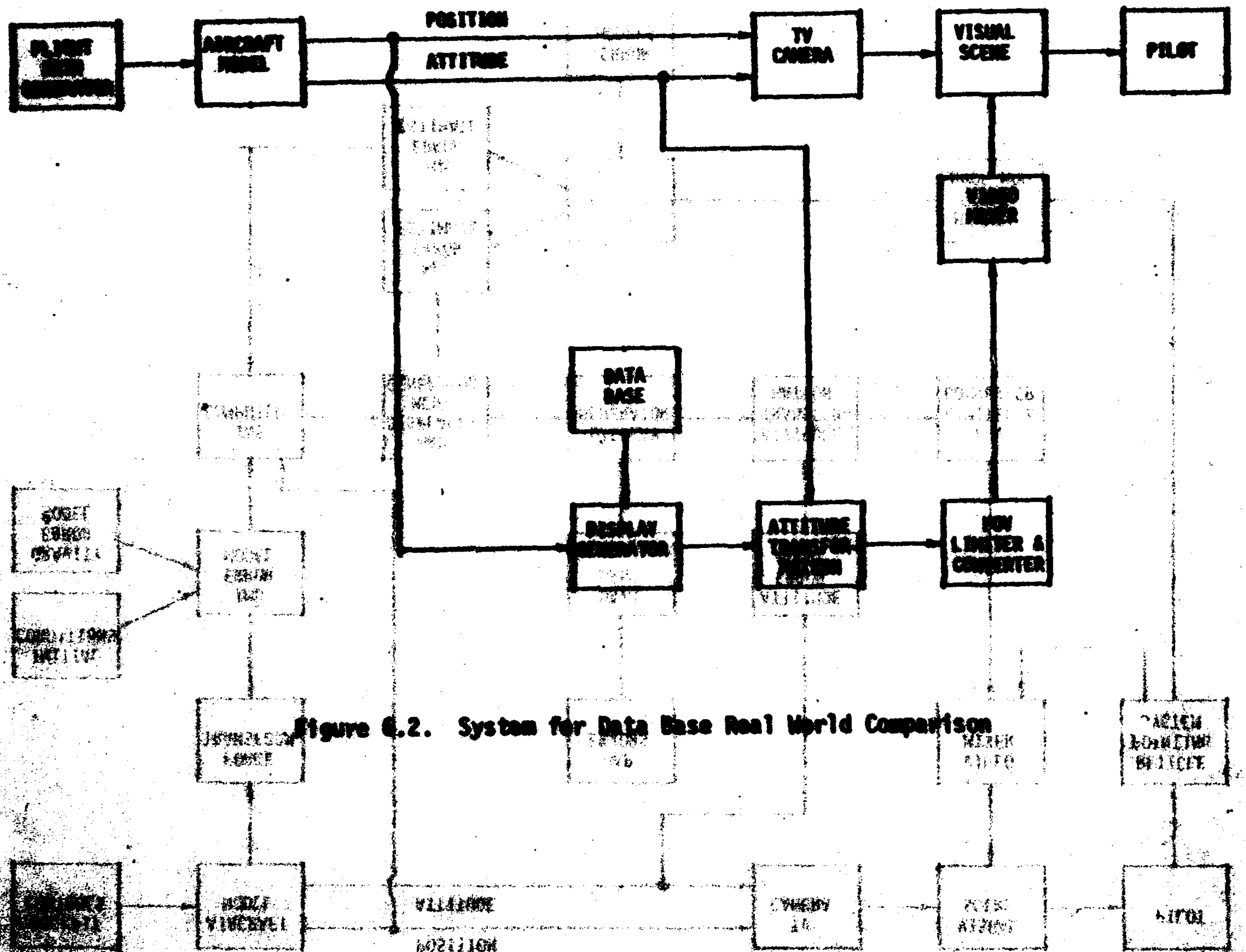

Figure 6.2. System for Data Base Real World Comparison

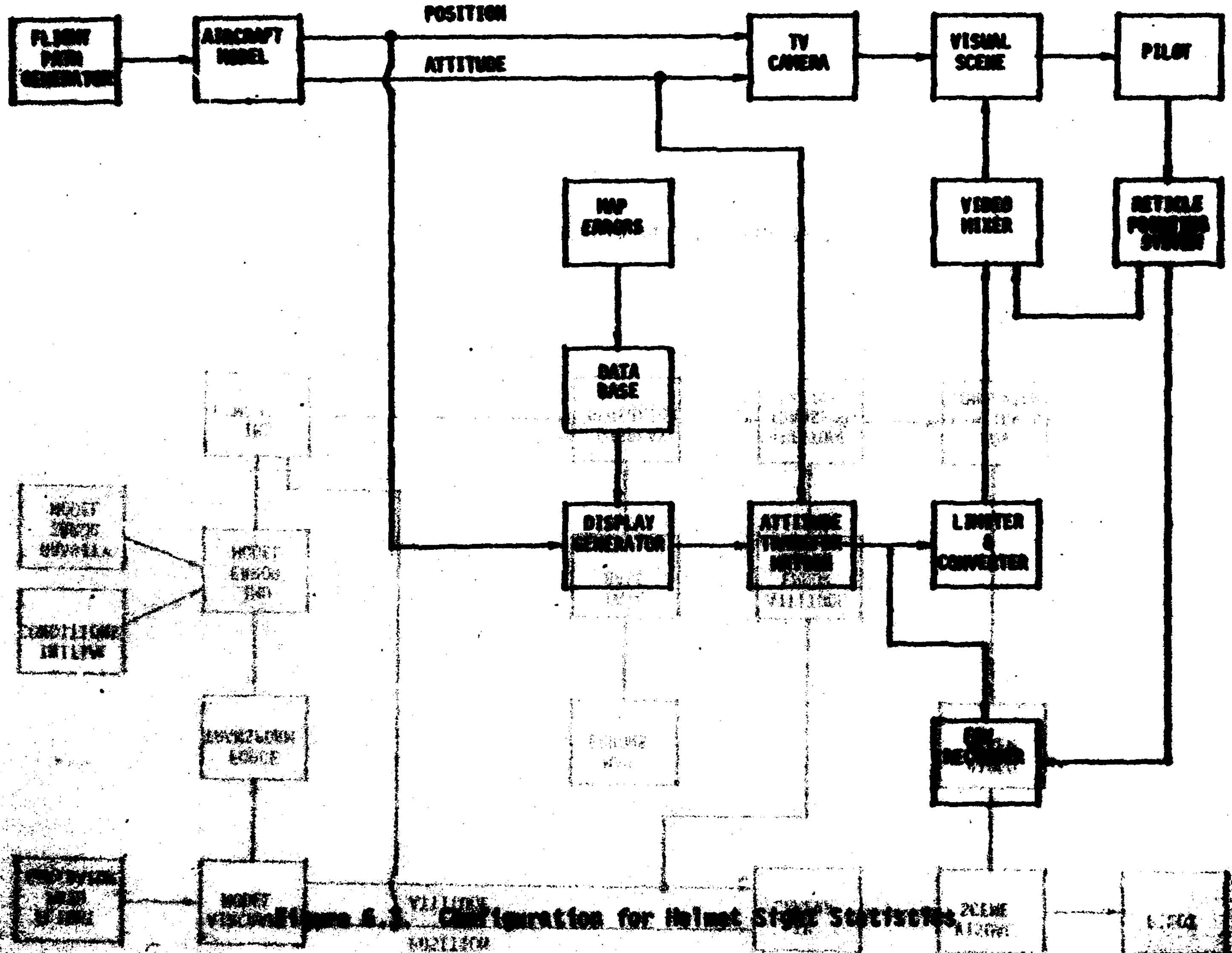

Figure [illegible]. Configuration for Helmet Sight Statistics

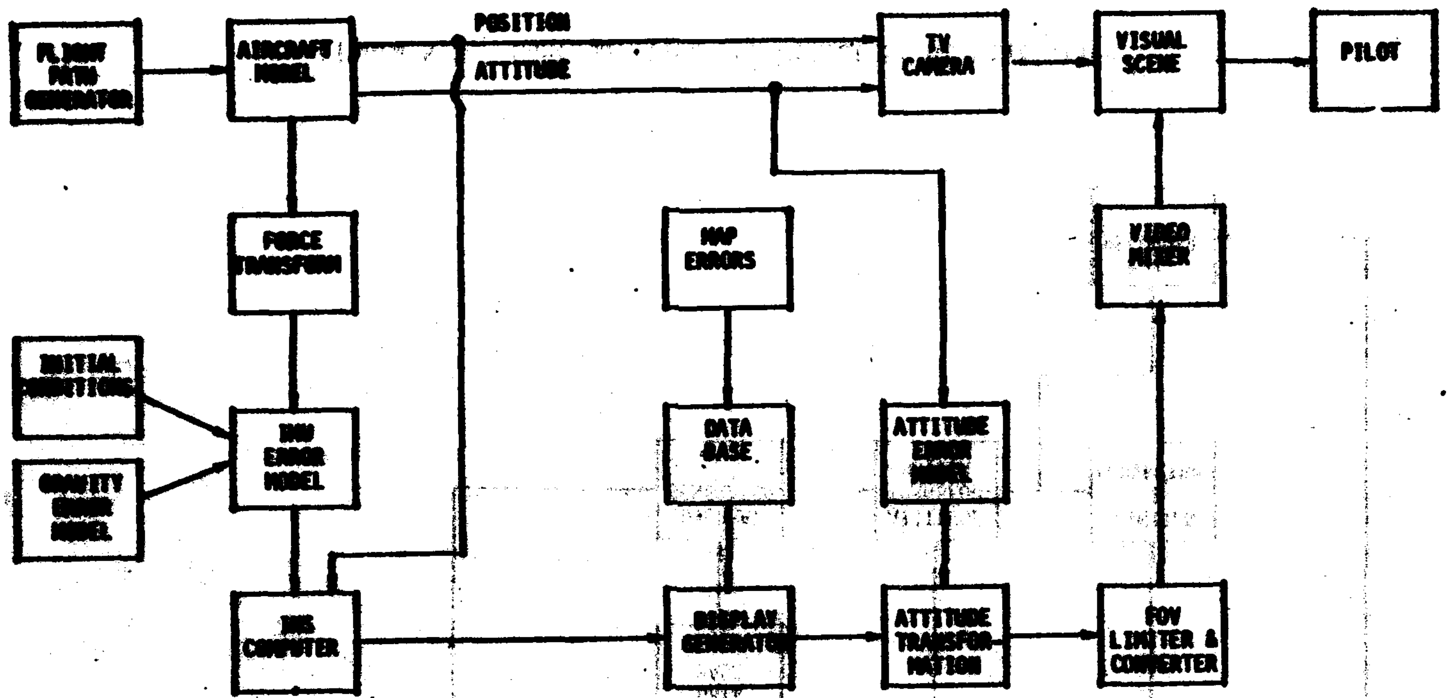

Figure 6.4. Addition of Error Models

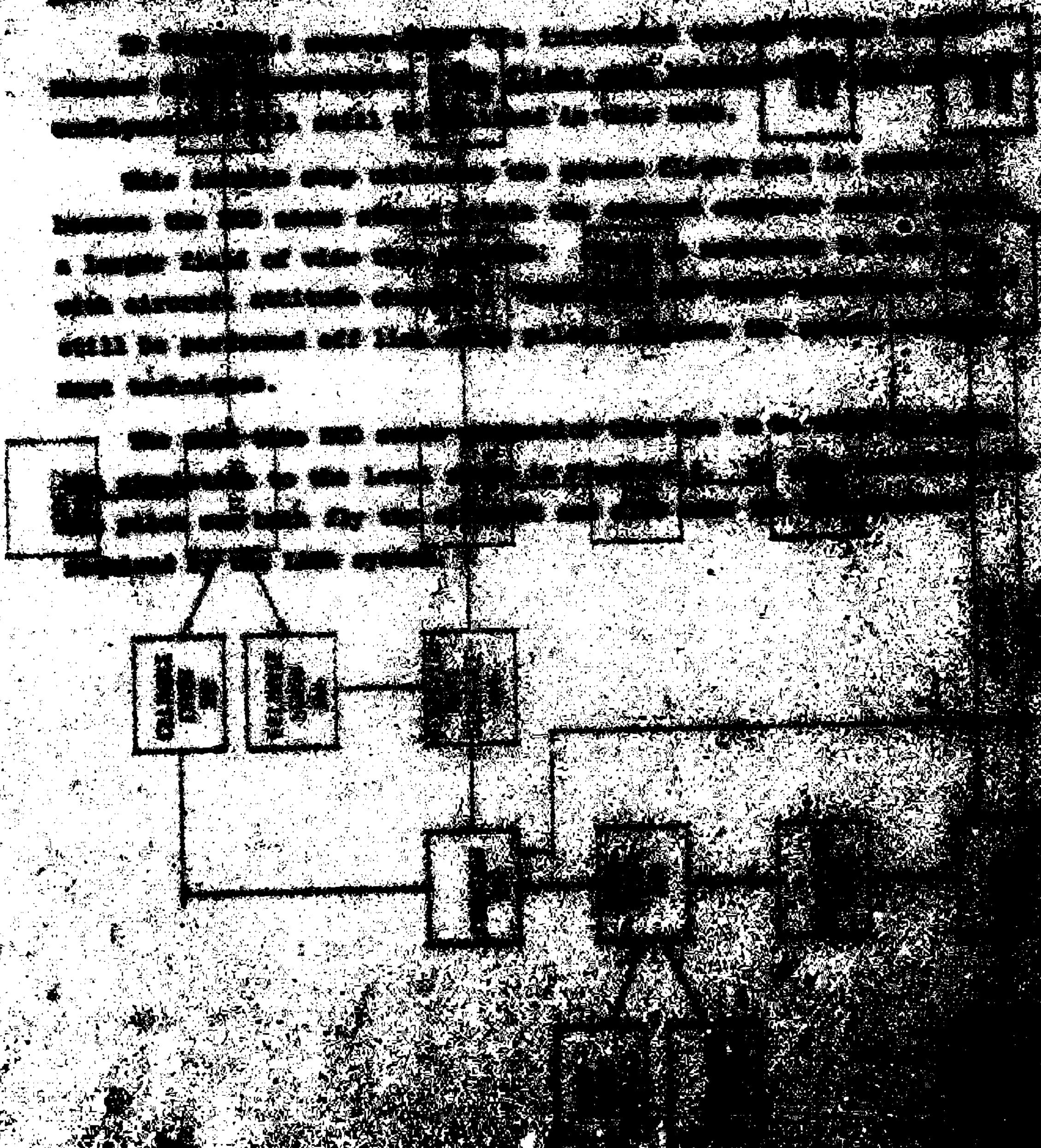

Figure 6.4. Navigation Filter Operation Assessment

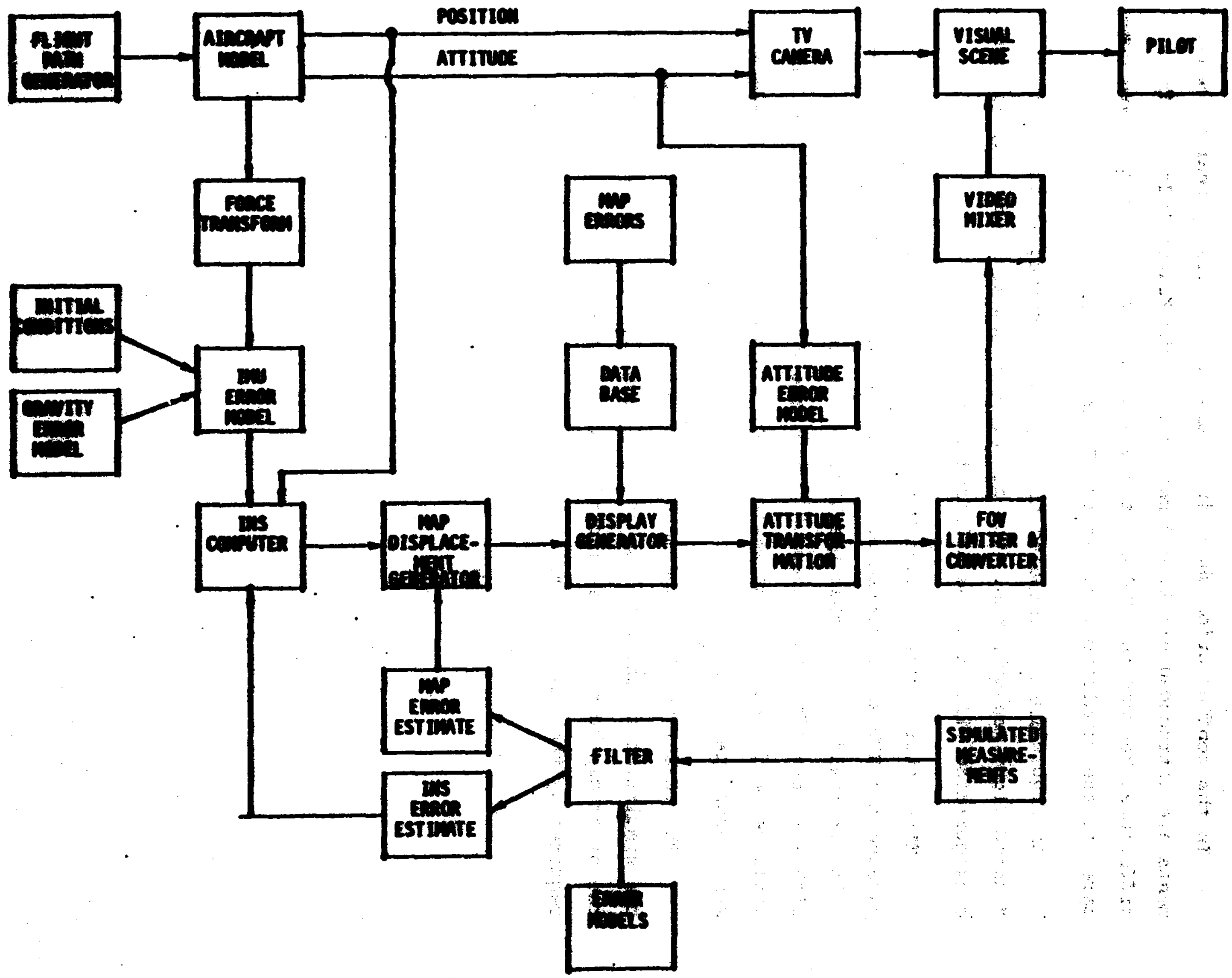

Figure 6.5. Navigation Filter Operation Assessment

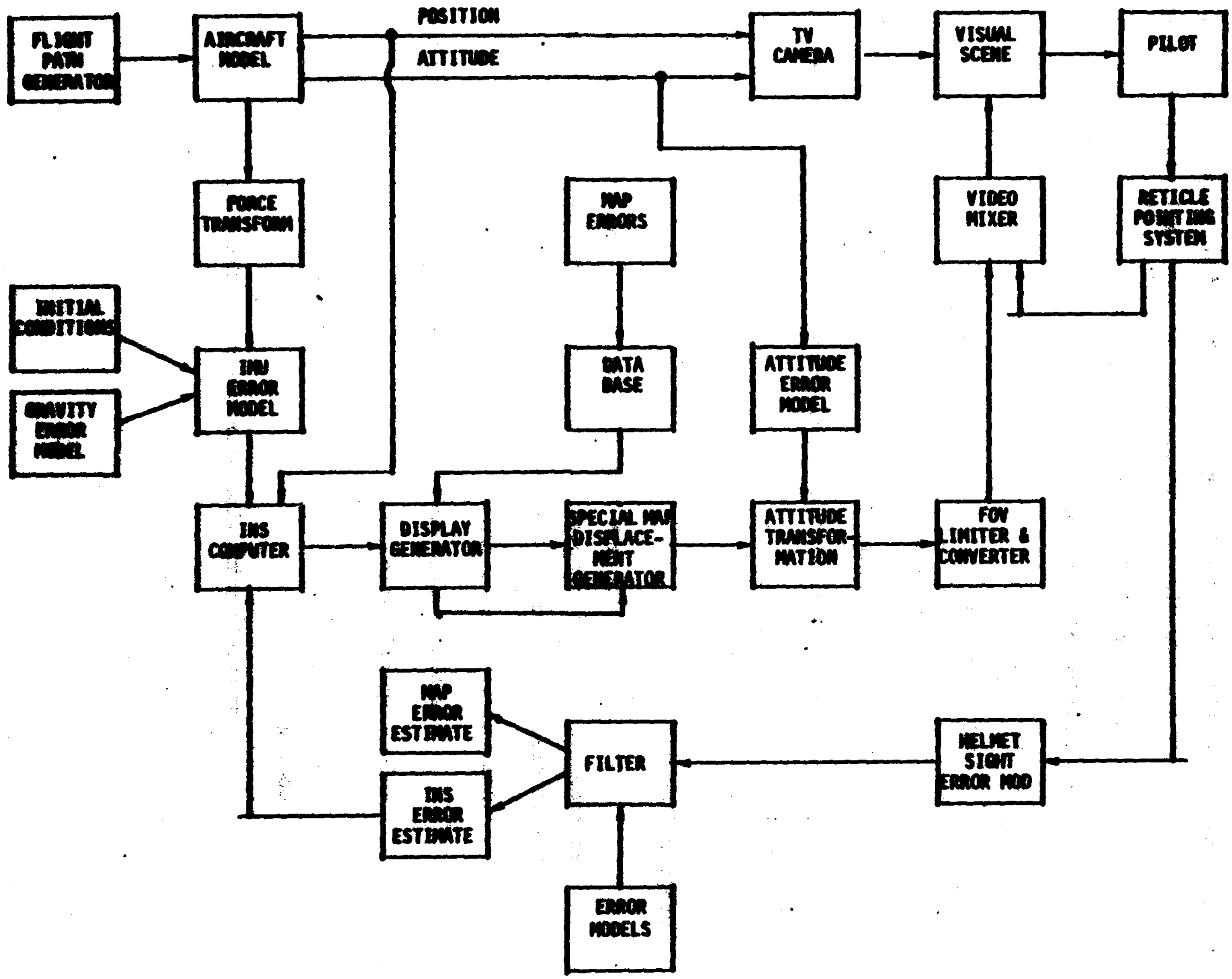

Figure 6.6. Addition of Actual Measurements

Summary

Step 1 Development and recording of a representative flight path

Step 2 Development of HUD display for the flight path, simulation of the HUD display superimposed on the "REAL world" display

Step 3 Collection of HMS pointing statistics

Step 4 Addition of error models

- 4a) IMU
- 4b) Attitude
- 4c) Map data base

Step 5 Addition of Kalman Filter with simulated measurements

Step 6 Replacement of simulated measurements with real measurements

Step 7 Full simulation

Program Elements

A modular approach has been recommended as the primary technical approach to the LANA simulation development. For each of the modules six general tasks can be defined:

Analytical Formulation

equations, error models, memory requirements, running time

Module Specification

input output format, running time, memory requirements

Coding

compatible with simulator computing facility

7.0 Software Development Requirements

7.1 Functional Specification

7.1.1 Introduction

The software described in this specification will utilise computing facilities available in a USAF flight simulator.

Within this simulator, an operator can use standard aircraft controls (stick and throttle) to "fly" a TV probe over a terrain board or alternately a prerecorded path can be repeatedly "flown" over the same board. A picture of the board, seen through the TV probe is presented to the pilot on a TV projection system.

The LAMA simulation will utilize the DMA digital data base of the board and superimpose on the TV display an abstract (ridges and essential cultural features) of the data base information simulating the display presented on the aircraft's HUD.*

The HUD display will be displaced relative to the TV probe display due to errors in the simulated aircraft navigation and attitude determination system.

A reticle will also be superimposed on the TV probe scene. The location of this reticle will be determined through a Helmet Mounted Sight measurement system in the simulator cockpit and on the helmet worn by the pilot/operator.

Bearing measurements made by the pilot/operator utilizing this simulated HMS will be used to update the simulated navigation system.

Before each flight it will be possible to select error models for the various system components. At the end of the flight hard copy records of system performance will be provided.

---

*Equipment to perform this function is now in development and will be delivered to the AFWAL early in 1983.

7.1.2 Interfaces

Inputs during simulation run:

True position, velocity, attitude, attitude rate are obtained from the aircraft type simulation available in the simulation facility.

Helmet Mounted Sight reticle bearing is obtained from the HMS readout system in the simulation cockpit.

A "bearing mark" input is provided as a switch closure on the stick of the simulator cockpit.

An abort command is available in the cockpit.

Simulated HUD display is available from the display generator.

<u>Inputs before simulation run:</u>

Values for error coefficients for the LAMA components, or alternately a code selecting a specific component error model.

The DMAC data base modified with TBD map errors.

Operator/Pilot identification.

Flight path type identification.

Narrative TBD used in output heading.

<u>Inputs after simulation run:</u>

Compute and print hard copy.

Reset and store data or reinitialize and change parameters.

<u>Outputs during simulation run:</u>

Simulated HUD display to video mixer.

Simulated reticle to video mixer.

Estimated position and heading to the display generator.

Abort indication during run.

<u>Outputs before simulation run (hard copy):</u>

Narrative TBD used to identify run including [illegible].

Flight path type.

Operator/Pilot identification.

Error values utilized.

DMA errors utilized.

Simulation ready or abort.

List of required additional data, software, hardware components.

Outputs after simulation run (hard copy):

Update location as a function of time
as a function of location.

Navigation error as a function of time
as a function of location.

RMS error for complete flight.

Peak error during flight and location.

Locations where errors exceeded RMS.

Time at beginning of simulation run.

Time at completion or abort of simulation run.

Reason for aborted run.

7.2 Timing Requirements

7.2.1 Introduction

Computationally the most difficult part of the simulation is the generation of the simulated HUD display. It has not been determined whether smooth motion of this display is required from a human factor standpoint; however, the display generator, which utilizes the DMA data base (under contract by AFWAL/AAA) will operate at TV compatible rates. Thus, smooth motion of the simulated HUD is possible and will be utilized as a baseline in this simulation development plan.

7.2.2 Requirements for individual modules:

Force Transformation

IMU Error Model

Gravity Error Model

The time steps have to be sufficiently short to keep specific forces approximately constant during the time steps. Non-real time simulations have shown that for ~ 2g turns 30 sec time intervals are sufficient. However, if tighter turns appear appropriate in the flight simulation, shorter intervals will be required. It is important to use the average specific force during the time interval and not to sample the specific force at the time of the update.

INS Computer.

In this module the Nav system error is added to the "true" position. The output has to be compatible with the display generator. Thus, every 1/30 sec true position has to be read, errors added to it to provide an output every 1/30 sec. (Note errors change only every 30 sec.)

MAP Displacement Generator.

In this module, the addition is also performed in 1/30 sec though the filter input changes very slowly. (It is recommended that this module be included in the INS module to reduce computational delay.)

Display Generator and Data Base.

These computational elements are under development. Inputs are required every 1/30 sec. Outputs are provided every 1/30 sec.

Attitude Transformation Module.

This module will be available as part of the Display Generator module. Attitude inputs are required every 1/30 sec.

Attitude Error Model.

Though the errors change slowly input from the TV probe and output have to be TV compatible (1/30 sec).

FOV Limiter and Converter.

This module converts from digital data to analog needed by the video mixer. Since the information is 1 bit (no addition or video or white saturation) the D to A function is simple, TV compatible operation is required.

Reticle Pointing System

This module reads the Helmet Sight and adds black saturation to the video at the reticle location. TV compatible operation is required.

Helmet Sight Error Model.

Operates after "Mark" interrupt? 3-4 times every 5 to 10 minutes.

Filter, Estimator.

Estimates need to be propagated at the error update rate (30 sec/step). State variables are recomputed after every measurement sequence (5 to 10 min intervals).

Force Transformation Module

Functional Requirements

The IMU error model needs acceleration at the IMU location in the IMU case coordinate system to generate the gyro "g" sensitive drift terms and the accelerometer bias and scale factor error.

Inputs: Aircraft CG acceleration

Aircraft Attitude rates

In local vertical, north coordinates

Outputs: Acceleration of the IMU outer case

Rotation rate of the IMU outer case

Update Time: ≈ 30 sec

Status

This is a new module. Analytical formulation and coding has to be performed. The coordinate transformations are simple. No major analytical work is required.

FORCE TRANSFORMATION MODULE
DEVELOPMENT PLAN

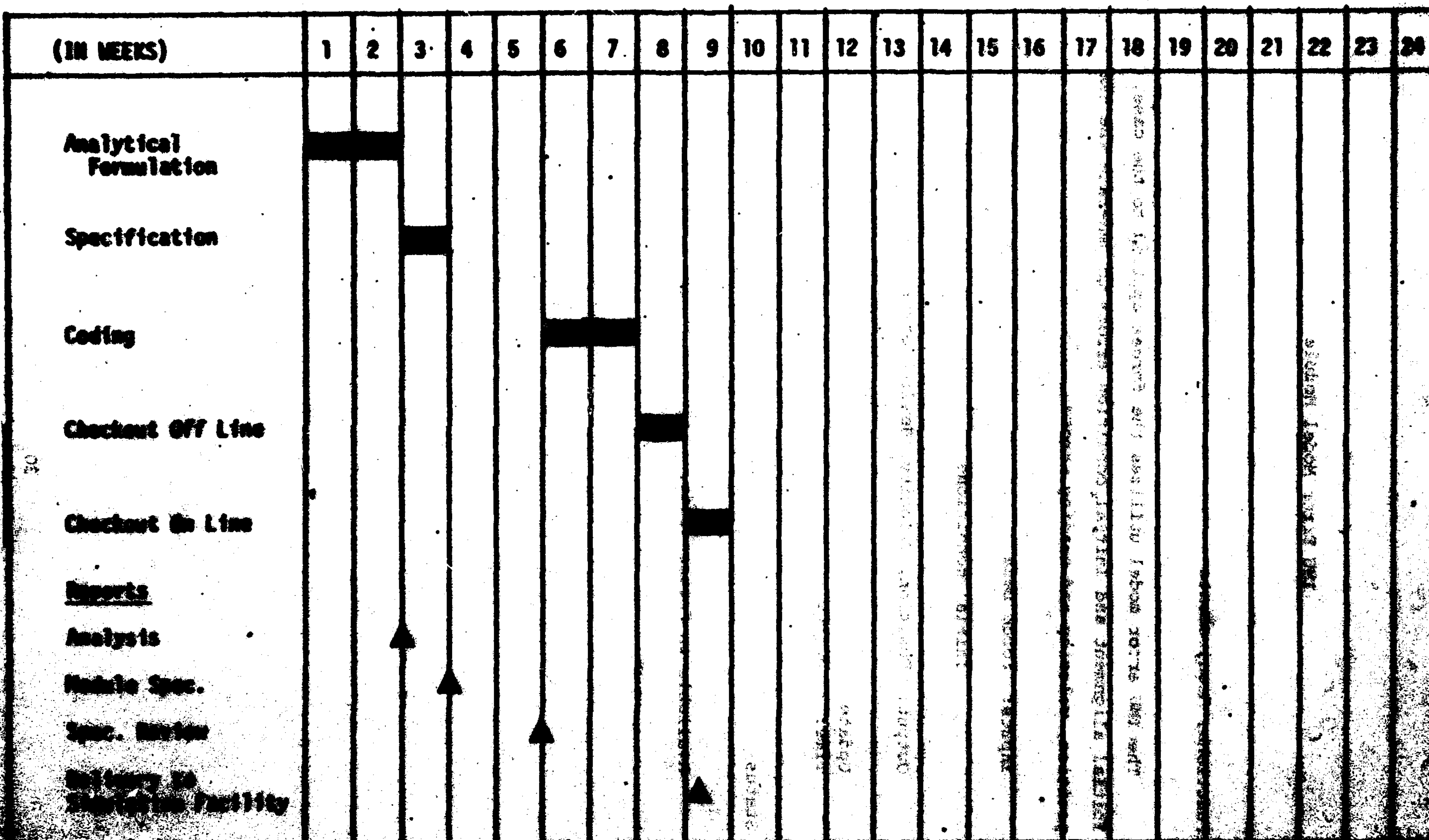

IMU Error Model Module

Functional Requirements

The IMU error model utilizes the forces applied to the case, initial alignment and initial condition errors to generate the IMU position, velocity and heading errors.

Inputs: Force Data

Initial conditions

Output: Position, Velocity, Heading error

Update Time: 30 sec

Status

Available in Fortran code.

IMU ERROR MODEL MODULE

DEVELOPMENT PLAN

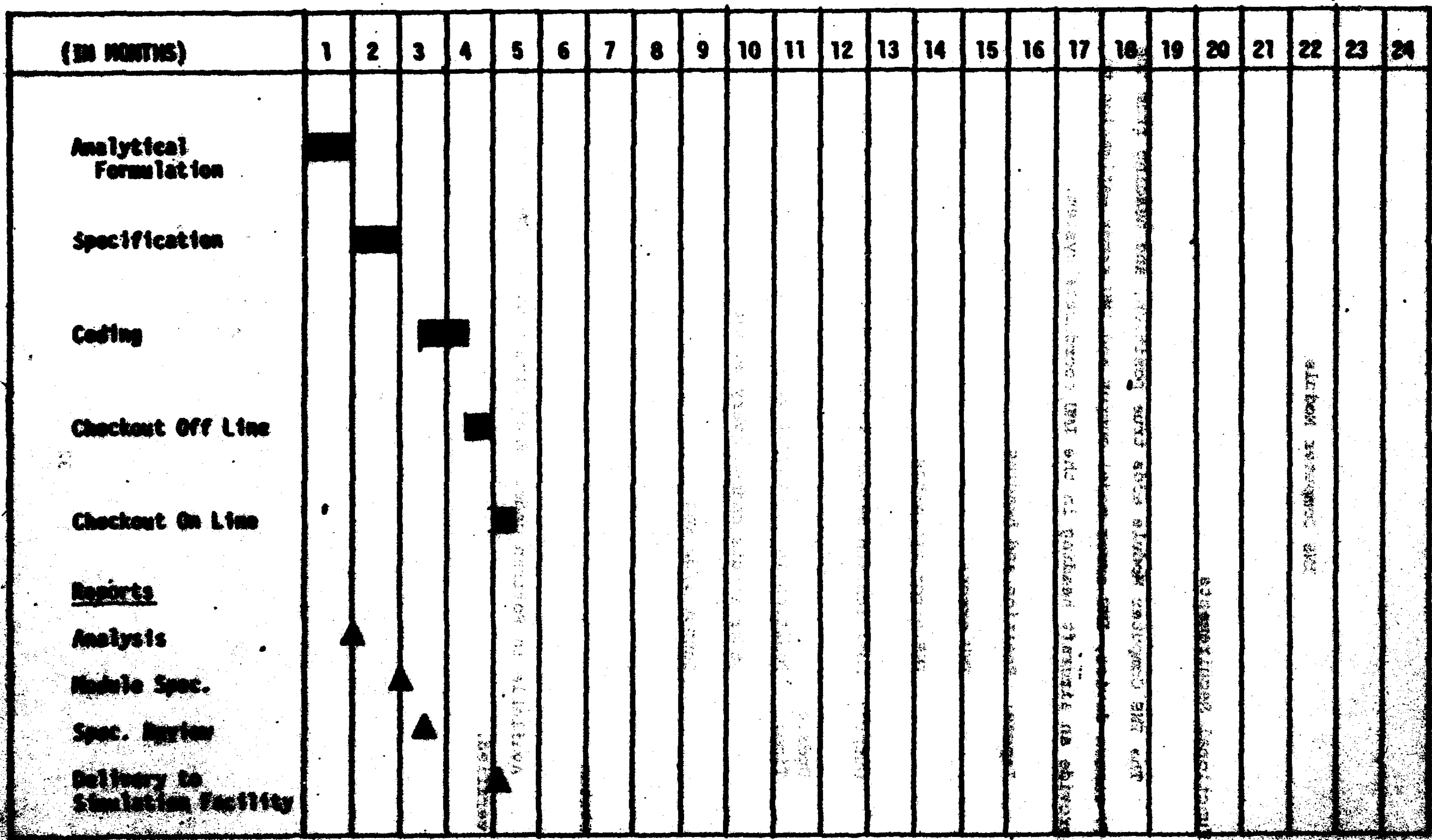

IMS Computer Module

Functional Requirements

The IMS Computer Module adds true position, and heading from the TV camera device, IMU error model output and IMU error estimation to provide an aircraft heading in the IMU coordinate system.

Inputs: Position and Heading

IMU errors

IMS error estimates

Output: Position and Heading in the IMU coordinate system

Update Time: Position input every 1/30 sec

Other inputs change every 30 sec

Output 1/30 sec

Status

Available in Fortran code. Real time running time needs to be verified.


THE COMPUTER MODULE
DEVELOPMENT PLAN
1
2
3
4
5
6
7
8
9
10
11
12
13
14
15
16

Map Displacement Generator
Module

Functional Requirements

The Map Displacement Generator utilizes the output of the INS computer and adds to the INS computed location the estimated error between the INS coordinate system and the Map coordinate system as needed by the Display Generator.

Inputs: Inertial Position, Heading

INS Map coordinate system error estimate

Outputs: Estimated Position in Map coordinates

Aircraft Heading in Map coordinates

Update Time: 1/30 sec

Status

This is a new module. Analytical formulation and coding has to be performed. No major analytical work is required.

MAP DISPLACEMENT GENERATOR MODULE
DEVELOPMENT PLAN

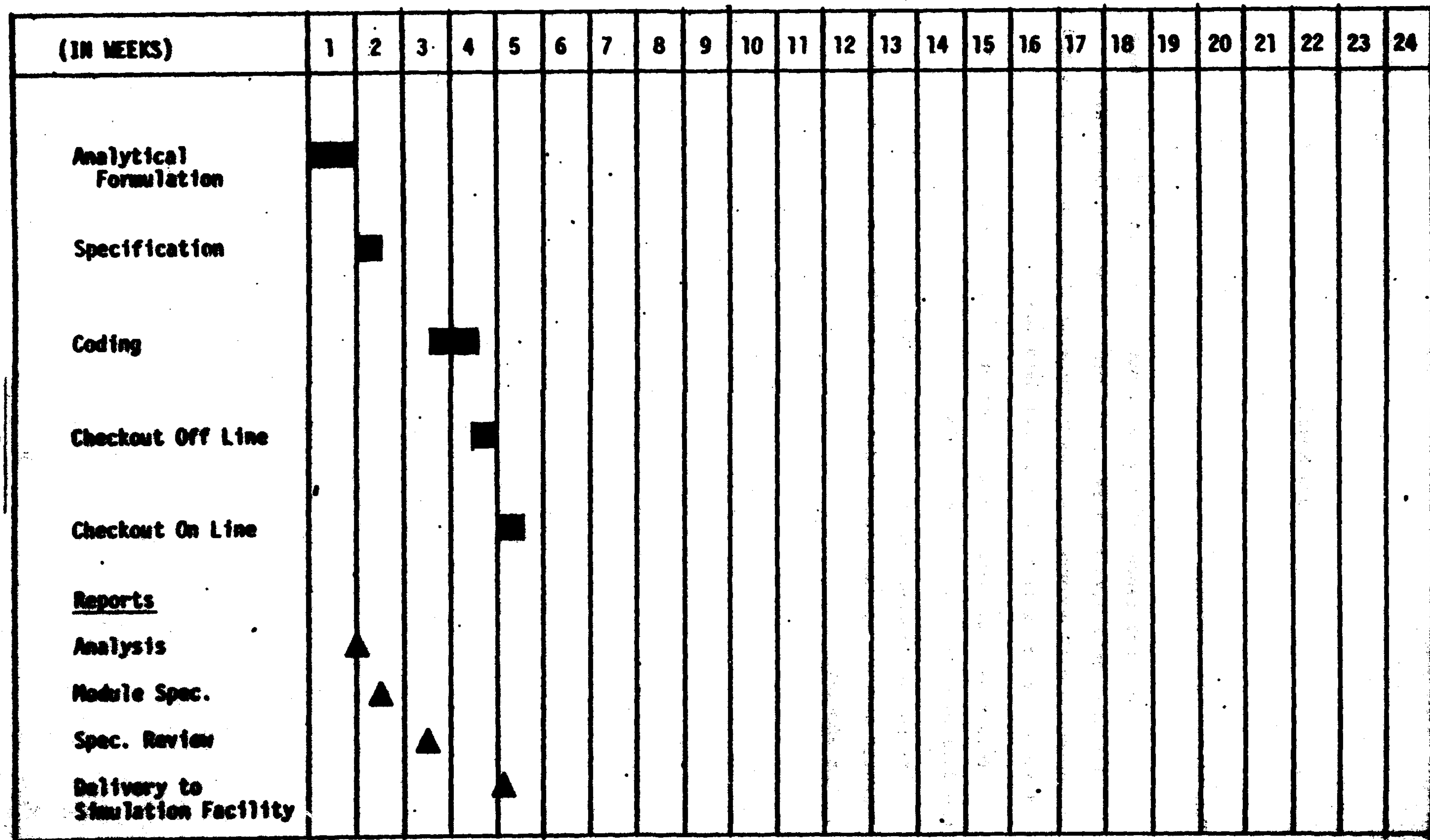

Data Base Model

Functional Requirements

This does not represent a module, but a one time effort to change the simulator data base to a realistic map. It will be necessary to introduce both uncorrelated and correlated errors into the data and to add and delete data from the cultural data base.

This task will require the use of an interactive terminal where the data base material can be displayed.

It is recommended that the DMAC be requested to provide both an "actual" and a "representative" data base for the land mass utilized in the simulation.

Display Generator Module

Functional Requirements

The display Generator utilizes the DMC data base and the estimate of aircraft position and heading to generate a "picture" larger than the picture displayed on the HUD. The total picture will be 45 deg horizontal and 30 deg vertical. The "picture" consists of ridges generated from the elevation data base and of surveyed landmarks generated from the cultural data base.

Input: Position and Heading in Map Coordinates

Output: "Picture" of the outside world

Update Time: 1/30 sec

Status

Hardware and software under development by AFWAL. Will be available in early 1983.

Analysis and coding to interface with simulation will be required.

Off line "Picture" development for early simulation development will also be required.

DISPLAY GENERATOR MODULE

DEVELOPMENT PLAN

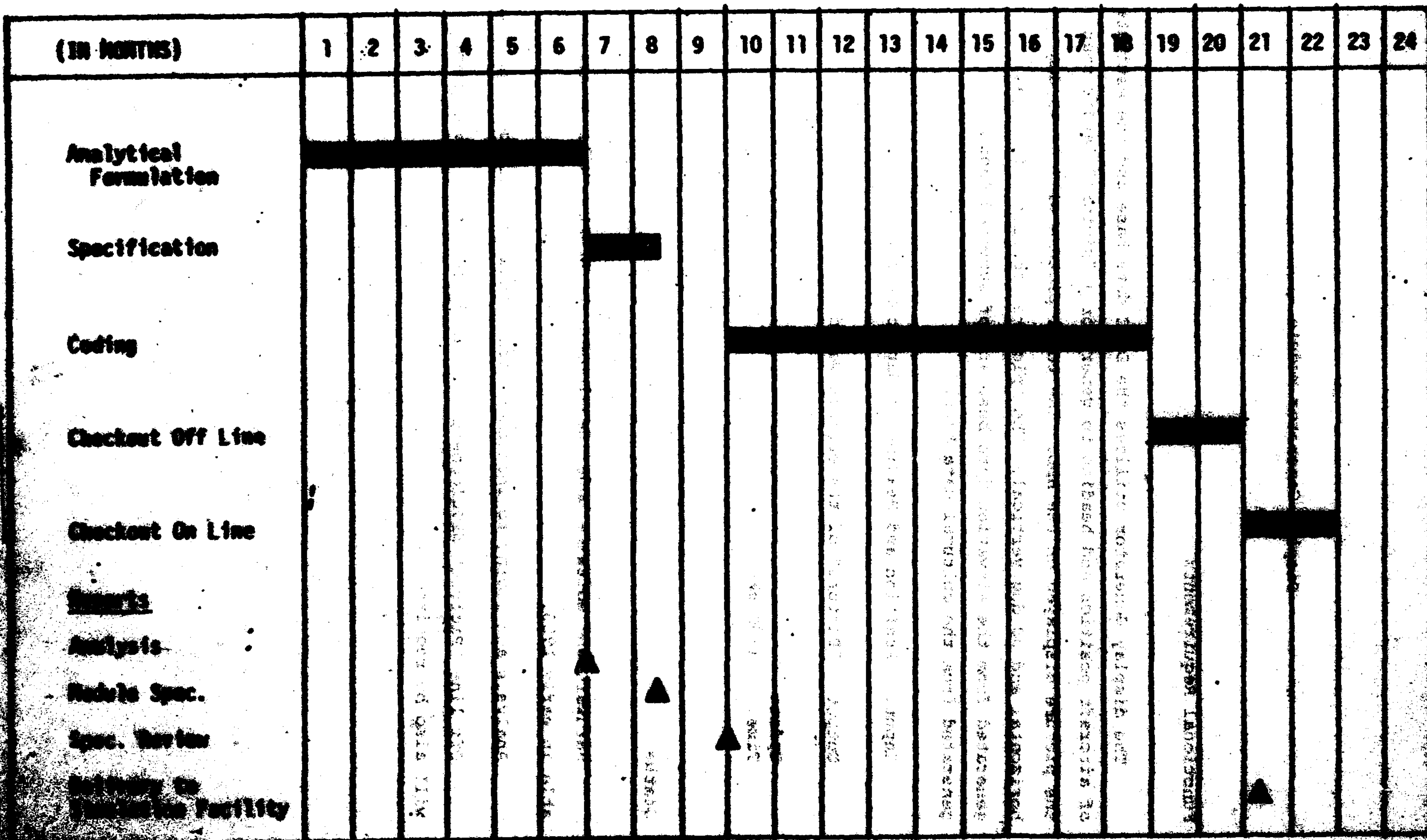

Attitude Error Module

Functional Requirements

The Attitude Error Module utilizes attitude data from the TV camera drive and adds errors to this data based on the aircraft attitude error model.

Inputs: Attitude from TV camera drive

Outputs: Aircraft attitude

Update Time: 1/30 sec

Status

This is a new module. Analytical formulation and coding has to be performed. No major analytical work is required.

Attitude Error Module
Development Plan

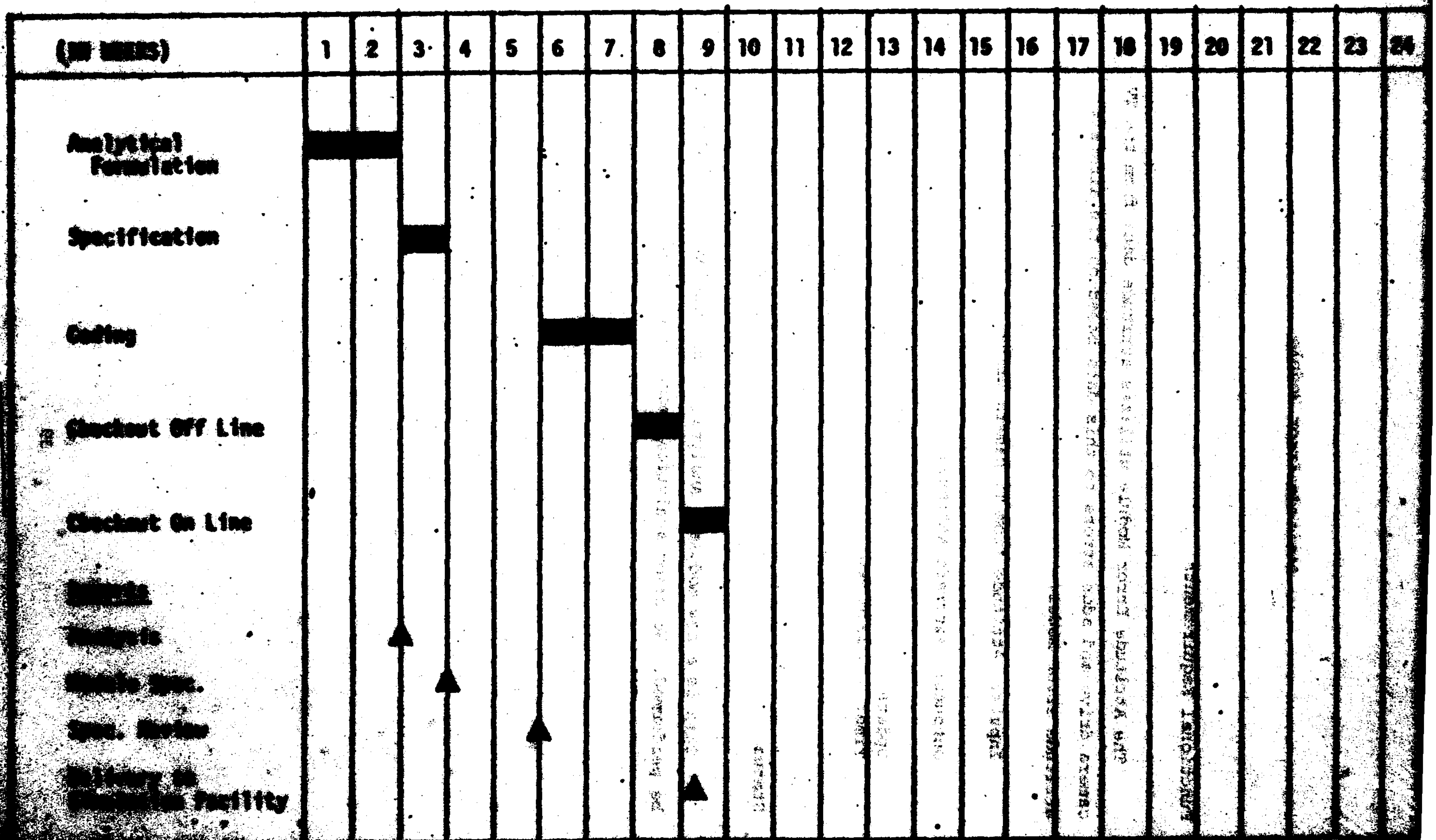

Attitude Transformation

Functional Requirements

The Attitude Transformation Module utilizes the picture from the display generator and the estimated aircraft attitude to generate a 30 deg horizontal by 20 deg vertical picture for display on the HUD.

Inputs: "Picture" from the display generator

Estimate of A/C attitude

Output: "Picture" for display on the HUD

Update Time: 1/30 sec (TV compatible)

Status

Will be included in display generator development.

Attitude Transformation

Development Plan

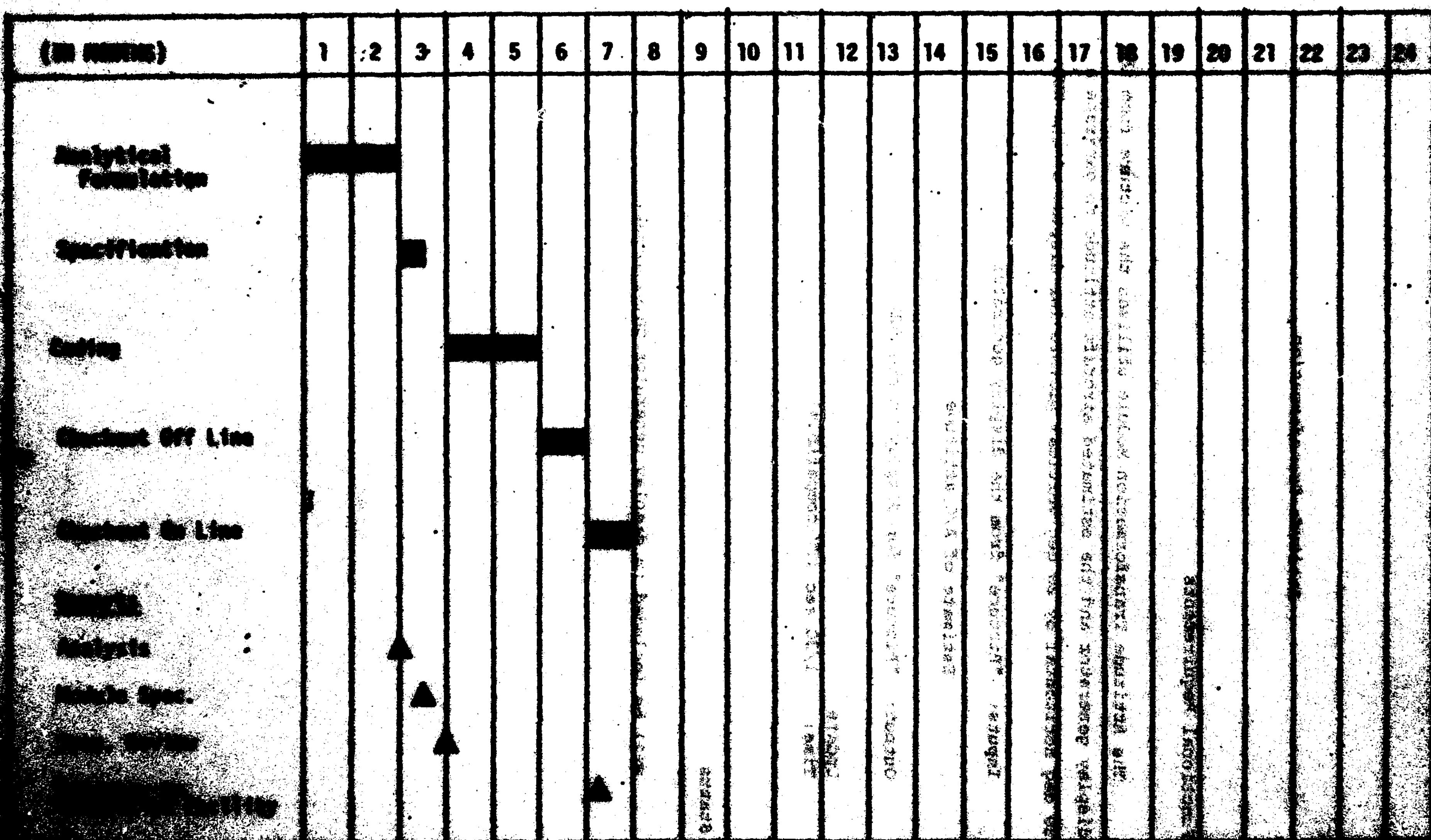

Helmet Sight Error Module

The Helmet Sight Error Module utilizes the crosshair location in the video and adds errors to this data based on the Helmet Sight Error Model, and converts this location to a unit vector in aircraft coordinates. In addition, the direction of the unit vector is changed slightly by the HMS error model.

Input: Location of crosshair in visual scene (Line #, Pixel #)

Output: Unit vector to selected location with added noise

Update
Time: By interrupt. A group of 3 approximately every 10 MS.

Status

This is a new module. Analytical formulation and coding has to be performed. No major analytical work is required.

Helmet Sight Error Module

Development Plan

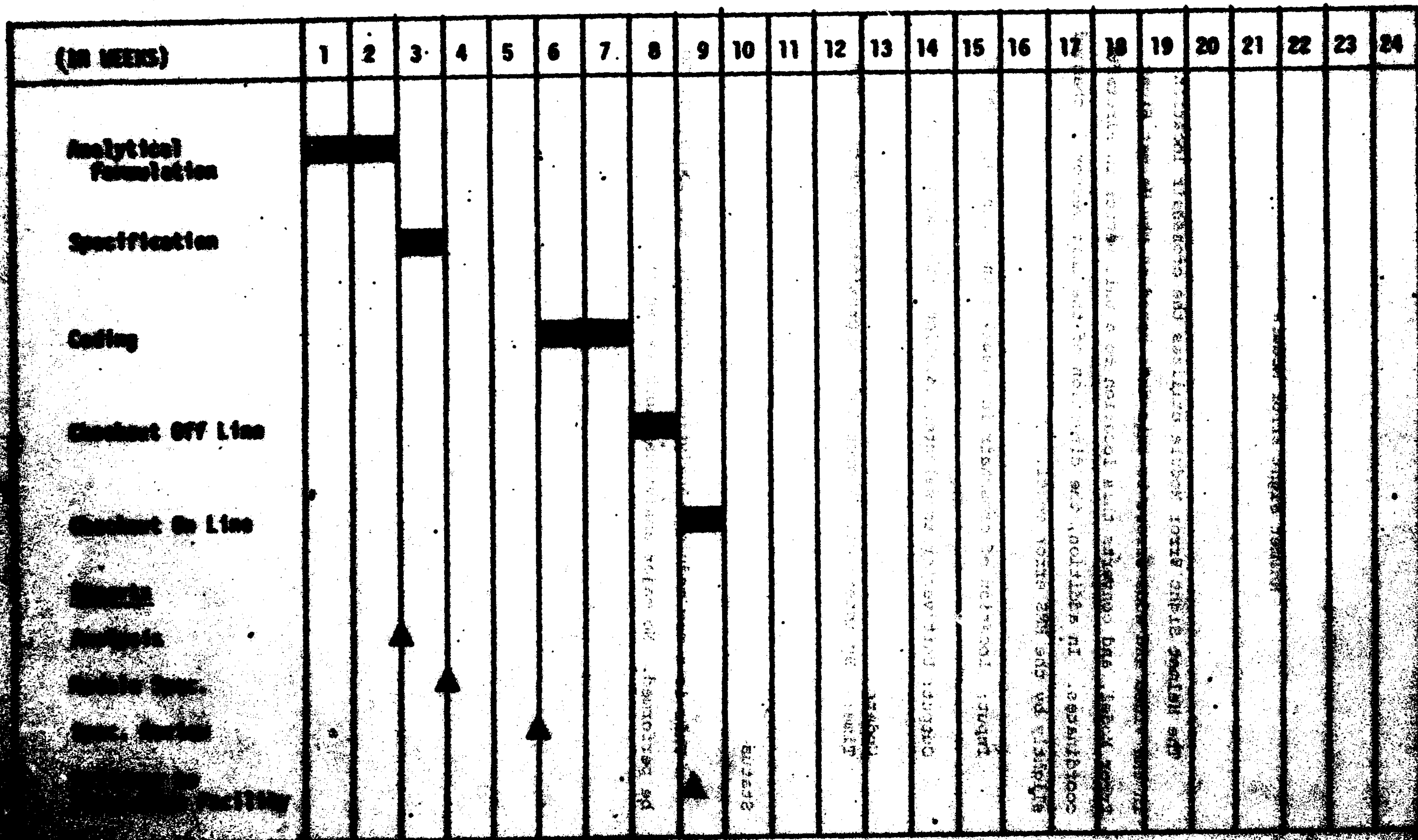

Filter

The Filter utilises:

- Location of landmarks from the data base
- Aircraft estimated position and heading
- Aircraft attitude
- Direction to selected landmark
- The relevant error moduels for the various components

and estimates:

- Errors between the INS and map coordinate system
- INS position and heading errors

Inputs and outputs are given above.

Status

Complete filter formulation is required, though various parts have been developed. Coding for real time performance is required.

FILTER DEVELOPMENT PLAN

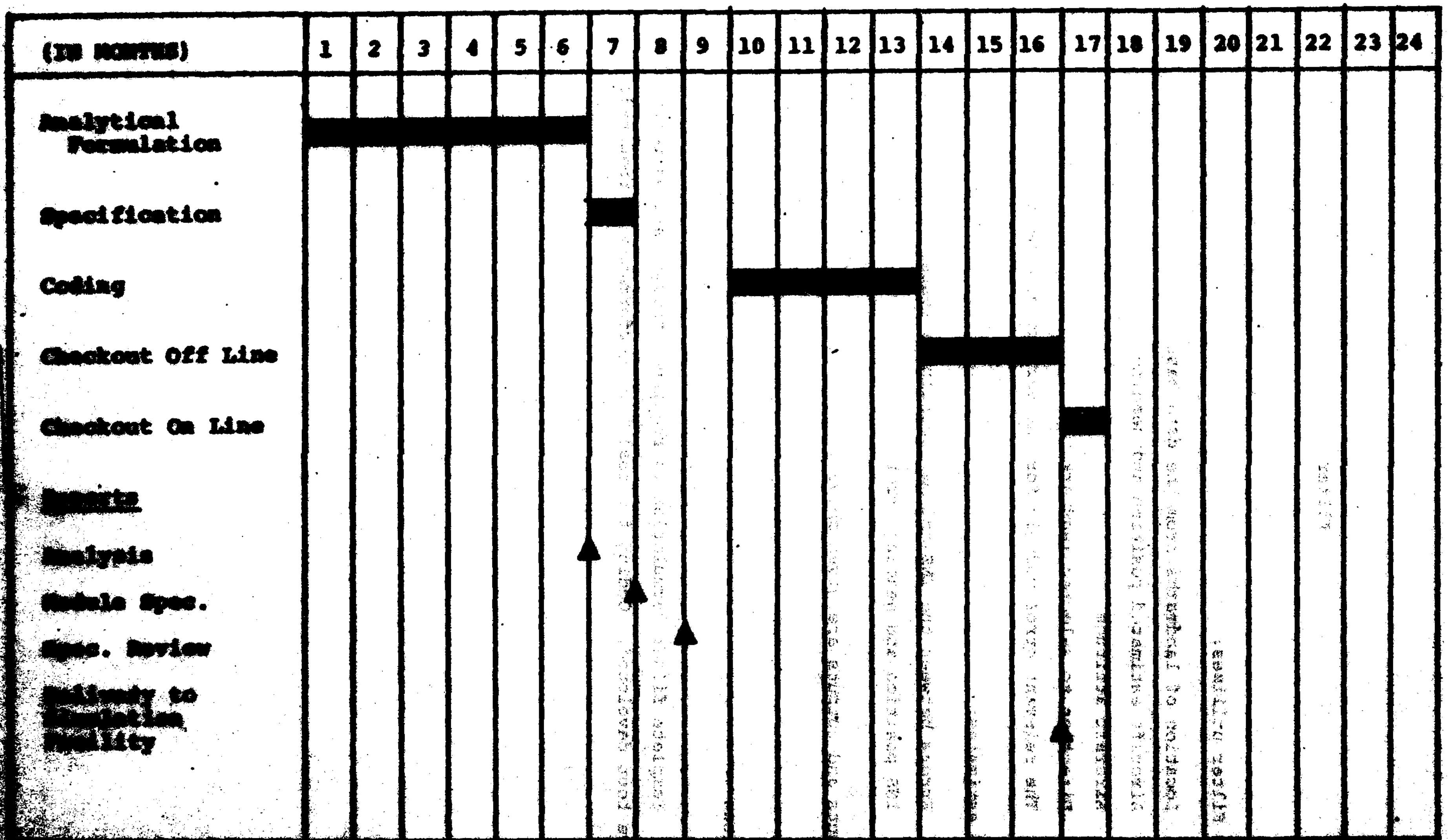

System Executive

Functional Requirements

Provide the data flow between modules, interrupts for measurements, system status checks, system failure interrupt displays, synchronization between the flight path and data base.

This is a module required only for the simulation and does not represent parts of the airborne system.

Update Time: NA

Status

This is a module peculiar to the simulation facility. Careful detailed specification based on the functional spec (sec. 7.2) is required to insure that speed is not affected by module cycle time.

SYSTEM EXECUTIVE
DEVELOPMENT PLAN

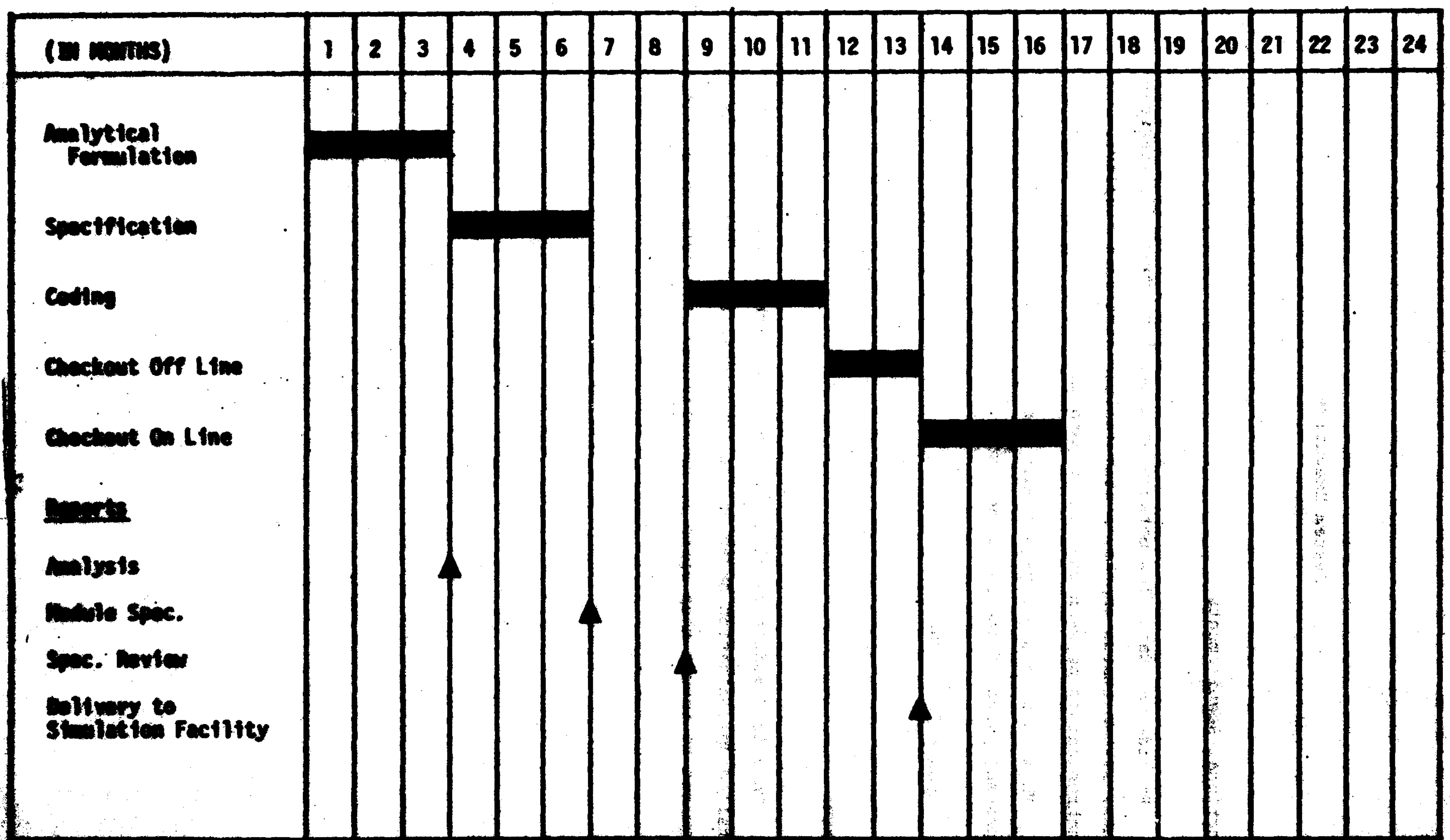

Special Map
Displacement Generator

Functional Requirements

This module is required during system checkout. It provides correction for the map error estimate when the standard trajectory is utilized.

Inputs: Picture from display generator map error estimate.

Output: Correct Picture

Update Time: 1/30 sec

Status

Module required during system development. No major analytical effort is required.

Special Map Displacement Generator

Development Plan

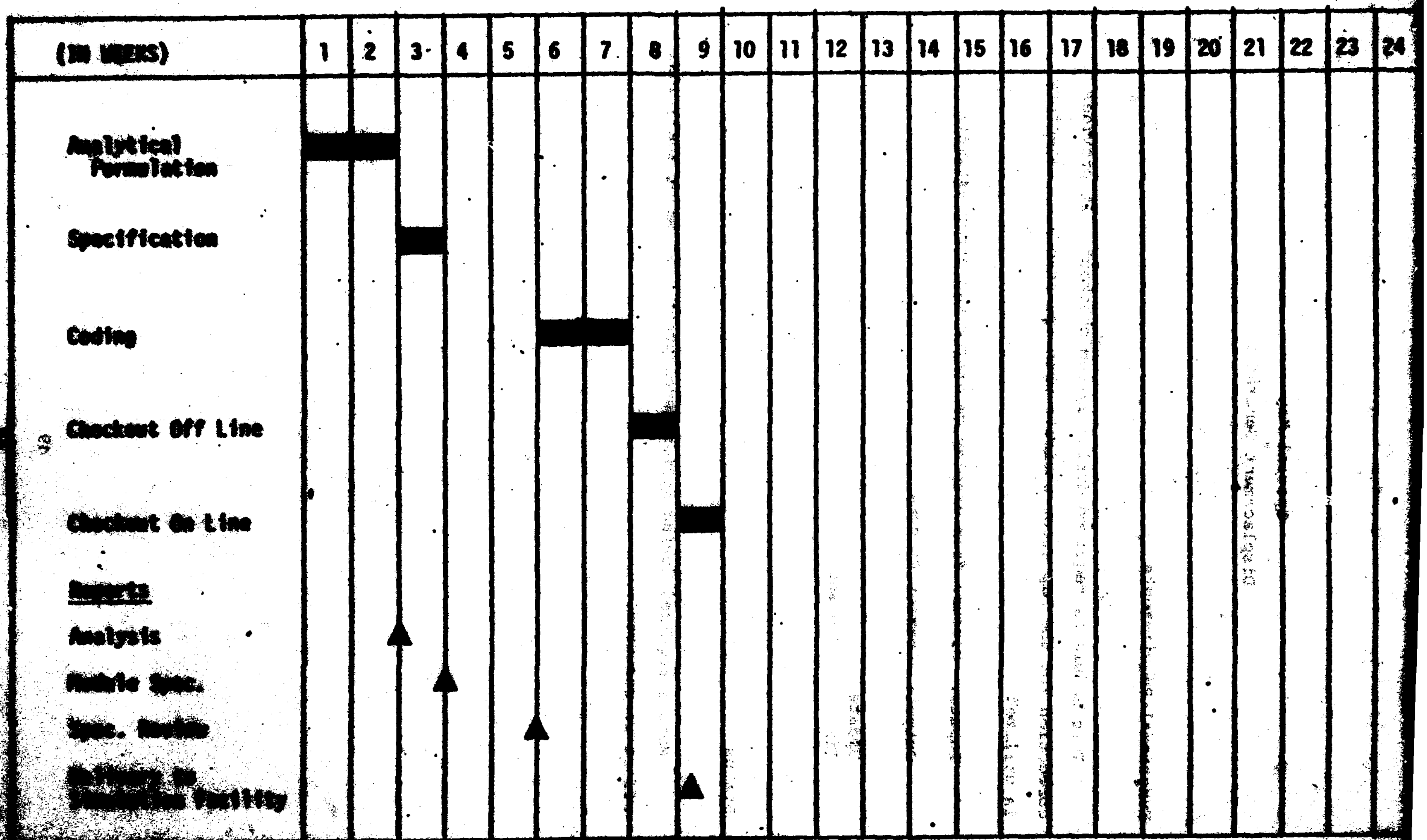

Summary

The total anticipated effort for the development of the Rotorcraft Simulation is shown below.

Supervisory personnel, Support personnel, publications of reports, interfacing with simulation facility personnel has not been included in the summary. The time estimates are in person months.

Module	Eng/Analyst	Programmer
Force Transformation	1	1
IMU Error Model	2.5	1
INS Computer	2	1.5
Map Displacement Generator	1.5	1
Display Generator	9	24
Attitude Transformation	2	2
Attitude Error	1	1
Helmet Flight Error	1	1
Filter	9	8
System Executive	6	6
Special Map Displacement	1	1
TOTAL:	35.5	47.5

8.0 Further Exploitation of the Data Base

The present LAMA configuration represents a first step in the utilization of the DMAC data base for navigation system updates. The system in its present form is designed for daytime operation.

For night time operation, a FLIR can provide the "real world" display in the aircraft cockpit. The pilot can still use the helmet sight to point at a landmark (shown on the FLIR display) and update the inertial navigator as is proposed in the daytime configuration.

For adverse weather operation (in a two seater configuration) the second crew member can use a SLR as the primary navigation sensor and compare the SLR image with the DMAC generated view (looking to the side of the flight path) while the pilot views a data base generated image of the world as seen in front of the aircraft.

In areas with large elevation changes, clues can be provided to the pilot showing potential exits or warning the pilot about areas where rapid elevation changes exceed the performance of his aircraft.

Real time changes in the cultural data base of a given operating area can also add to the effectiveness of the system; especially addition of known threats. This addition would allow crews to avoid known high threat areas when these crews are assigned targets beyond these areas.

APPENDIX A

This appendix presents a summary of work performed by [illegible] of the C.S. Draper Laboratory under 1979 IR&D project 110 during the initial development of the LANA concept.

1.0 INTRODUCTION

As the vehicle flies by a landmark, the line of sight from the vehicle to the landmark in local level frame coordinates is computed from the vehicle position estimate obtained from the inertial navigator and the landmark location obtained from a map. [Map errors for the landmarks are assumed to be zero mean random variables modeled as a 300 ft. 1σ Gauss-Markov process with an assumed correlation distance of 15,000 ft.] The deviation of the optically measured line of sight from the computed line of sight constitutes the measurement for an extended Kalman filter. The actual line of sight optical measurement is specified by an azimuth and elevation angle with respect to the local level frame. A number of such measurements can be taken per landmark.

The inertial system error model uses 17 states and was obtained from "Inertial Navigation System Error Models" by W. Widnall and P. Grundy, TR-03-73, May 1973 Intermetrics, Inc. Since the simulations were only to a first order, no attempt was made to introduce scale factor errors or g-sensitive terms into the inertial system error model. Consequently, a benign environment was assumed for the vehicle even for the case of a strapdown inertial system.

The vehicle was assumed to be at a constant altitude of [illegible] flying from east to west at a constant velocity [illegible] were evenly spaced along the vehicle flight [illegible] path by approximately [illegible]. [See Figure [illegible] for [illegible] geometry.]

A high performance [illegible] and a low cost [illegible] (LCIGS) [illegible] both used in various runs. [See Table 3-1 for the specifications [illegible] for these systems.] For most of the runs, the systems were [illegible]

to be initialized via GPS as determined from data supplied by [illegible].*
In some of the runs for LCIGS, a 1°/hr initial drift and a 1' or initial misalignment were introduced with non-calibration obtained via the optical measurements on evenly spaced landmarks in a [illegible] landmark calibration phase of flight.

For either the high performance or LCIGS cases, position errors are dominated by the map errors. The utility of the [illegible] arrangement is therefore manifested by a systematic means of aligning the inertial navigator to prevent excessive error growth between landmarks when the map cannot be used rather than in any significant reductions to the absolute value of position errors over the map errors. The relative position error with respect to a landmark is significantly reduced and for LCIGS remains below 100 ft., 1σ for about a minute after passing the landmark.

A summary of the significant results obtained from the simulations is presented in Section 2.

Section 3 is a description of the simulations and of the results.

2.0 SUMMARY OF SIMULATION RESULTS

The following is a summary of the principal results obtained from the computer runs.

For optimum measurement geometry of the [illegible] with azimuth angles of 45°, 135°, the [illegible] deviation for the filter estimate [illegible] will be dominated by the map error. Increasing the [illegible] if they are evenly spaced [illegible] which therefore results in lower position [illegible]. [The lowest position error for the [illegible] 63 meters for the high performance [illegible]]

With the optimum geometry, [illegible] measurement, which is [illegible] runs. (See Table 3-1 for the specifications used [illegible].) For most of the runs, the systems were assumed

*CSDL internal communication.

[illegible] are taken. [The errors include velocity misalignments, [illegible] accelerometer biases.]

That measurement geometry is restricted to [illegible] than say 40°, that three measurements per landmark (with azimuth angles as far apart as possible) are required to [illegible] the optimum case.

Increasing the number of evenly spaced landmarks caused LCIGS horizontal position errors to approach the high performance position errors when using fewer landmarks. For example, a run made for LCIGS with 20 evenly spaced landmarks over a 1200 second period resulted in horizontal position errors before and after measurements at the last landmark of 87.3 and 67.6 meters respectively, which roughly correspond to high performance system errors using only 9 landmarks.

LCIGS horizontal velocity errors were never lower than [illegible] although for a number of cases the errors were close to 1 fps. In contrast, the high performance system had velocity errors as low as 0.6 fps.

The relative position with respect to the last landmark [illegible] the target was reached was less than 100 ft. for a [illegible] of time for both the high performance system and LCIGS.

For many computer runs, the time intervals [illegible] too small to allow propagation of relative errors to [illegible] as 100 ft. [illegible], in [illegible] relative [illegible] the [illegible] point [illegible] a 100 ft. relative error [illegible]

Number of Landmarks	High Performance [illegible]	[illegible]
[illegible]	[illegible]	[illegible]
9	[illegible]	[illegible]
20	—	[illegible]

[illegible] Time [illegible] Is Below 100 Ft.

When an initial gyro drift error of 1°/hr is introduced into the LCINS in place of the [illegible] GPS derived value of 0.1°/hr, gyro calibration using the optical measurements on 11 evenly spaced landmarks [illegible] period of less than 1500 seconds are effective in reducing the drift error to 0.067°/hr. Following this calibration and maintaining the same spacing between landmarks, the horizontal position errors are comparable to the high performance system position errors at the 9th landmark when 5 landmarks are used. [These are 124 and 75 meters before and after the measurements.] Velocity errors are comparable to LCINS velocity errors at the 9th landmark (.86, .44 m/s before and after the measurements) when 9 landmarks and GPS initialization are used. The same steady-state results are obtained when the initial misalignment is also set at 1 mr (along with the 1°/hr drift).

3.0 SIMULATION RESULTS

A number of computer runs were made for both a high and low performance inertial system with a vehicle flying at a constant altitude of 100 ft. and constant velocity of 800 fps from west to east at a constant latitude of 45°. Horizontal map errors were assumed to be 300 ft., 1σ independent Gauss Markov processes along [illegible] with a correlation distance of 15,000 ft. Vertical map errors were assumed to be Gauss Markov with a 100 ft. 1σ error and the same correlation distance. Landmark locations were [illegible] the vehicle path at ground level. Initialization of vehicle position, velocity and alignment was assumed to be [illegible] GPS [illegible] errors. [illegible] 5 landmarks [illegible] vehicle path were used for the optical measurements [illegible] elevation. Total time of travel from the FEBA line [illegible] assumed to have occurred) to the [illegible] Figure 3-1 is a [illegible] and [illegible] with [illegible] at 45° [illegible]. [illegible] to scale.)

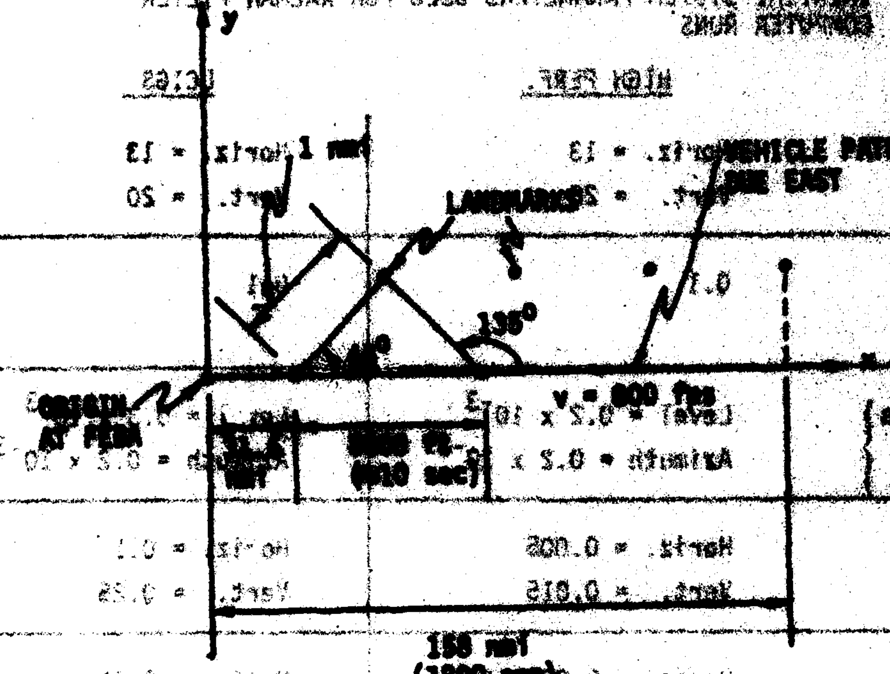

Figure 3-1. Vehicle Path and Landmarks (45°, 135°) Azimuth Measurements at Each Landmark

Table 3-1 is a list of the initial errors and system parameter errors used for the high performance and low performance [illegible] inertial systems.

Table 3-1. INERTIAL SYSTEM PARAMETERS USED FOR KALMAN FILTER COMPUTER RUNS

PARAMETER	HIGH PERF.	[illegible]
Initial Position (ft.)	Horiz. = 13 Vert. = 20	Horiz. = 13 Vert. = 20
Initial Velocity (fps)	0.1	0.1
Initial Misalignments (rad)	Level = 0.2×10^{-3} Azimuth = 0.2×10^{-3}	Level = 0.[illegible] Azimuth = 0.2×10^{-3}
Gyro Drift Bias (^{o}/hr)	Horiz. = 0.005 Vert. = 0.015	Horiz. = 0.1 Vert. = 0.25
Gyro Random Walk in Rate $((^o/hr)^2/hr)$	Horiz. = 0.000016 Vert. = 0.000225	Horiz. = 0.01 Vert. = 0.0625
Accelerometer Bias (μg)	Horiz. = 50 Vert. = 100	Horiz. = 100 Vert. = 1[illegible]
Accelerometer Random Walk in Acceleration $((\mu g)^2/hr)$	100	225

For both systems, inertial system errors in the [illegible] optical measurements [illegible] the basic inertial system model equations used. The horizontal errors in position, velocity, and misalignment are the outputs of the standard Schuler loop presented in Figure 3-2.

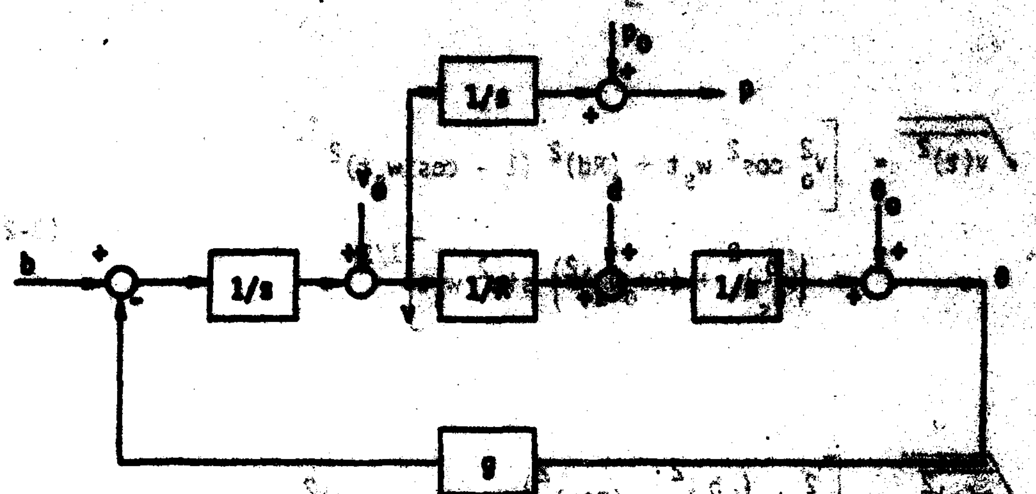

b = accelerometer bias
d = gyro drift
v_0 = initial velocity
p_0 = initial position
θ_0 = initial misalignment
g = gravity

R = earth rate
v = velocity
p = position
θ = misalignment
s = Laplace transform variable

Figure 3-2. Schuler Loop

The [illegible] random walk [illegible] Figure 3-2. [illegible] been neglected.

$$\sqrt{\overline{\theta(t)^2}} = \left[\left(\frac{d}{w_s}\right)^2 \sin^2 w_s t + \theta_0^{\,2} \cos^2 w_s t \right]^{1/2}$$

$$\sqrt{\overline{v(t)^2}} = \left[v_0^2 \cos^2 w_s t + (Rd)^2 \, (1 - \cos w_s t)^2 + \left\{ \left(\frac{b}{w_s}\right)^2 + (R\theta_0 w_s)^2 \right\} \sin^2 w_s t \right]^{1/2} \qquad (3\text{-}2)$$

$$\sqrt{\overline{p(t)^2}} = \left[p_0^2 + \left\{ \left(\frac{b}{w_s^2}\right)^2 + (R\theta_0)^2 \right\} (1 - \cos w_s t)^2 + \left(\frac{v_0}{w_s}\right)^2 \sin^2 w_s t + (Rd)^2 \left(\frac{\sin w_s t}{w_s} - t\right)^2 \right]^{1/2} \qquad (3\text{-}3)$$

with $w_s = \sqrt{g/R}$

Horizontal errors for the high performance system were dominated by the effects of the initial misalignment angles assumed for the horizontal axes. The Schuler oscillation tended at first to reduce the misalignment angle. The LCINS system was also dominated by the effects of the initial misalignment angles [illegible] gyro drift term was sufficiently large to cause the misalignment errors to increase significantly with time rather than to decrease as in the high performance system.

The vertical channel position error was due to the external bias. Vertical velocity errors tended to be very small.

Table 3-2 lists the inertial system position errors at each landmark before and after the optical measurements are incorporated. Corresponding velocity errors are listed in Table 3-3. The propagation of the high performance system errors between landmarks is "driven" mainly by the misalignment error. Because the gyro drift is low, the horizontal misalignment angles are rapidly reduced by the filter with no propagation of misalignment error between measurements until the effects of the random walk in gyro drift become large enough relative to the reduced misalignment error. In the case of LCIGS, there is a strong initial driver of misalignment angle between measurements due to the large gyro drift.

The use of more evenly spaced landmarks within the 20 minute interval obviously results in less inertial system error propagation between the more closely spaced landmarks. Runs were made with 9 evenly spaced landmarks for the high performance system and LCIGS. The position errors and velocity errors just before and after the measurements at each landmark are listed in Tables 3-4 and 3-5. Comparison with the 5 landmark case (Tables 3-2 and 3-3) shows a considerable lowering of errors. Errors immediately after a set of measurements are still dominated by a priori map error but do show a 40% reduction from the 100 meter map position error at the 9th landmark for the high performance system and a corresponding 23% reduction for LCIGS. Velocity errors for the high performance system are below 1 fps in the target area for either 5 or 9 landmarks. LCIGS velocity error while reduced when 9 landmarks are used is still considerably above 1 fps. [i.e., 2 fps before measurements, 1.3 fps after measurements, at the 9th landmark.]

All of the above runs for LCIGS assumed a modest initial gyro drift for LCIGS (.3°/hr horizontal drift, 0.25°/hr vertical drift). It was desired to see the effect of a much larger initial gyro drift, 1°/hr, assuming no GPS calibration for drift. The optical measurements were for 19 evenly spaced landmarks as previously, but over a time interval of 2400 seconds so that the FEBA line was assumed to be traversed at 1200 seconds. Thus about 10 landmarks were in effect used to "pre-calibrate" the LCIGS with the 1°/hr initial drift during the first 1200

Table 3-2. INERTIAL SYSTEM POSITION ERRORS WITH KALMAN FILTER

	High Performance System Position Errors (Meters)		LCIGS Position Errors (meters)	
Landmark	Before Meas.	After Meas.	Before Meas.	After Meas.
1	53.6	53.6	87.3	81.6
2	188.6	85.7	256.4	90.0
3	182.1	85.7	218.2	87.3
4	143.6	81.4	231.8	90.0
5	124.3	75.0	245.5	90.0
	Above from Fig. 4		Above from Fig. 16	

Table 3-3. INERTIAL SYSTEM VELOCITY ERRORS WITH KALMAN FILTER

	High Performance System Velocity Errors (m/s)		LCIGS Velocity Errors (m/s)	
Landmark	Before Meas.	After Meas.	Before Meas.	After Meas.
1	0.47	0.41	0.73	0.55
2	0.77	0.35	1.1	0.43
3	0.48	0.23	0.86	0.49
4	0.31	0.18	1.04	0.57
5	0.29	0.23	1.03	0.49
	Above from Fig. 6		Above from Fig. 18	

Table 3-4. INERTIAL SYSTEM POSITION ERRORS - 9 LANDMARKS

Landmark	High Performance System Position Errors (meters)		LCIGS Position Errors (meters)	
	Before Meas.	After Meas.	Before Meas.	After Meas.
1	56.3	49.8	83.2	67.7
2	106.1	72.3	141.3	81.3
3	122.0	75.5	139.4	79.4
4	112.5	73.9	127.7	77.4
5	109.3	69.9	125.8	77.4
6	91.6	65.9	129.7	78.4
7	85.2	64.3	135.5	81.3
8	80.4	62.7	135.5	79.4
9	80.4	62.7	131.6	77.4
	Above from Fig. 25		Above from Fig. 29	

Table 3-5. INERTIAL SYSTEM VELOCITY ERRORS - 9 LANDMARKS

Landmark	High Performance System Velocity Errors (m/s)		LCIGS Velocity Errors (m/s)	
	Before Meas.	After Meas.	Before Meas.	After Meas.
1	.46	.41	.76	.57
2	.58	.4	.85	.48
3	.5	.31	.66	.42
4	.37	.24	.61	.44
5	.27	.19	.66	.50
6	.23	.17	.75	.53
7	.21	.17	.77	.53
8	.22	.18	.72	.48
9	.24	.21	.66	.44
	Above from Fig. 26		Above from Fig. 30	

seconds. In all of the applicable [illegible], an approximate steady-state condition is reached in about 1500 seconds for the [illegible] horizontal navigation channels. There is a slight asymmetry between the results for the horizontal channels which is due to the optical azimuth measurement angles not being exactly 45^0, and 135^0.

A more realistic but far from optimum choice of azimuth angles was chosen to be the set 20^0, 30^0 with the geometry depicted in Figure 3-3.

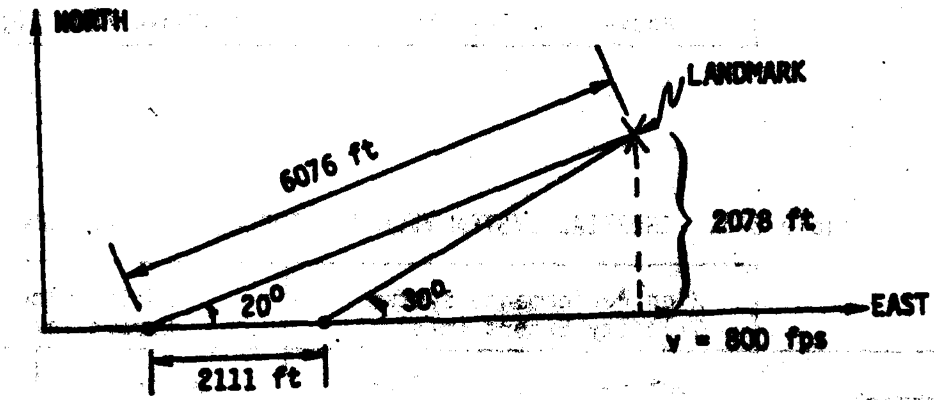

Figure 3-3. Measurement Geometry for 20^0, 30^0 Azimuth Angle Set.

Position and velocity errors just before and right after the measurements made at each landmark are listed in Tables 3-6 and 3-7, respectively. East position and velocity errors are higher than the north errors because of the asymmetry in measurement coefficients due to the 20^0, 30^0 set which does not occur with the ideal 45^0, 135^0 set. Both the north and east position errors are higher than in the ideal case (Tables 3-2 and 3-3). Here, unlike the ideal case additional measurements per landmark and/or better choice of measurement geometry help in reducing the errors, but in any event, errors are not better than in the ideal case.

Table 3-6. HIGH PERFORMANCE SYSTEM POSITION [illegible] MEASUREMENT ERROR, 20°, 30° SET OF [illegible]

	East Position Error (Meters)		[illegible]	
Landmark	Before Meas.	After Meas.	Before Meas.	After Meas.
1	54.3	56.3	[illegible]	[illegible]
2	188.8	152.7	194.6	[illegible]
3	337.6	188.8	222.7	116.8
4	325.9	188.8	302.6	[illegible]
5	285.3	176.8	168.6	[illegible]

Table 3-7. VELOCITY ERRORS CORRESPONDING TO POSITION ERRORS IN TABLE 3-6

	East Velocity Error (Meters/s)		North Velocity Error (Meters/s)	
Landmark	Before Meas.	After Meas.	Before Meas.	After Meas.
1	0.45	0.43	0.46	0.45
2	0.86	0.62	0.79	0.41
3	0.88	0.51	0.57	0.29
4	0.62	0.36	0.36	0.23
5	0.44	0.31	0.32	0.23

Table 3-8 lists position and velocity errors for the high performance system for various combinations of azimuth measurement angles, two or three measurements per landmark and measurement noise. Comparing the 1 mr and 5 mr noise cases for angles of [illegible]$^\circ$, 30° and [illegible]$^\circ$, [illegible]$^\circ$, confirm the results obtained for 45°,135° that there is insignificant change in error when the 5 mr noise is reduced to 1 mr. There is a significant reduction in errors when 3 measurements per landmark are used for the case of non-ideal azimuth angles that are constrained to be less than 45°. Also, the further apart in value the azimuth angles are, the smaller the resulting errors.

Table 3-8. HIGH PERFORMANCE SYSTEM - 5 LANDMARKS - [illegible] AZIMUTH MEASUREMENT ANGLES, NUMBER OF [illegible] PER LANDMARK, AND MEASUREMENT NOISE

[illegible]

CASE	East Position Error (m)		North Position Error (m)		East Velocity Error (m/sec)		[illegible] (m/sec)	
	Before	After	Before	After	Before	After	[illegible]	[illegible]
10^0, 30^0 5 mr	160.7	97	128.6	80.4	.31	.27	.3	.23
10^0, 30^0 1 mr	158.6	96.4	129.7	80	.31	.28	.3	.23
10^0, 20^0, 30^0 5 mr	122	100.7	122	75	.28	.28	.29	.22
10^0, 30^0, 42^0 5 mr	120	87.9	124.3	77	.28	.23	.3	.23
10^0, 42^0 5 mr	135	94.3	126.4	78.2	.3	.26	[illegible]	.23
20^0, 30^0 5 mr	285.3	176.8	168.6	105.9	.44	.31	.32	.23
20^0, 30^0 1 mr	281.3	180.8	168.6	105.1	.46	.32	.32	.23
45^0, 135^0 5 mr	124.3	75	[illegible]	[illegible]	[illegible]	[illegible]	[illegible]	.23

APPENDIX B

Draper Laboratory developed an extensive guidance simulation in support of the Cruise Ballistic Missile guidance study contract [illegible]. Bearing measurements to known landmarks were added to the simulation and the latter phase of the [illegible] trajectory was utilized to determine the performance of the [illegible] concept.

The work described in this Appendix was performed by Mr. [illegible] Landis.

Error models utilized for the simulation are described in the main section of this report.

The simulated landmarks are located 1 km off the flight path. Sightings are made when the landmark is 3, 2 and 1 km in front of the aircraft.

The rapid error growth after each measurement is due to the gravity anomaly model utilized and also due to large accelerometer errors.

Two sets of runs were completed utilizing 100 m landmark uncertainties and 10 meter landmark uncertainties. The differences between these two cases are slight, since the nav set errors grow rapidly and since the errors are only plotted at fixed time intervals (approximately 2 minutes after the measurement is made).

1. Overall Program Description

1.1 Introduction

This memorandum presents a fairly detailed mathematical description of the covariance simulation program used in the Cruise Ballistic [illegible] Study. The purpose of the program is a statistical analysis of the propagation of guidance system errors. The program assumes an error [illegible] model as a set of first-order linear time-varying differential [illegible] forced by white noise, together with linear noise corrupted [illegible]

Based on such a model, the main parts of [illegible] must be:

- Calculate [illegible] flight path.
- Propagate error-covariance matrix.
- Calculate measurement matrices for a given measurement [illegible] at selected times.
- Perform measurement update of error-covariance matrix assuming least-squares Kalman filter algorithm.
- Derive outputs of interest from error-covariance matrix.
- Iterate the above steps, according to a user-defined schedule.

Some of these steps contain rather weighty sub-steps; for example, the first requires a calculation of specific-force time history, [illegible] requires calculation of navigational reference locations in inertial space.

1.2 Program Inputs

The main input quantities to the program are the following:

- Trajectory time-history and related information (including coordinate systems in which data is given).
- Covariance matrix of guidance system initialization errors.
- Numerical values for parameters in the IMU error model (including instrument errors and gravity anomaly).
- Numerical values for parameters in the measurement model.
- User inputs describing the [illegible].
- User inputs describing the [illegible] time-step lengths, [illegible]).

1.3. Program Outputs

The program will print the position, velocity and [illegible] (RMS values) at various points along the trajectory, given in [illegible] local level, and flight-path coordinate frames.

1.4 Data Flow Diagrams

The architecture discussed in the preceding sections will now be illustrated by two diagrams. The first is a program-architecture schematic, shown in Figure 1.1.

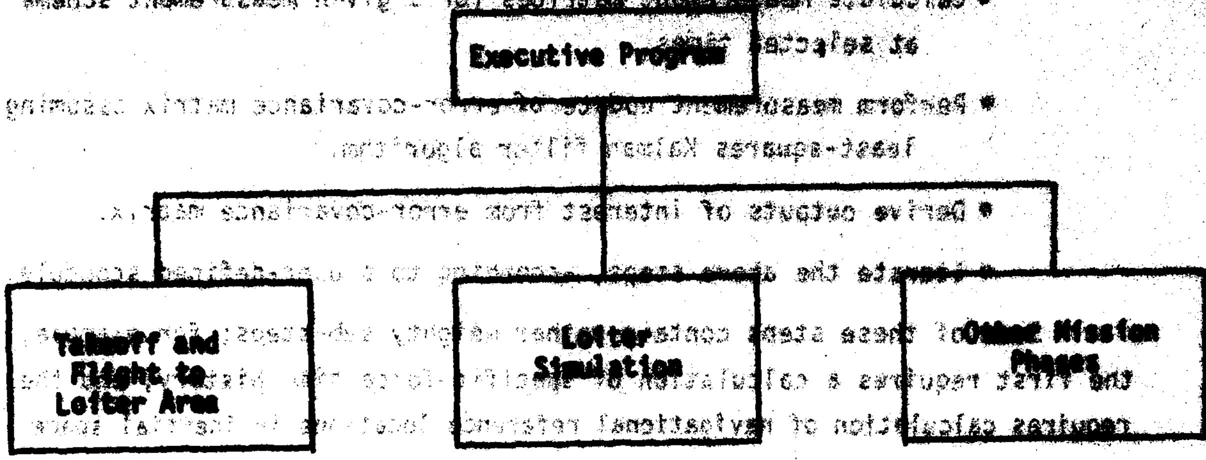

Figure 1.1. Architecture Schematic

An executive or bookkeeping program is shown. This program decides (from user inputs) on the order of phases, and sees to it that the various subroutines are executed in the corresponding order. It also allows for omitting a given phases. (This will occur, for instance, if a final-takeoff-covariance, stored on a file, is to replace a fresh takeoff-simulation). Any other bookkeeping related to the overall phasing structure of a mission will be included. The boxes in Figure 1.1 do not necessarily represent separate programs — generally the simulations will differ only in the trajectory calculations.

The second diagram illustrates the data-flow internal to any phase. It is shown in Figure 1.2.

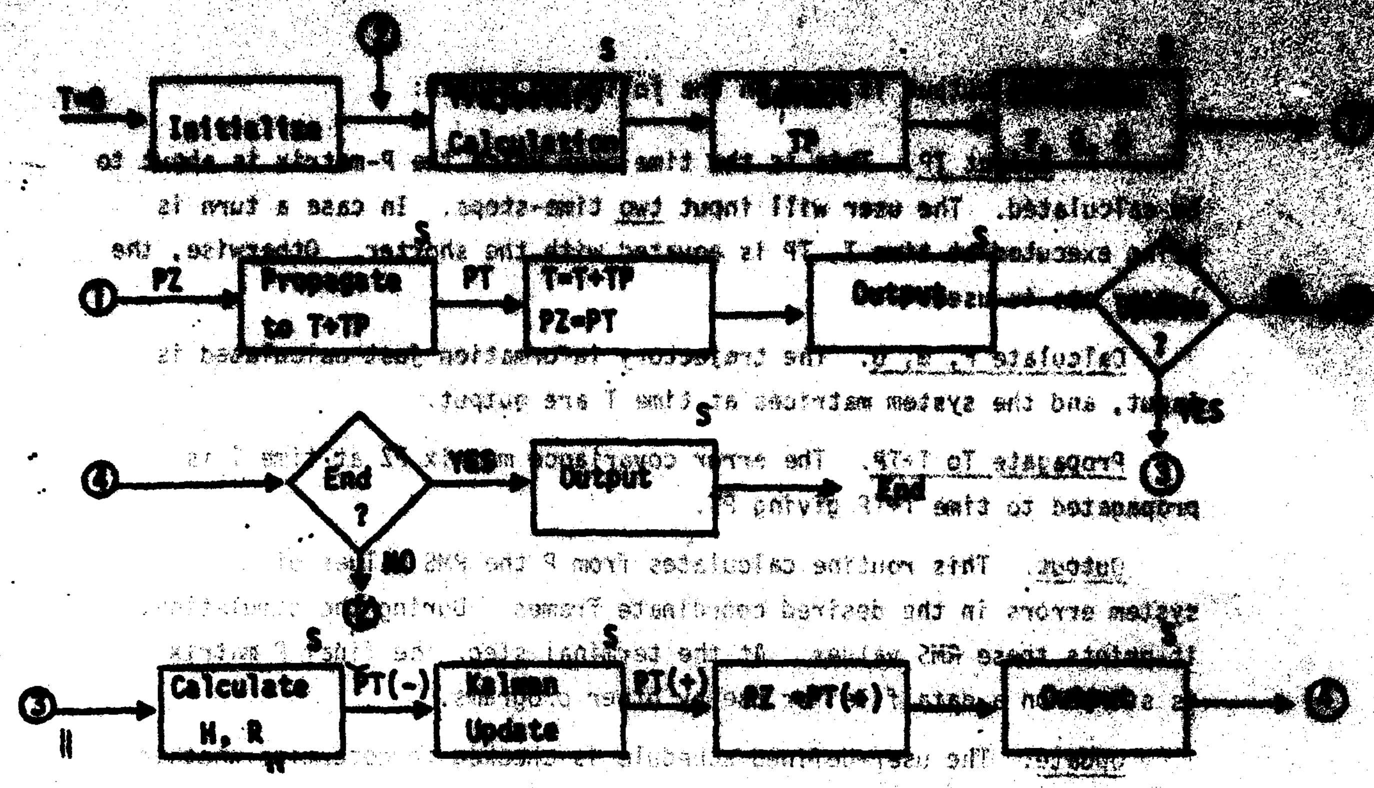

Figure 1.2. Data Flow Diagram

In Figure 1.2, each block with an "S" above it represents a separate subroutine. The other blocks represent operations in the program controlling the phase. The individual blocks will be briefly summarized.

Initialize. The user inputs are read, and, when necessary, logic in subroutines is initialized. The initial P matrix, P(0), is set up.

Trajectory Calculation. The main inputs are time and a flag to indicate phase. The outputs are:

- position, velocity, specific force in inertial space (frame as defined before)
- all the coordinate transformations required by the subroutines.
- a flag indicating whether a sharp turn is being executed.

The last output is seen in the following figure:

Select TP. This is the time over which the P-matrix is about to be calculated. The user will input two time-steps. In case a turn is being executed at time T, TP is equated with the shorter. Otherwise, the longer one is used.*

Calculate F, G, Q. The trajectory information just calculated is input, and the system matrices at time T are output.

Propagate To T+TP. The error covariance matrix PZ at time T is propagated to time T+TP giving PT.

Output. This routine calculates from P the RMS values of system errors in the desired coordinate frames. During the simulation, it prints these RMS values. At the terminal step, the final P matrix is stored on a data file for use by other programs.

Update. The user-defined schedule is checked to determine whether an update is to be performed and, if so, which type.

Calculate H, R. The inputs to this subroutine include time, location, and an indication of the type of measurement employed (e.g. star-tracker, landmark, bearing measurement, etc.). The outputs are the measurement matrices H and R. Intermediate calculations, such as position and velocity of landmarks in inertial space, must be made in order to calculate these outputs.

Kalman Update. The error covariance matrix PT is updated using a Kalman filter algorithm, giving the updated matrix PT(+). The system and measurement matrices are input.

It remains to give a mathematical description of what is involved in each of the steps just mentioned. This is the main concern of Section 2.

*The main motivation for this is the Sitting path, which combines line segments and rounded turns, the latter requiring more frequent recalculation of system matrices.

2. Mathematical Model

2.1 Introduction

The purpose of Section 2 is to present a mathematical model which describes the propagation of errors through the guidance system. Detailed equations are presented explicitly only for some components of the model, such as the system matrices. Many segments are handled more generally with references to other literature which provides the details. Also, several parts of the model are given only in preliminary form, and are to be refined (see Section 3).

The order of presentation of the model does not follow the flow of the logic in Figure 1.2. (Rather, the most natural mathematical order was chosen). Therefore, the following list of correlations between Figure 1.2 and the subsections of Section 2 will be helpful to the reader:

Initialize: Section 2.4.5
Trajectory Calculation: Section 2.5
Calculate F,G,Q: Section 2.4.3
Propagate to T+TP: Section 2.3
Output: Section 2.6
Calculate H,R: Section 2.4.4
Kalman Update: Section 2.3

Throughout this section, an error quantity is described as the computed (or observed) value minus the true value of the quantity. All of these errors are considered as random variables and, therefore, (since they are time-dependent) as stochastic processes.

2.2 Linear Error Model Equations

The basic assumption employed in this memorandum is that system errors can be represented mathematically in the form

$$\dot{\bar{x}}(t) = F(t)\,\bar{x}(t) + G(t)\bar{w}(t) \qquad t \geq t_0$$

$$\bar{z}(t_i) = H_i\,\bar{x}(t_i) + \bar{v}(t_i) \qquad i = 1, 2, \ldots$$

where

$\bar{x}(t)$ = n-dimensional state vector

$\bar{w}(t)$ = m-dimensional continuous white-noise forcing vector

$\bar{z}(t)$ = ℓ-dimensional measurement (or observation, or output) vector, available at certain discrete times $t_i \geq t_0$

$\bar{v}(t_i)$ = ℓ-dimensional measurement noise vector

$F(t)$, $G(t)$, and H_i are real matrices of appropriate dimensions.

The noise statistics associated with the above system are given by the following equations:

$$E[\bar{x}(t)] = E[\bar{w}(t)] = E[\bar{v}(t)] = \bar{0}$$

$$E[x^{\alpha}(t)w^{\beta}(t)] = 0 \qquad t \geq t_0$$

$$E[\bar{w}(t)\bar{w}'(\tau)] = Q\delta(t-\tau) \qquad t, \tau \geq t_0$$

$$E[w^{\alpha}(t)\; v^{\beta}(\tau)] = 0 \qquad t, \tau \geq t_0$$

$$E[\bar{v}(t_i)\;\bar{v}'(t_j)] = R_i\delta_{ij}$$

Note: x^{α} here denotes the α-th component of the vector $\bar{x}$.

This model is a natural one for inertial navigation systems. The main limitation it imposes is the following: the error source $\bar{y}_e(t)$ must be expressed as the output of a white-noise forced "shaping filter," i.e. in the form

$$\bar{y}_e(t) = H_e\bar{x}_e(t) + \bar{v}_e(t)$$

where

$$\dot{\bar{x}}_e(t) = F_e(t)\bar{x}_e(t) + G(t)\bar{w}_e(t)$$

where $\bar{v}_e(t)$ and $\bar{w}_e(t)$ are stationary continuous white-noise processes. In most cases, a model of this form arises naturally, but in others (the main example is gravity anomaly) another form of model (e.g. colored-noise forced) arises more naturally. In these latter cases, an approximating white-noise forced model must be derived.

2.3 Covariance Calculation (Propagate And Update P)

The covariance propagation method is based upon the following assumptions: the information about error states provided by external measurements is incorporated by means of a Kalman filter. This procedure allows for a calculation, in the navigation computer, of a running estimate $\hat{x}(T)$ of the error state vector $\bar{x}(t)$, which is used to correct the indications of position, velocity, and attitude provided by the inertial navigator. The actual equations used will not be repeated here; rather we refer to Chapter 4 of Applied Optimal Estimation ed. by A. Gelb (Ref. 2) particularly to the tables on Page 110 and 123.* Mention should be made of the fact that the Kalman-filter assumption is an idealization since such an algorithm would be too unwieldy for IMU computers. However, the assumption is warranted by the fact that the weighting of measurements is done in actual systems in a way which is intended to approach optimality within realistic computational constraints.

In studying the propagation of errors through the guidance system via covariance analysis, one is interested in the time evolution of the covariance of the estimation error defined by

$$\tilde{x}(t) = \hat{x}(t) - \bar{x}(t)$$

Let

$$P(t) = E[\tilde{x}(t)\tilde{x}'(t)] \quad t \geq t_0$$

* Note that in our model the dynamics are continuous but Kalman updates are discrete, so that both tables apply

Then it may be shown that between measurements P(t) is a solution of the Riccati differential equation

$$\dot{P}(t) = F(t)\,P(t) + P(t)F^{T}(t) + G(t)Q(t)G^{T}(t)$$

(Alternatively, the propogation of P(t) can be represented by in discrete form by

$$P(t+\Delta t) = \Phi\, P(t)\Phi' + QK$$

where a discretized form of the process is employed). The update of the covariance is given by

$$P(t_k+) = (I-K_kH_k)P(t_k-)(I-K_kH_k)' + K_kR_kK'_k$$

where K_k is the Kalman gain matrix. All of these calculations are presented in full detail in Ref. 2.

Of course, the calculation of P(t) using the equations presented above can only be accomplished if the system and measurement matrixes are known. These issues are addressed in Section 2.4.

2.4 Guidance Error Model Description

The preceding section discussed error covariance propagation in linear systems in general. The guidance subsystem error model (including the model for gravity anomalies which effect it) is a linear system of the form described in Section 2.2. Before the specific characteristics and dynamics of the guidance subsystem error model are described, it is convenient to introduce the coordinate frames in which the quantities of interest are defined

2.4.1 Coordinate Frames

In this section, the coordinate frames to be used by the program are described. The three axes of each of these frames form a right-handed set, and their origin is the center of the earth. Note that several of these frames are fixed in inertial space, and others are not. Most of these frames are described in Britting's book (Ref. 1). We will use two to designate the beginning of a mission.

(1). Inertial -Equatorial Frame (i-frame). This is the frame in which the trajectory position, velocity, and specific forces will be given, as well as ephemeris data for measurement beacons or landmarks and reflectors. x^i, y^i lie in the equatorial plane with x^i through the Greenwich meridian at t=0. The z^i axis points to the North Pole. The frame is inertial.

(2). Earth-Frame (e-frame). This frame coincides with the i-frame at t=0 but is fixed relative to the earth. Thus, it rotates about z^i at rate Ω^e.

(3). Geographic frame (n-frame). This frame has its axes aligned with north, east and down directions at the present location (time t) of the vehicle. It is a natural frame in which to express the rms output errors. This frame rotates with the earth and the vehicle.

(4). Flight-path* frame (t-frame). This frame is used to specify gravity models. The geographic frame is rotated about the z axis, so that the x axis points in the vehicle direction of flight. Thus, the x^t and y^t axes form an along/cross track reference system.

(5). Platform-frame (p-frame). This frame is a natural one for specifying the errors in inertial instruments. The axes are the output axes of the accelerometers, with the x^p, y^p axes parallel to the platform.

2.4.2 System State Vector

This section presents the physical meaning of the elements of the state vector $\bar{x}(t)$ in the linear error model equation. The basic form of the 62-dimensional vector is

$$\bar{x}'(t) = [\overline{\delta r}'(t)\ \overline{\delta v}'(t)\ \bar{\psi}'(t)\ \bar{d}'(t)\ \bar{a}'(t)\ \bar{x}_G'(t)\ \bar{x}_A'(t)\ \overline{\delta h}_{ref}'(t)]$$

In this equation, $\overline{\delta r}$ and $\overline{\delta v}$ are 3-dimensional position and velocity errors in the i-frame, and $\bar{\psi}$ is the 3-dimensional platform misalignment (attitude) error vector, coordinatized in the i-frame.

The following paragraphs describe gyro and accelerometer errors. These errors are modelled in accordance with, and use the notation of, Ref. 3.

*Also called the track frame, since it has along-track, cross-track and down axes.

The vector $\bar{d}(t)$ is the 30-dimensional gyro drift vector. It is here assumed that three gyros have their input axes aligned along the platform (p-frame) x, y and z axes respectively. The first 10 elements of $\bar{d}$ correspond to the x-gyro and are defined as follows:

$$d_1 = D_{BX} \quad \text{bias drift vector}$$

$$\left.\begin{aligned} d_2 &= D_{IX} \\ d_3 &= D_{OX} \\ d_4 &= D_{SX} \end{aligned}\right\} \quad \text{Unbalance Drift Error Coefficients}$$

$$\left.\begin{aligned} d_5 &= D_{IIX} \\ d_6 &= D_{OOX} \\ d_7 &= D_{SSX} \\ d_8 &= D_{IOX} \\ d_9 &= D_{OSX} \\ d_{10} &= D_{SIX} \end{aligned}\right\} \quad \text{Compliance Drift Error Coefficients}$$

(In these equations, the symbols I, O, and S refer the input-output-spin axes of the gyro). Similar definitions hold for d_{11} through d_{30} with all these drift biases assumed to be statistically independent.

The 15-dimensional vector $\bar{a}(t)$ represents the accelerometer errors. The input axes of the three accelerometers are along the platform X,Y,Z axes respectively. The first 4 elements of $\bar{a}(t)$ are defined as follows:

$$a_1 = K_X = \text{bias error}$$

$$a_2 = K_{IX} = \text{scale-factor error coefficient}$$

$$a_3 = K_{IIX} = \text{scale-factor non-linearity coefficient}$$

$$a_4 = K_{CAX} = \text{cross-axis non-linearity coefficient}$$

Elements 5 through 12 of $\bar{a}$ are similarly defined with reference to the Y and Z accelerometers. Elements 13 through 15 represent mounting misalignment errors as follows:

$a_{13} = \delta_{21}$

$a_{14} = \delta_{31}$

$a_{15} = \delta_{32}$

where δ_{ij} = misalignment angle from i-th to j-th axis.

The three dimensional vector $\bar{x}_G$ represents the gravity anomaly errors, refered to f-frame coordinates. Specifically

x_{G1} = along-track vertical deflection

x_{G2} = cross-track vertical deflection

x_{G3} = anomaly magnitude/g_N,

where g_N = average surface gravity. (The scaling of the latter by g is merely a convenience).

The remaining states refer to the altitude damping based on altimeter measurements. Third order damping is assumed (as in Ref. 4), and this gives rise to three damping states, one for each i-frame axis. The three-dimensional vector $\bar{x}_A(t)$ represents these states. (The δa notation of Ref. 4 is not used to avoid confusion with accelerometer errors). The two-dimensional vector $\delta\bar{h}_{ref}$ represents altimeter errors, and is defined as

$\delta h_{ref\ 1}$ = 1st order Markov error

$\delta h_{ref\ 2}$ = bias error

This completes the description of the error-state vector.

2.4.3 System Matrices (F, G, Q)

The system matrices describe the fundamental error dynamics of the IMU. The matrices defined here are based on three sources of information:

Space-stable IMU dynamics (Ref. 1)

Third-order altitude damping (Ref. 4)

Inertial-instrument error models (Ref. 3)

The reader of this memorandum desiring detailed interpretation of the system matrices should refer to these sources.

The dynamics matrix F(t) has dimension 62 by 62, in accordance with the dimension of the error-state vector $\tilde{x}(t)$. F(t) is presented in partitioned form as:

$$F(t) = \left[\begin{array}{cccccccc}
F_{1,1}(t) & I_3 & 0_{3x3} & 0_{3x30} & 0_{3x15} & 0_{3x3} & 0_{3x3} & F_{1,8}(t) \\
F_{2,1}(t) & 0_{3x3} & F_{2,3}(t) & 0_{3x30} & F_{2,5}(t) & F_{2,6}(t) & F_{2,7}(t) & F_{2,8}(t) \\
0_{3x3} & 0_{3x3} & 0_{3x3} & F_{3,4}(t) & 0_{3x15} & 0_{3x3} & 0_{3x3} & 0_{3x2} \\
\multicolumn{8}{c}{\longleftarrow\!\!-\!-\!-\!-\;0_{45x62}\;-\!-\!-\!-\!\!\longrightarrow} \\
\multicolumn{5}{c}{\longleftarrow\!\!-\!-\;0_{3x54}\;-\!-\!\!\longrightarrow} & F_{6,6}(t) & 0_{3x3} & 0_{3x2} \\
F_{7,1}(t) & \multicolumn{6}{c}{\longleftarrow\!\!-\!-\;0_{3x57}\;-\!-\!\!\longrightarrow} & F_{7,8}(t) \\
\multicolumn{7}{c}{\longleftarrow\!\!-\!-\;0_{2x60}\;-\!-\!\!\longrightarrow} & F_{8,8}(t)
\end{array} \right]$$

where

I_3 = 3 by 3 identity

0_{ixj} = i by j matrix of 0's

The sub-matrices $F_{i,j}(t)$ are now defined. $F_{1,1}(t)$ is 3 by 3 related to altitude damping. Let

$$\bar{u}_R = \frac{\bar{R}^i(t)}{|\bar{R}^i(t)|}$$

$$U = \bar{u}_R \, \bar{u}_R'$$

where $\bar{R}^i(t)$ is i-frame position. (These quantities will be used frequently in subsequent equations). Then

$$F_{1,1}(t) = -k_1 U.$$

where k_1 is a damping coefficient. $F_{1,8}(t)$ is 3 by 2, representing the effect of altimeter errors. The definition is

$$F_{1,8}(t) = k_1[\bar{u}_R : \bar{u}_R].$$

(The colon signifies justaposition of matrices).

$F_{2,1}(t)$ is 3 by 3, and is defined as

$$F_{2,1}(t) = F^S_{2,1}(t) + F^D_{2,1}(t)$$

$F^S_{2,1}(t)$ reflects Schuler dynamics, and is

$$F^S_{2,1}(t) = \frac{3\omega^2{}_s(t)}{|\bar{R}^i(t)|^2} \bar{R}^i(t)\bar{R}^{i\prime}(t) - \omega^2{}_s(t) I_3$$

where $\omega_s(t)$ is the Schuler frequency:

$$\omega^2{}_s(t) = \frac{C_g}{|\bar{R}^i(t)|^3}$$

$$C_g = 4.84814\text{x}10^{-6} \text{ rad/sec}$$

$F^D_{2,1}$ (t) reflects altitude damping and is defined

$$F^D_{2,1}(t) = -k_2 U$$

where k_2 is a damping coefficient.

The $F_{2,3}(t)$ matrix is 3 by 3, and models the error in indicated acceleration caused by platform alignment errors. We designate by $\bar{f}^i(t)$ the specific force acting on the instruments. Then

$$F_{2,3}(t) = \begin{bmatrix} 0 & -f^i_3(t) & f^i_2(t) \\ f^i_3(t) & 0 & -f^i_1(t) \\ -f^i_2(t) & f^i_1(t) & 0 \end{bmatrix}$$

The matrix $F_{2,5}(t)$ is 3 by 15. This matrix models the acceleration indication errors (bias, g-sensitive, etc). (For further explanation, see Ref. 3). To describe this matrix, we let

$$\bar{f}^p(t) = C^p_i \, \bar{f}^i \, (t)$$

where C^p_i is the transformation from the i to the p frame. (This will be a program input representing nominal platform orientation). Then dropping the t's for convenience:

$$F_{2,5}(t) = C^i_p \begin{bmatrix} 1 & f^p_1 & (f^p_1)^2 & (f^p_2)^2 + (f^p_3)^2 \\ 0 & 0 & 0 & 0 \\ 0 & 0 & 0 & 0 \end{bmatrix}$$

$$\begin{matrix} 0 & 0 & 0 & 0 & 0 & 0 & 0 \\ 1 & f^p_2 & (f^p_2)^2 & (f^p_1)^2 + (f^p_3)^2 & 0 & 0 & 0 \\ 0 & 0 & 0 & 0 & 1 & f^p_3 & (f^p_3)^2 \end{matrix}$$

$$\begin{matrix} 0 & & f_1^p & 0 & 0 \\ (f_1^p)^2+(f_2^p)^2 & 0 & f_1^p & f_2^p & \end{matrix}\Bigg]$$

The matrix $F_{2,6}(t)$ reflects the effect of gravity anomaly on system errors. It is given by:

$$F_{2,6}(t) = g_N \, C_t^i$$

where g_N is average gravity at sea-level. Note that the t to i transformation is time-varying. It will be provided by trajectory calculations.

$F_{2,7}(t)$ is 3 by 3, and is part of the altitude damping dynamics. It is simply

$$F_{2,7}(t) = -I_{3x3}$$

$F_{2,8}(t)$ is 2 by 3, reflecting the effect of altimeter errors. It is defined by

$$F_{2,8}(t) = k_2[\bar{u}_R \,:\, \bar{u}_R]$$

where k_2 is a damping coefficient.

[illegible] in Ref. 3). To describe [illegible] coordinates in the [illegible]

$$f^{G1} = \begin{bmatrix} 1 & 0 & 0 \\ 0 & -1 & 0 \\ 0 & 0 & [illegible] \end{bmatrix} f^P$$

$$f^{G2} = \begin{bmatrix} 0 & 1 & 0 \\ 0 & 0 & -1 \\ -1 & 0 & 0 \end{bmatrix} f^P \qquad f^{G3} = \begin{bmatrix} 0 & [illegible] & [illegible] \\ -1 & 0 & 0 \\ 0 & -1 & 0 \end{bmatrix} f^P$$

In these equations f^P is defined as earlier in this section. Then,

$$F_{3,4} = C_p^i \begin{bmatrix} F_{G1} & 0 & 0 \\ 0 & F_{G2} & 0 \\ 0 & 0 & F_{G3} \end{bmatrix}$$

in which the F_{Gi}'s and 0's are all 1 by 10 matrices, and for i=1,2,3

$$F_{Gi} = [1 \quad f_1^{Gi} \quad f_2^{Gi} \quad f_3^{Gi} \quad (f_1^{Gi})^2 \quad (f_2^{Gi})^2 \quad (f_3^{Gi})^2 \quad f_1^{Gi} f_2^{Gi} \quad f_2^{Gi} f_3^{Gi} \quad f_1^{Gi} f_3^{Gi}]$$

We note that rows 10 through 54 of the F(t) matrix are composed entirely of 0's. This reflects the fact that all of the instrument error coefficients are treated as random constants-that is, in the absence of an external update, they do not deviate from their original (t=0) values.

The $F_{6,6}$ matrix is 3 by 3 and [illegible] [illegible] (already [illegible]) [illegible]. It therefore applies principally to the latter [illegible] [illegible] of this Appendix). The form of this matrix is [illegible]

$$F_{6,6}(t) = \begin{bmatrix} -\beta_{GRAV} & 0 & 0 \\ 0 & -\beta_{GRAV} & 0 \\ 0 & 0 & -\beta_{GRAV} \end{bmatrix}$$

Here β_{GRAV} is the inverse correlation-time of the model, which is calculated by

$$\beta_{GRAV} = \frac{V_g}{D_g},$$

with V_g = ground speed, D_g = characteristic distance of gravity anomaly field.

$F_{7,1}(t)$ is 3 by 3 and is another altitude damping term. It is

$$F_{7,1}(t) = k_3 \, U$$

where k_3 is a damping coefficient.

$F_{7,8}(t)$ is 3 by 2, reflecting effect of altimeter errors. Its definition is

$$F_{7,8}(t) = -k_3[\bar{u}_R \; \vdots \; \bar{u}_R]$$

$F_{8,8}(t)$ is 2 by 2, and provides the altimeter error model. It's definition is

$$F_{8,8}(t) = \begin{bmatrix} -\beta_{ALT} & 0 \\ 0 & 0 \end{bmatrix}$$

where β_{ALT} is the Markov time-constant.

The white-noise spectral density matrix $Q(t)$ is 4 by 4 diagonal. Define

$$q_{11} = q_{22} = 2\beta_{GRAV}\,\sigma_{VD}^2$$

$$q_{33} = 2\beta_{GRAV}(\sigma_{ANOM}/g_N)^2$$

where β_{GRAV} is defined above ($F_{6,6}(t)$), and σ_{VD} is the vertical deflection standard deviation and σ_{ANOM} is the anomaly (magnitude) standard deviation.* Define

$$q_{44} = 2\beta_{ALT}\,\sigma_{ALT-M}^2$$

where β_{ALT} is the time constant of the altimeter Markov error, and σ_{ALT-M} is the standard deviation of this same error.

The G matrix is 62 by 4, and inputs the white driving noise into the gravity and altimeter error models. It is defined as follows:

$$\begin{bmatrix} 0_{54\times4} \\ I_3 \;\vdots\; 0_{3\times1} \\ 0_{3\times4} \\ [0 \;\; 0 \;\; 0 \;\; 1] \\ [0 \;\; 0 \;\; 0 \;\; 0] \end{bmatrix}$$

This completes the description of all of the error model system matrices. It is to be noted that the variables used in computing these matrices are:

- Numerical parameters for instrument and gravitational error models;
- Position and specific force in inertial space.
- Coordinate transformation matrices.

These values are all available from the program, the first group from user input and the others from the trajectory calculations.

---

*Units: σ_{VD} angular, σ_{ANOM} acceleration.

2.4.4 Measurement Matrices (H,R)

The CBM program utilizes two fundamental classes of external updates. For the tactical application a bearing measurement to know landmarks has been added to the CBM program. We note that the calculations require the following inputs:

- Position and velocity in i-frame
- Time into mission, to calculate i-frame location of land stations
- Standard deviation of update-station ephemeris errors.

2.4.5 Initial Covariance Matrix

In solving the Ricatti differential equation (Section 2.3.1) for P(t) a value of P(0) is required. This represents the covariance matrix of errors states prior to takeoff.*

However, the P(0) is itself a result of the errors in complex initial calibration and alignment procedure. The actual P(0) matrix will depend heavily on the particular mechanization of this procedure, on the time alloted to the procedure, and other factors. At the time of this writing, study in this area is still in progress. This section presents a simplified model, based on the assumption of uncorrelated error-states.**

P(0) is assumed diagonal, with P_i denoting the i-th diagonal element. The first 9 of these are

$$P_i = 0 \quad i=1 \text{ through } 6$$

$$P_i = [\sigma(\psi_0)]^2 \quad i = 7,8,9$$

where $\sigma(\psi_0)$ is the rms initial alignment error per axis. The next 30 terms are defined in terms of standard deviations of the gyro errors d_i, i=1,2,...30 listed in Section 2.4.2. It is assumed that these standard deviations are the same for all three gyroscopes, so that only ten standard deviations,

---

* The value of P(t) at the beginning of the loiter and phase is simply the terminal value from the preceding phase.

**For a gimbal-memory alignment system this assumption is fairly realistic.

$\sigma(d_i)$, i=1,2,...10 are input. For example, $\sigma(d_5)$ is the common standard deviation of the compliance drift error coefficient D_{II} for the three gyroscopes. Then define

$$P_{9+i} = P_{19+i} = P_{29+i} = [\sigma(d_i)]^2,$$

$$i = 1,2,\ldots,10$$

The next 15 diagonal elements represent accelerometer errors. The accelerometer standard deviations are given as $\sigma(a_i)$, i=1,2,3,4 and $\sigma(\delta)$, where δ is the mounting error misalignment. Then define

$$P_{39+i} = P_{43+i} = P_{47+i} = [\sigma(a_i)]^2,$$

$$i = 1,2,3,4$$

$$P_{52} = P_{53} = P_{54} = [\sigma(\delta)]^2.$$

The next three (gravity anomalies) are

$$P_{55} = P_{56} = \sigma_{VD}^2$$

$$P_{57} = (\sigma_{ANOM}/g_N)^2$$

σ_{VD} = standard deviation of vertical deflection

σ_{ANOM} = standard deviation of gravity anomaly

g_N = nominal gravity

Corresponding to the damping states,

$$P_{58} = P_{59} = P_{60} = 0$$

Finally, the altimeter errors are initialized by

$$P_{61} = \sigma_{ALT-M}^2$$

$$P_{62} = \sigma_{ALT-C}^2$$

This completes the description of the initial P matrix.

2.5 Trajectory Calculations

Many of the calculations in the other sections (particularly 2.4.3, 2.4.4, and 2.4.6) require current trajectory-related information. The list of required data, at any given time t, is:

$\bar{R}^i$ = i-frame position

$\bar{V}^i$ = i-frame velocity

$\bar{f}^i$ = i-frame specific force

V_g = ground speed

C_n^i, C_t^i = direction cosine-matrices

The equations for calculating these are not reproduced here. Obviously they will be different for the several phases of a mission.

The loiter-phase trajectory includes some segments with sharp turns, where system-dynamics vary, and some long straight segments, where they are stable. Therefore a flag will be output to indicate, for the given time, which of these segment types the missile is located on. Such a flag will not be required for the other phases.

2.6 Output Calculations

There are two classes of output of interest. The first is the standard deviation of major IMU errors, presented as a function of time. The second is the complete covariance matrix at the end of the phase, which is to be used to initialize the succeeding phase.

The IMU errors of interest are position, velocity and alignment errors coordinatized in the i and n-frames. (Velocity is with respect to inertial space, regardless of the frame it is coordinatized in). Partition the P matrix at time T as

$$P(t) = \begin{bmatrix} P_R & - & - \\ - & P_V & - \\ - & - & P_\psi \end{bmatrix}.$$

in which all the sub-matrices are 3x3, and the spaces are not of interest here. Then

$$\sigma(\delta r_\alpha^i) = P_R(\alpha,\alpha) \ , \ \alpha=1,2,3$$

$$\sigma(\delta V_\alpha^i) = P_V(\alpha,\alpha) \ , \ \alpha=1,2,3$$

$$\sigma(\psi_\alpha^i) = P_\psi(\alpha,\alpha) \ , \ \alpha=1,2,3$$

where $\overline{\delta r}^i$, $\overline{\delta V}^i$, $\overline{\psi}^i$ are i-frame IMU errors. Next calculate

$$P_R^n = C_i^n P_R C_n^i$$

$$P_V^n = C_i^n P_V C_n^i$$

$$P_\psi^n = C_i^n P_\psi C_n^i$$

Then the n-frame outputs may be calculated from these matrices just as in the case of the i-frame outputs. Both sets of standard deviations may be calculated continously in time from the current P(t) matrix.

The second output is simply the entire P matrix at the end of a phase, and requires no further discussion.

References

1. Britting, K., Inertial Navigation Systems Analysis, Wiley Interscience, 1971.

2. Gelb, A., ed. Applied Optimal Estimation, M.I.T. Press, 1974.

3. Sciegienny, J., "CBM Space-Stabilized IMU Error Model," CSDL Interlab Memorandum JS-15C-002-81, Feb. 1981

4. Widnall, William S. and Peter A. Grundy, Inertial Navigation System Error Models, Intermetrics TR-03-73, Intermetrics Incorporated, 11 May 1973.

AD-A119 700 CHARLES STARK DRAPER LAB INC CAMBRIDGE MA F/G 17/7
LOW ALTITUDE NAVIGATION AUGMENTATION SYSTEM.(U)
DEC 81 D A KOSO F33615-80-C-1209
UNCLASSIFIED CSDL-R-1526 AFWAL-TR-81-1222 NL

2 2

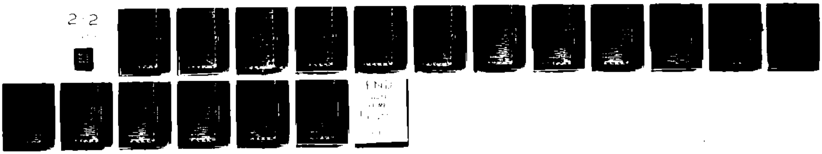

LOITER PHASE

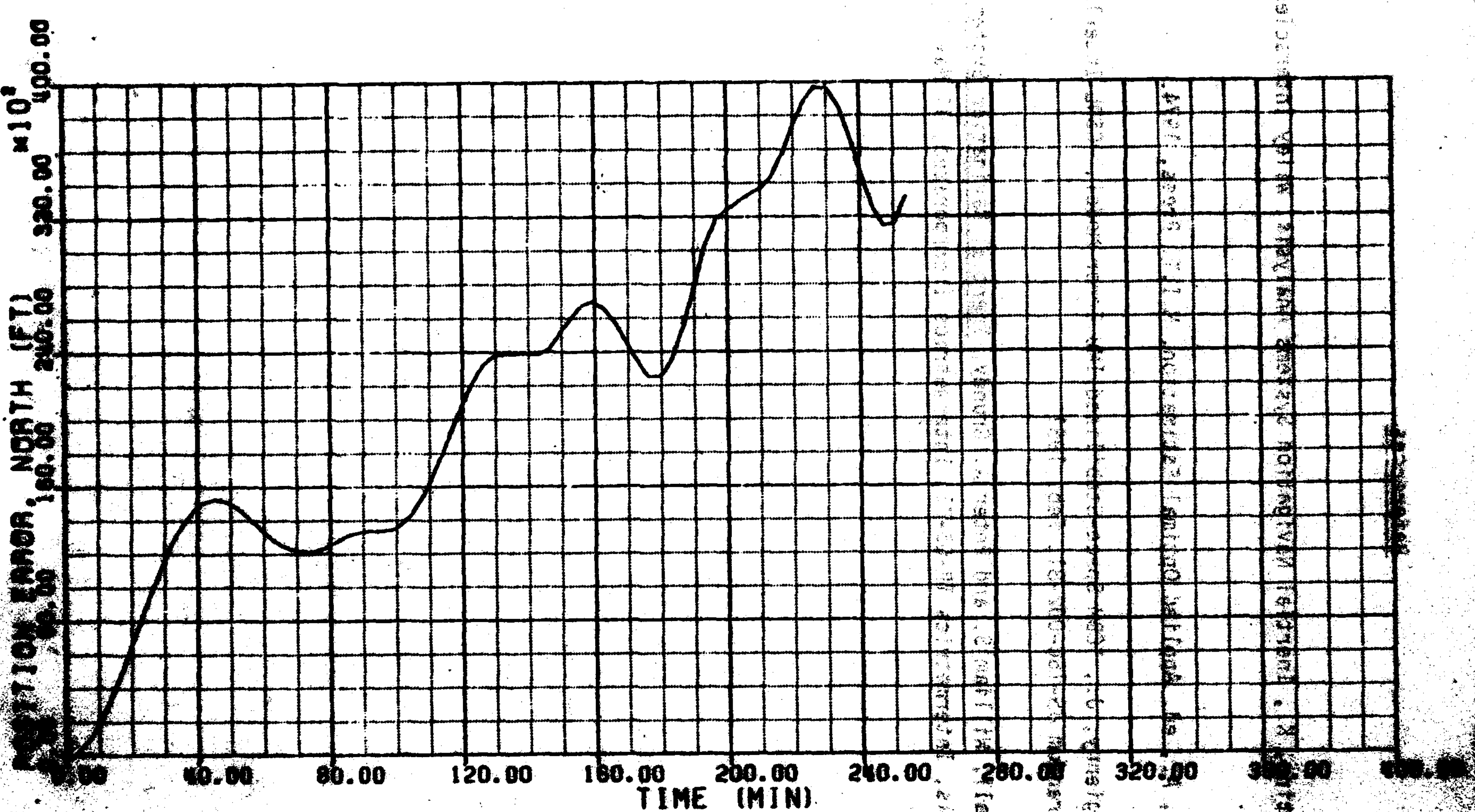

NO UPDATE

LØITER PHASE

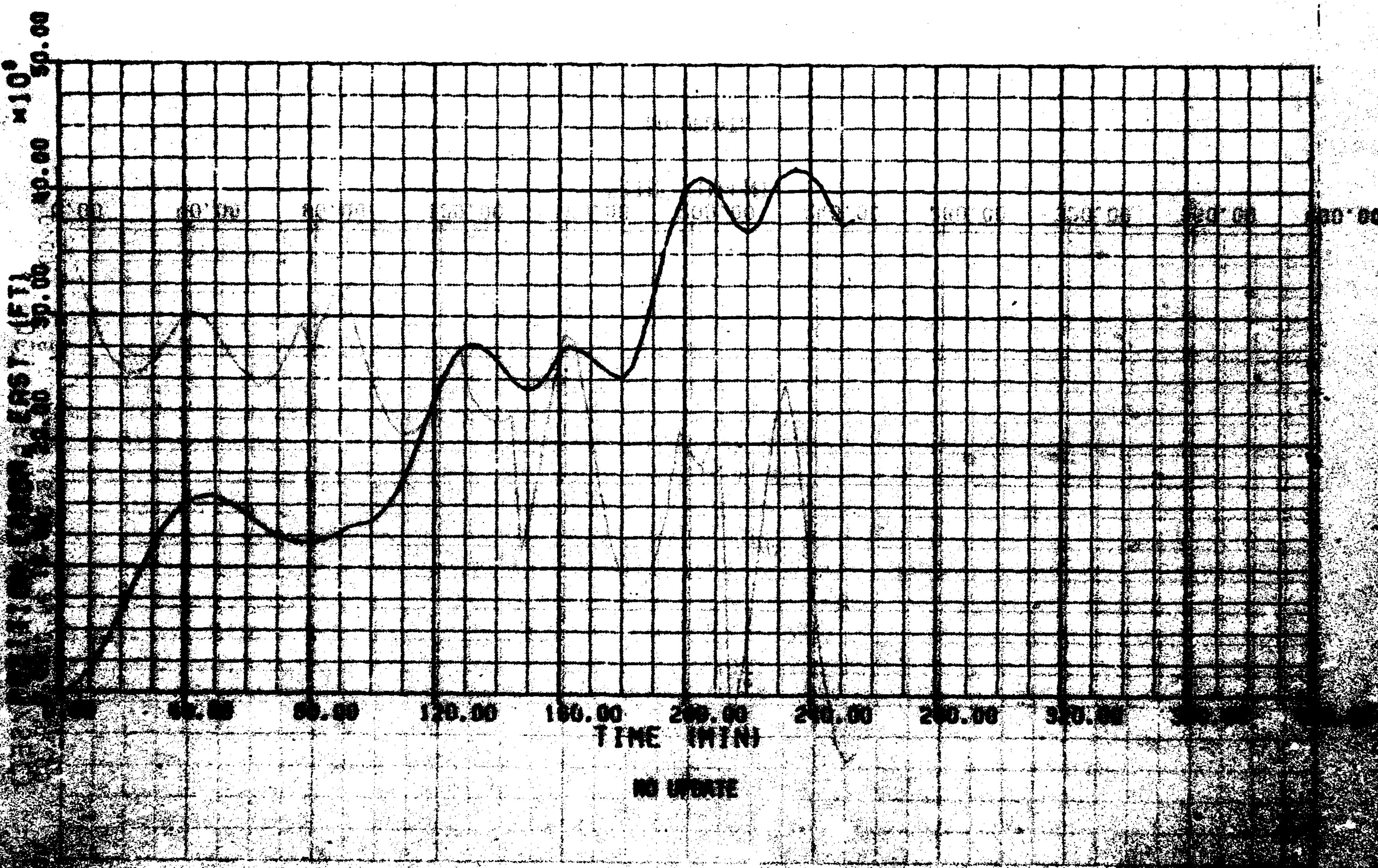

LØITER PHASE

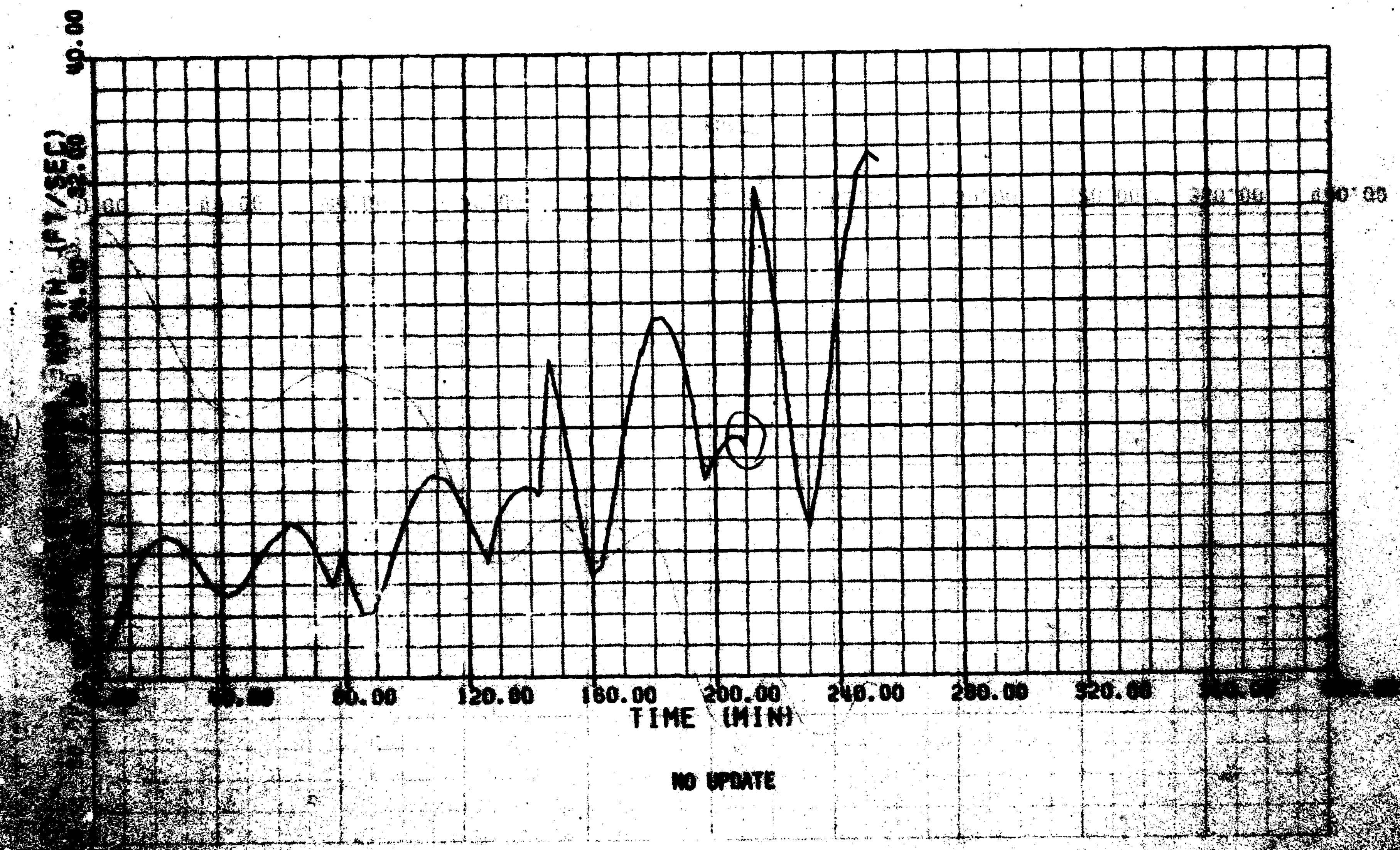

NO UPDATE

LØITER PHASE

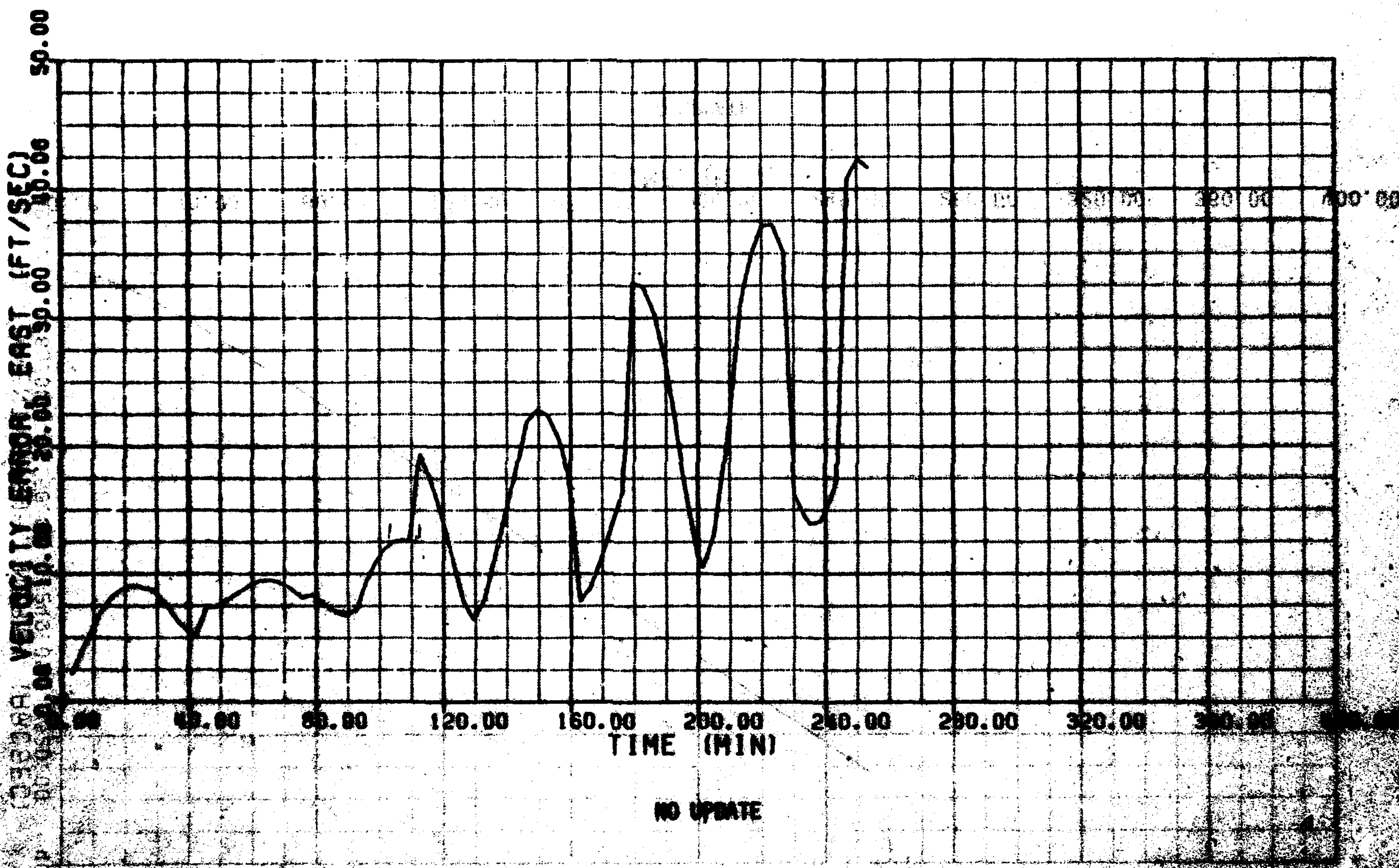

LØITER PHASE

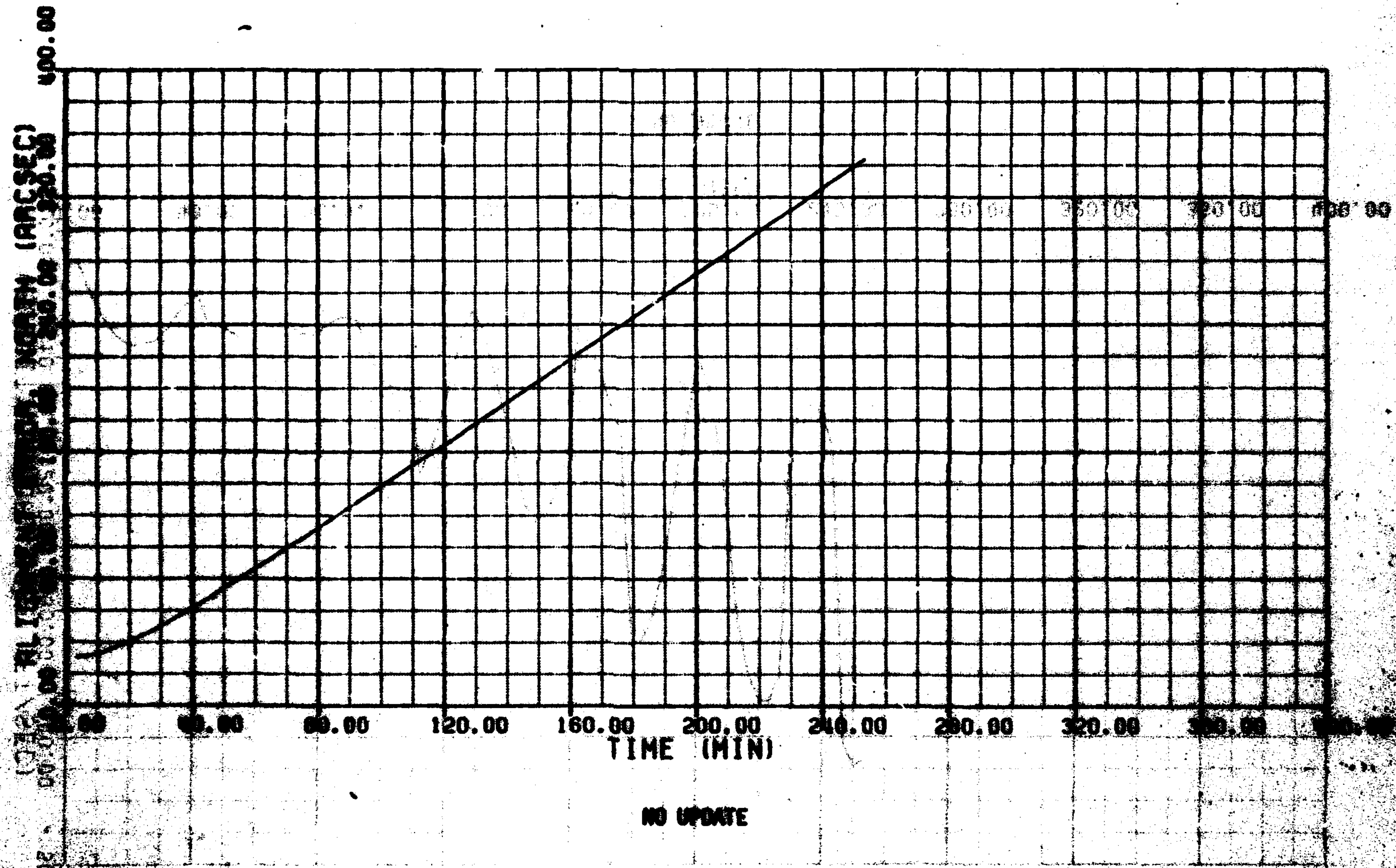

LØITER PHASE

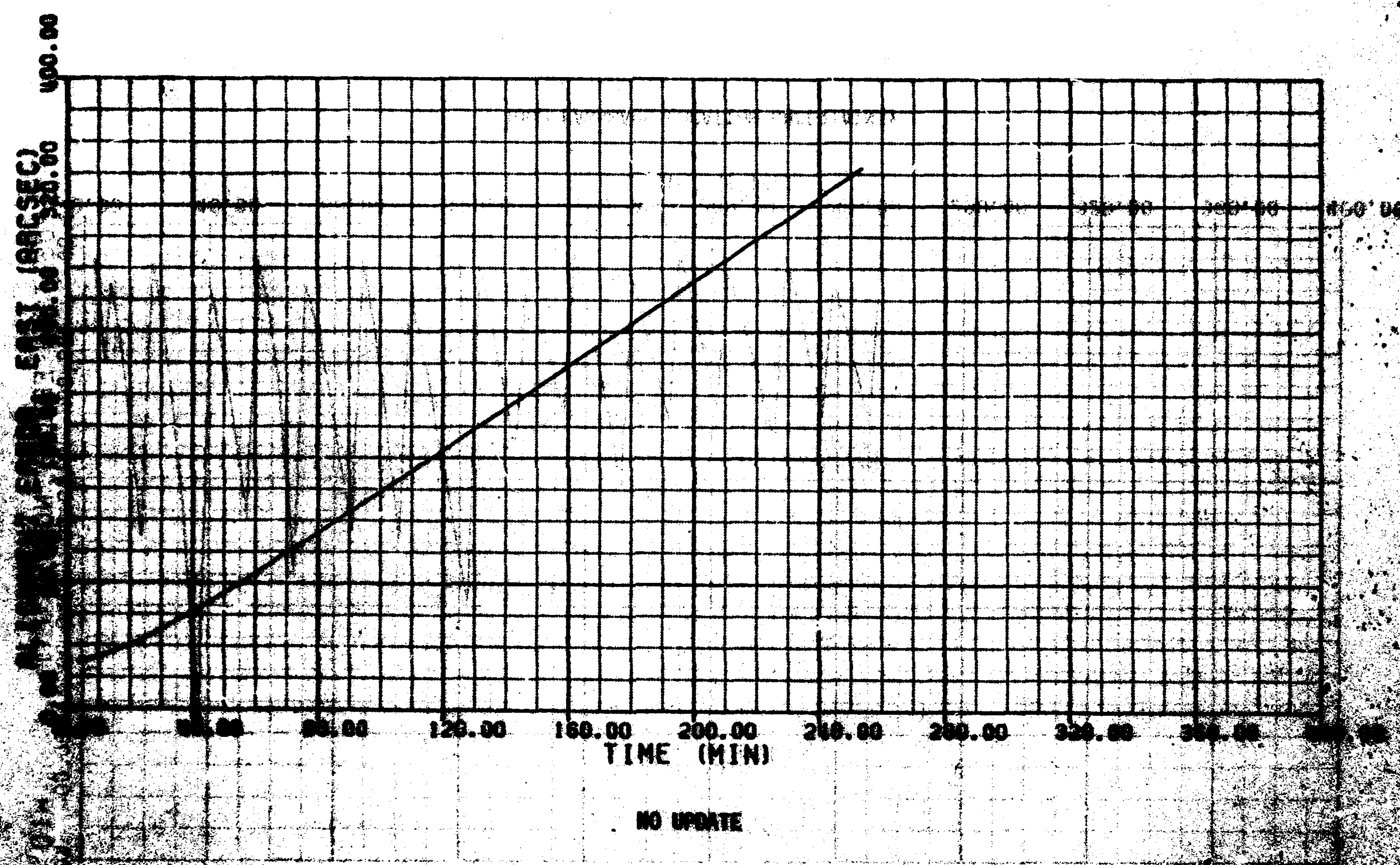

LØITER PHASE

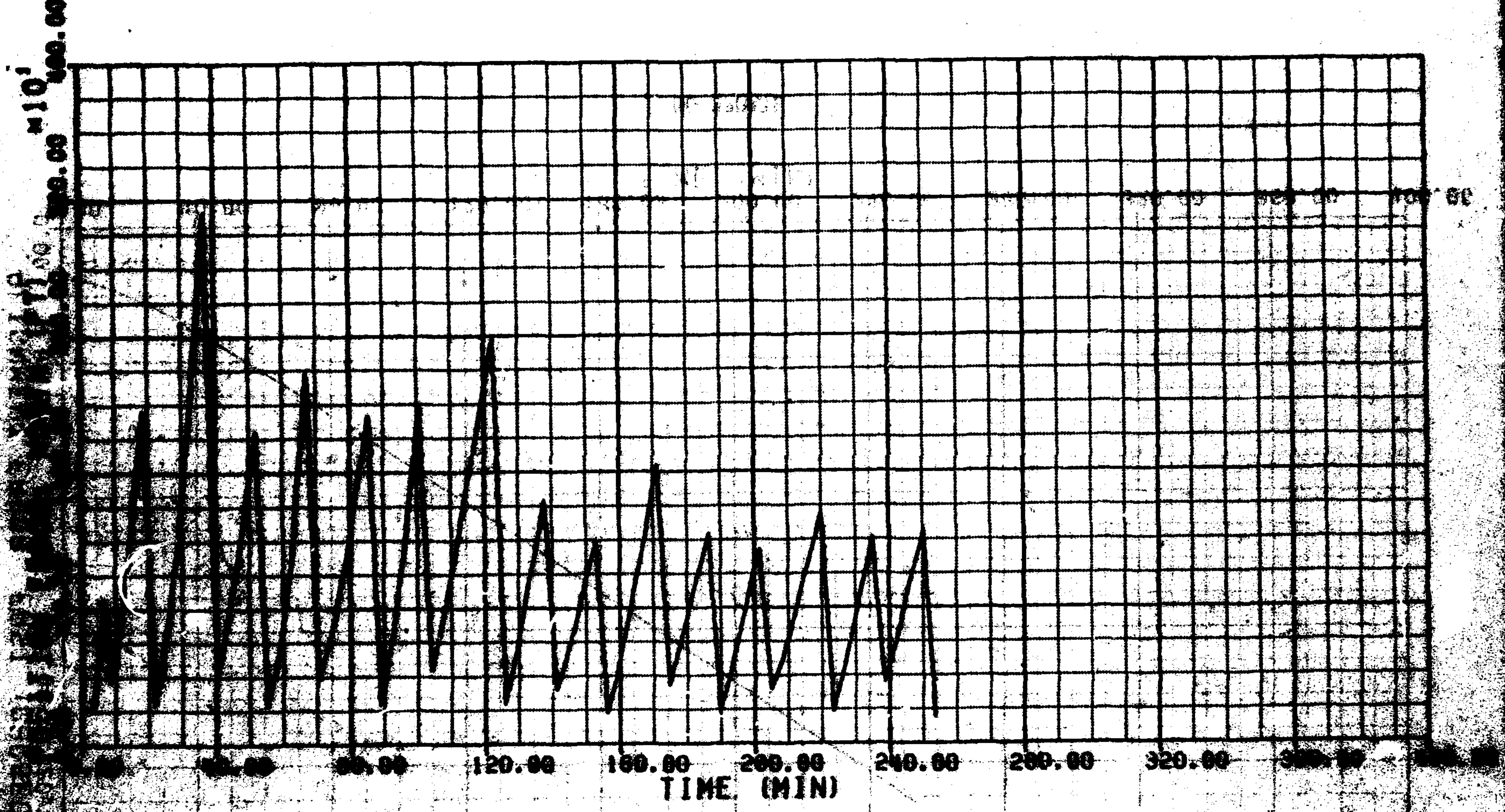

100M LANDMARK LOCATION UNCERTAINTY

LOITER PHASE

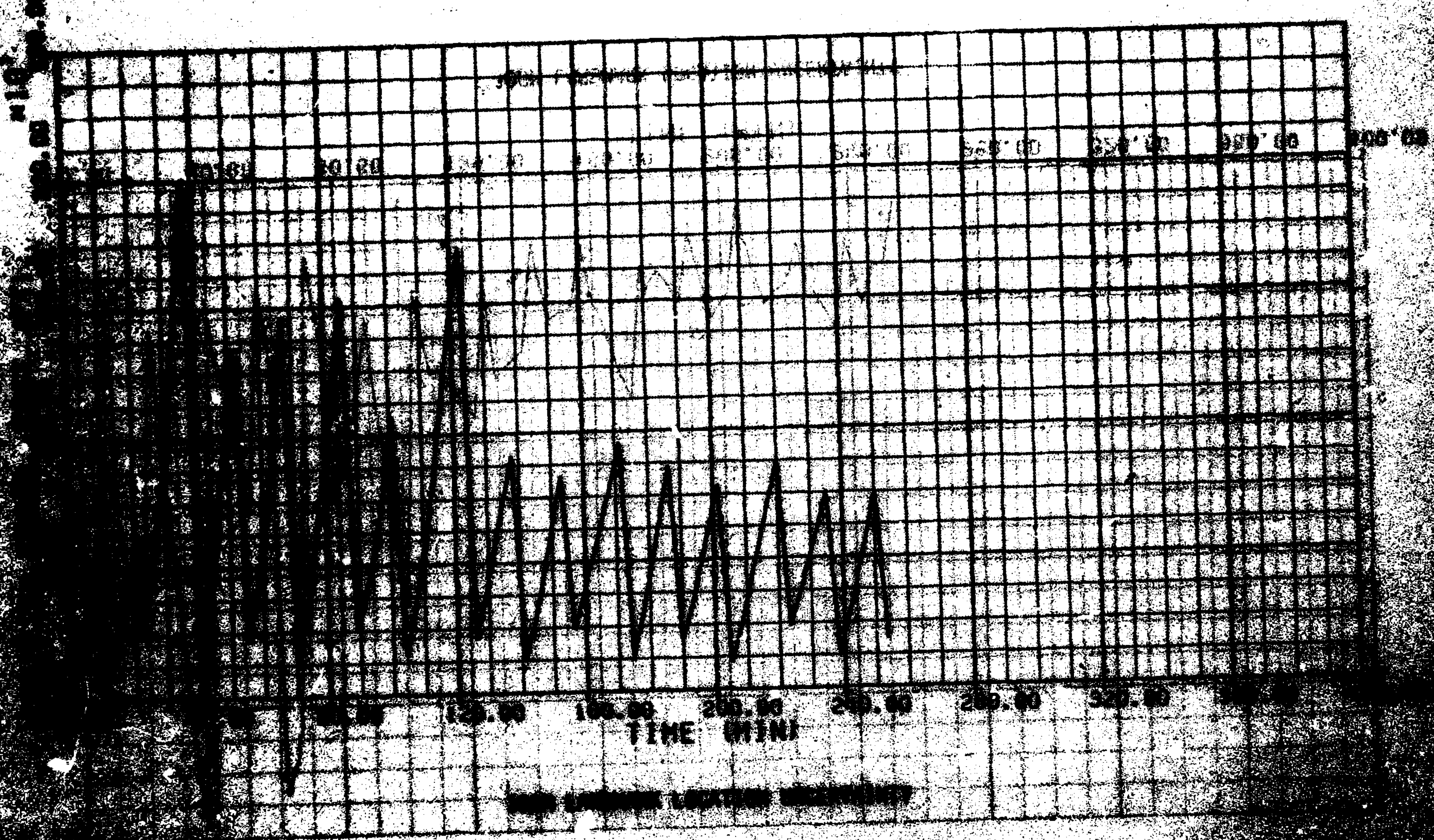

LØITER PHASE

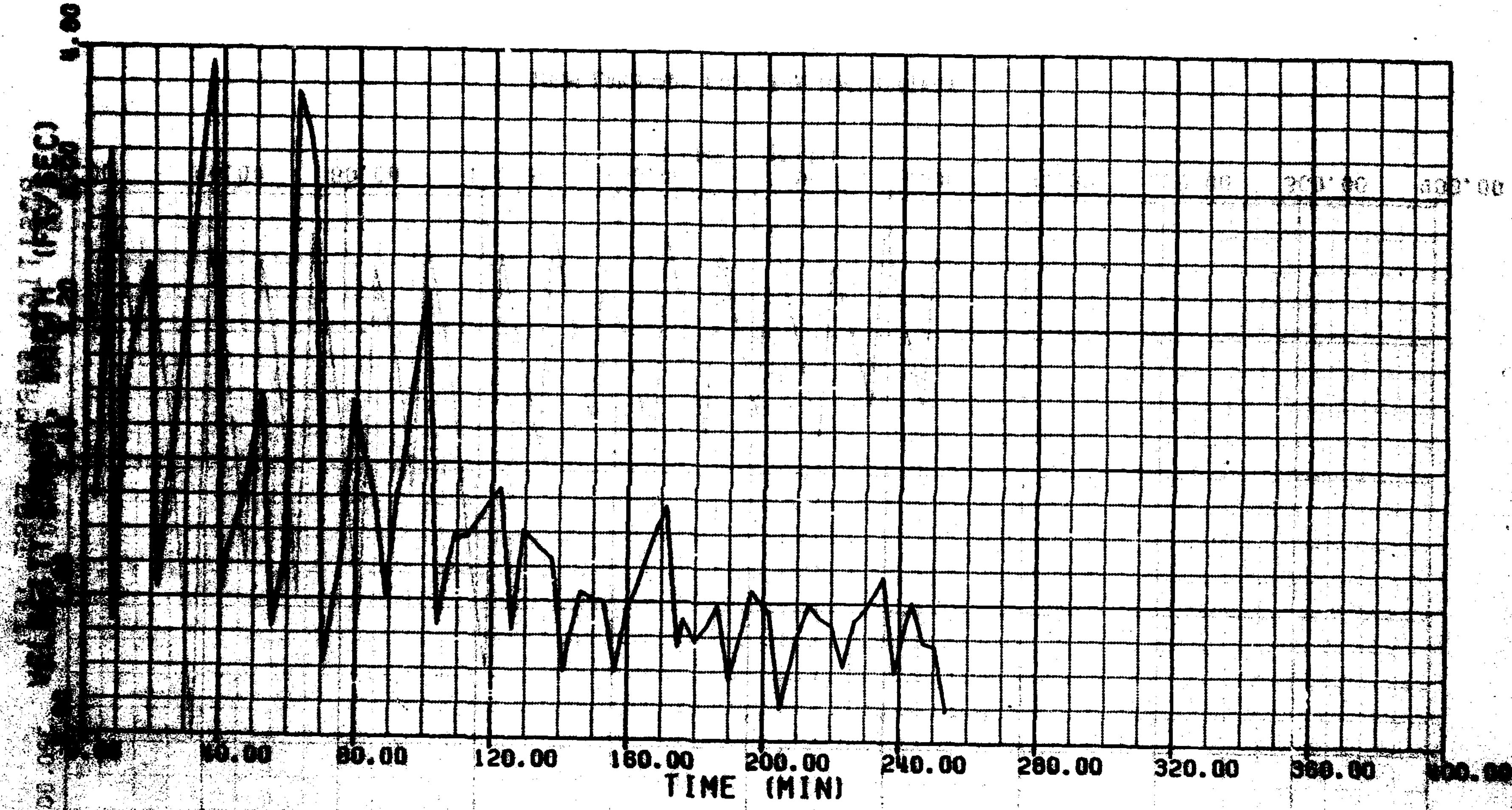

100M LANDMARK LOCATION UNCERTAINTY

LØITER PHASE

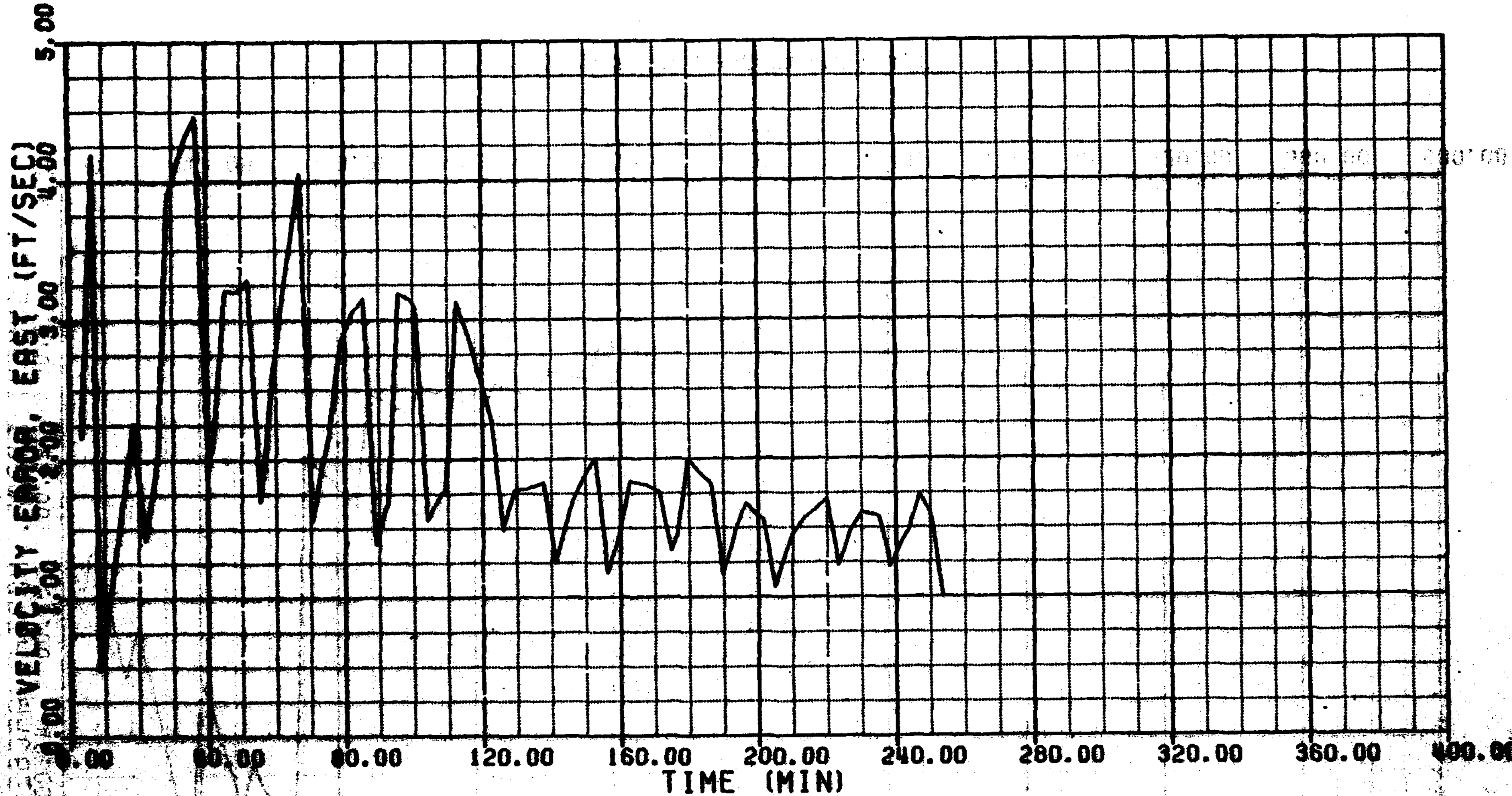

100M LANDMARK LOCATION UNCERTAINTY

LØITER PHASE

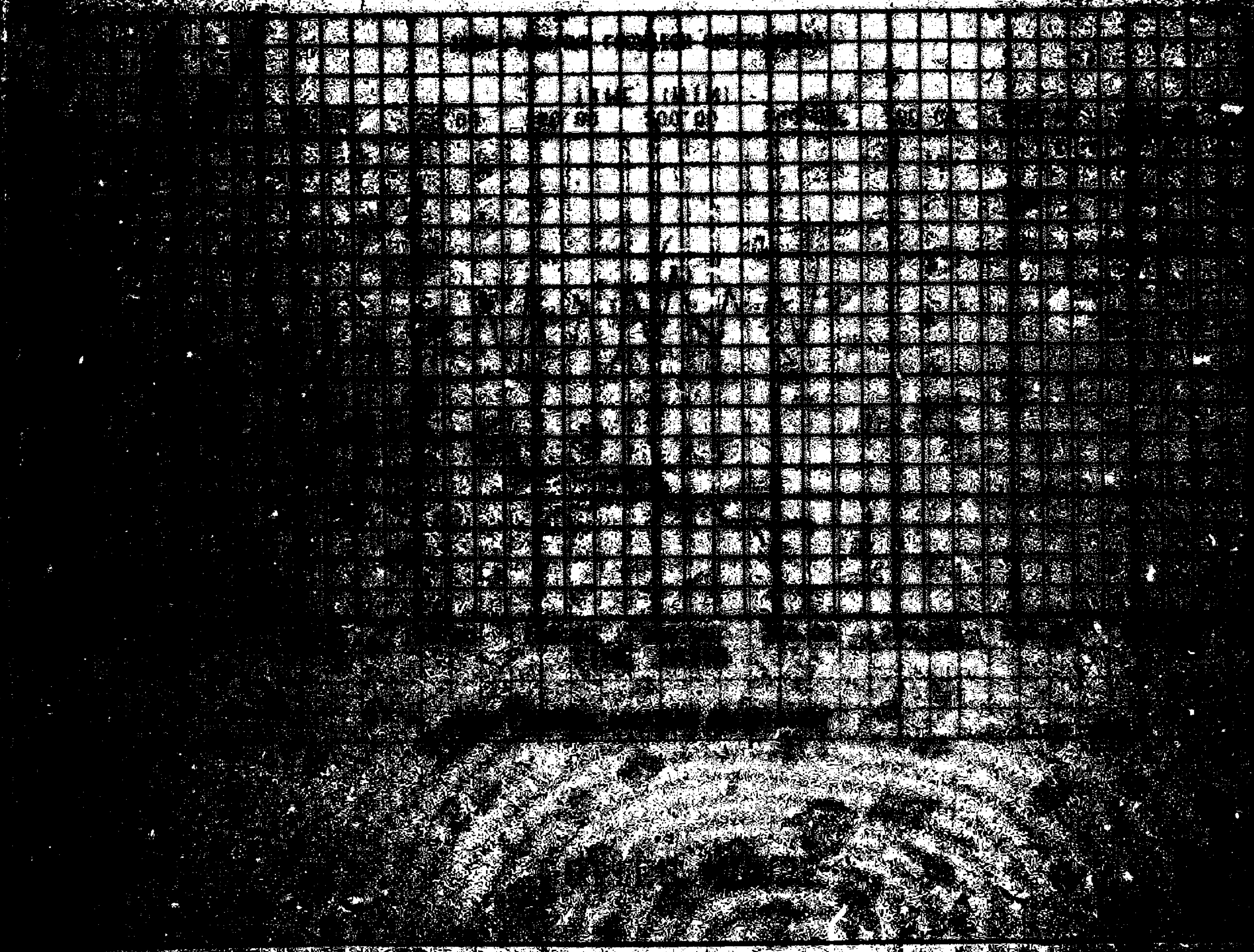

LØITER PHASE

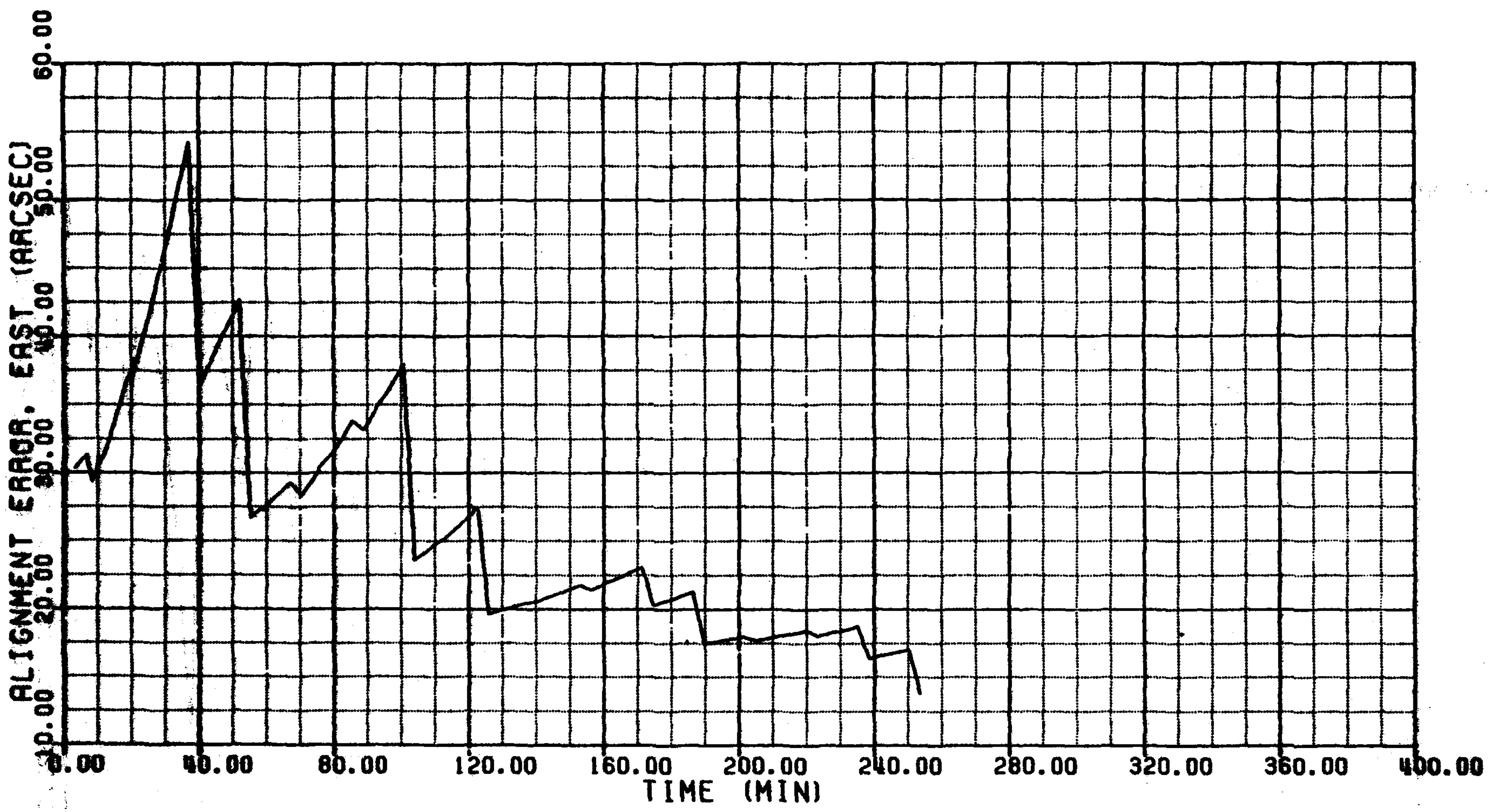

100M LANDMARK LOCATION UNCERTAINTY

LØITER PHASE

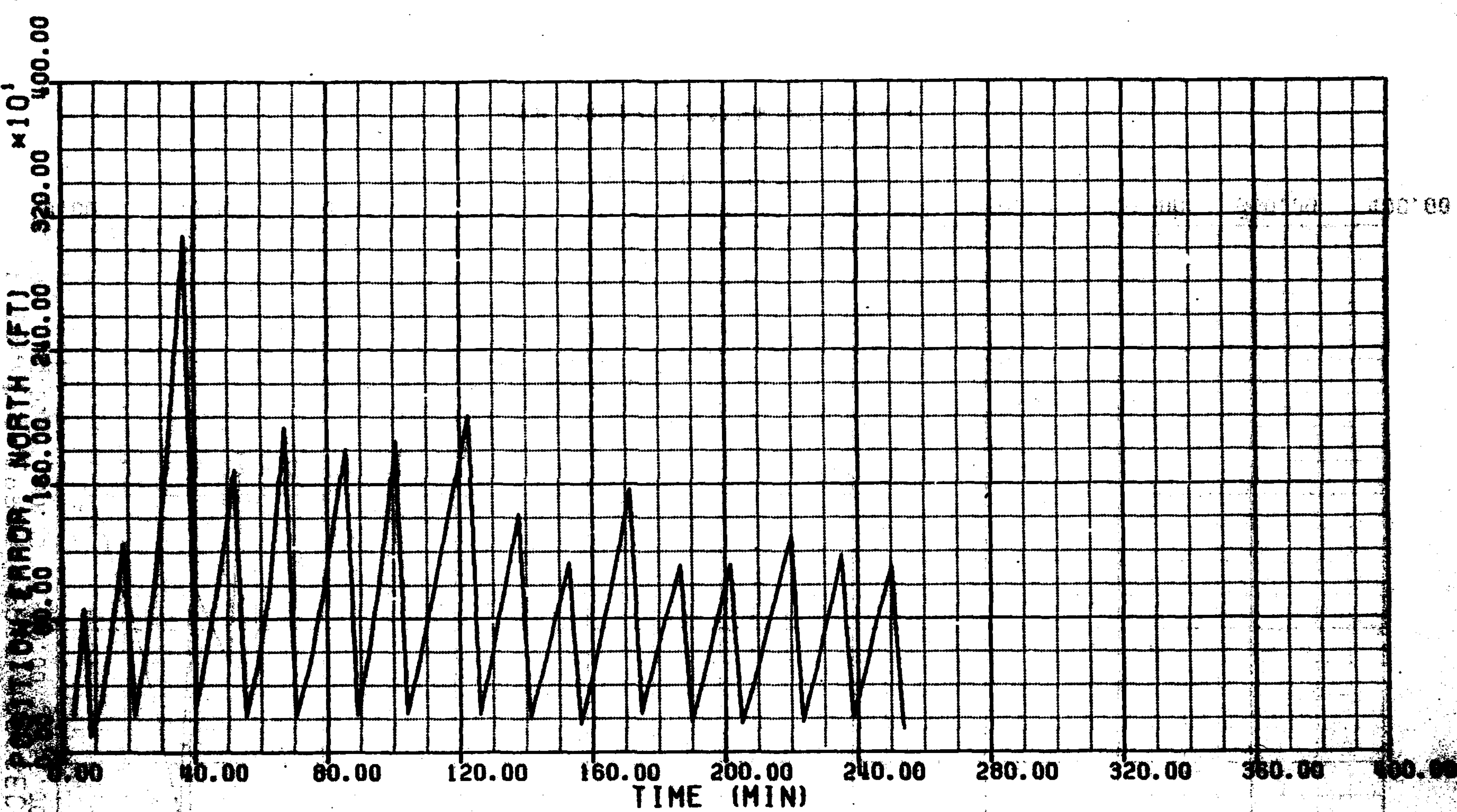

10M LANDMARK LOCATION UNCERTAINTY

LØITER PHASE

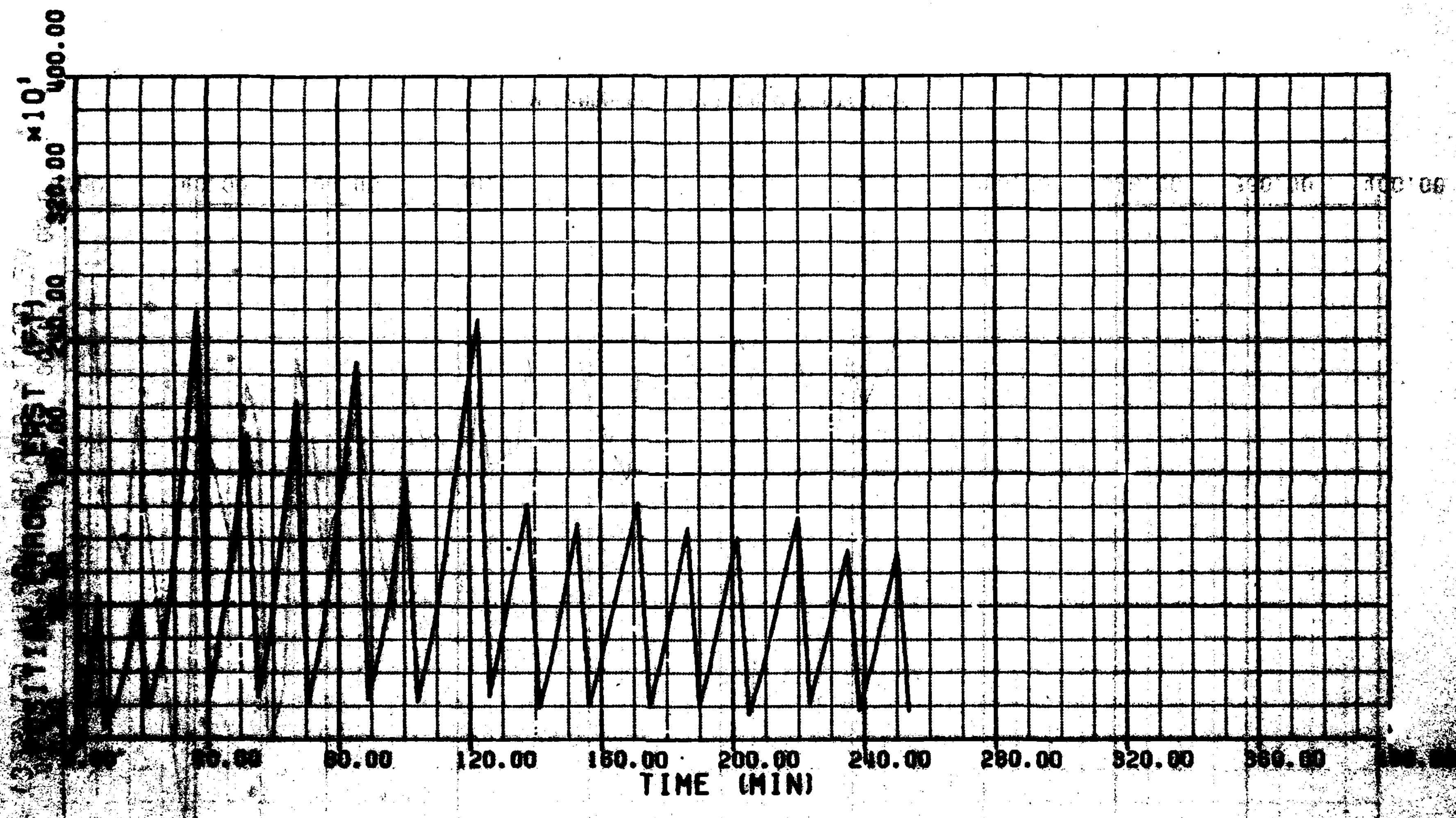

10M LANDMARK LOCATION UNCERTAINTY

LØITER PHASE

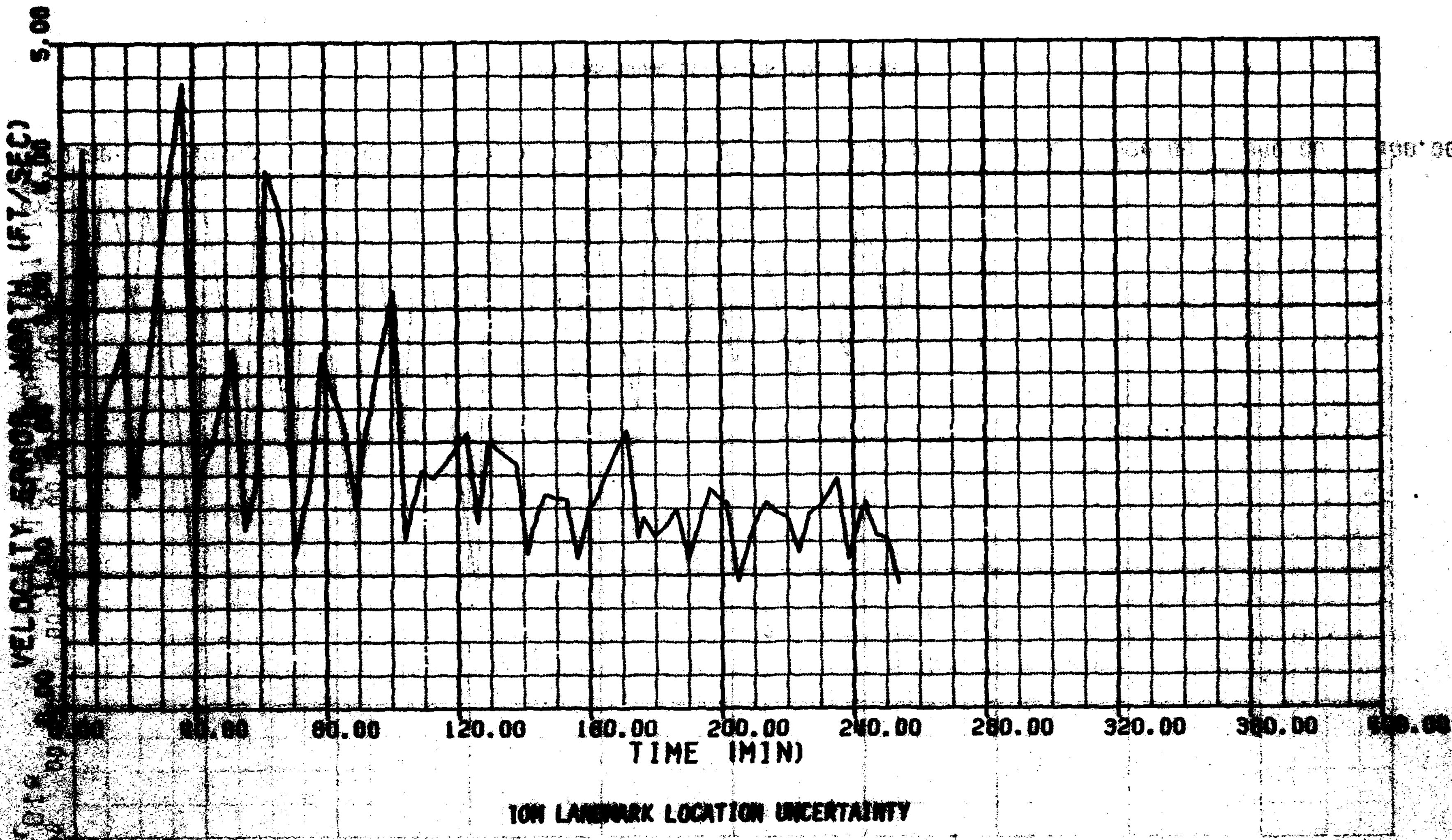

10M LANDMARK LOCATION UNCERTAINTY

LØITER PHASE

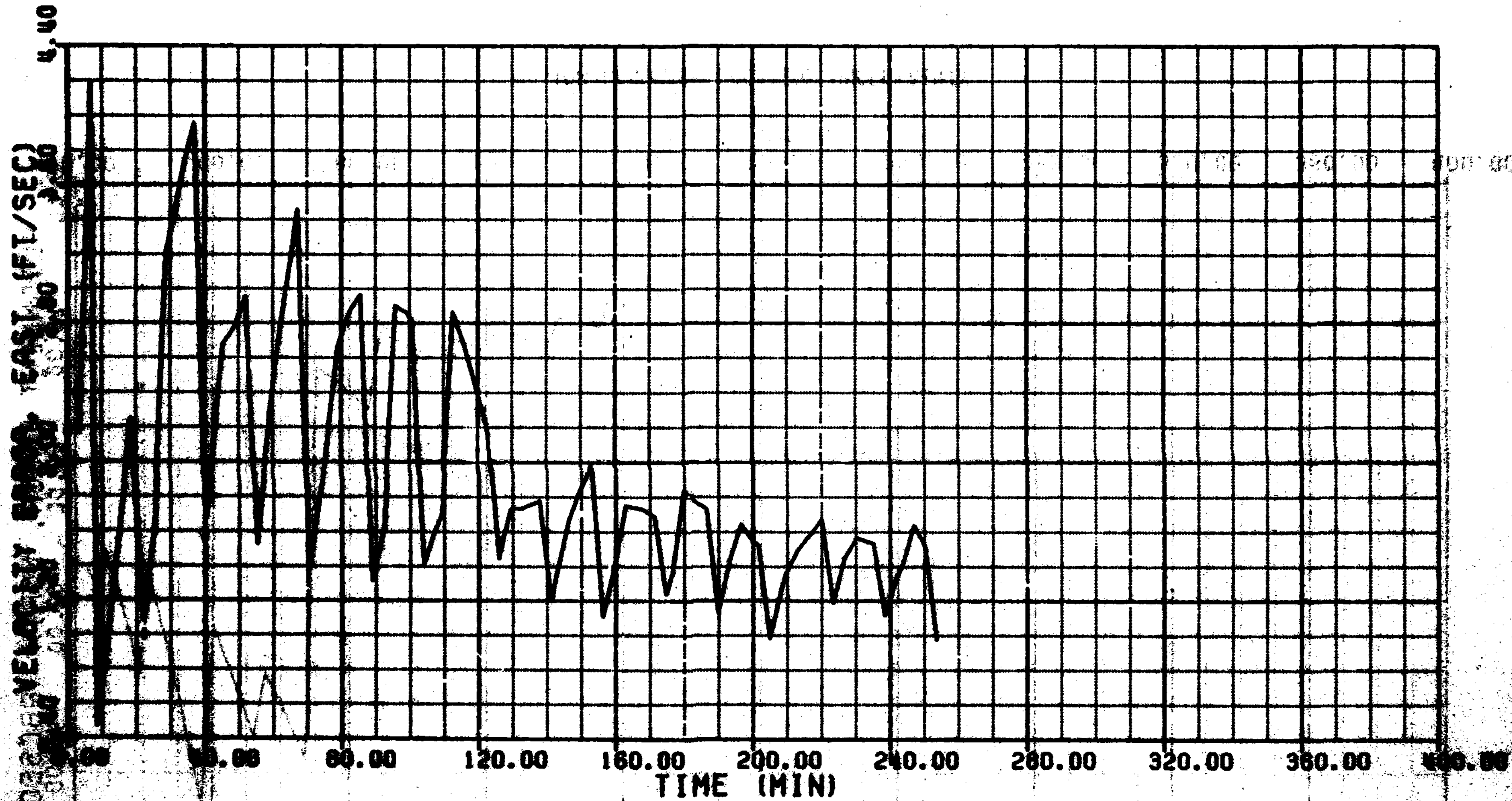

10M LANDMARK LOCATION UNCERTAINTY

LØITER PHASE

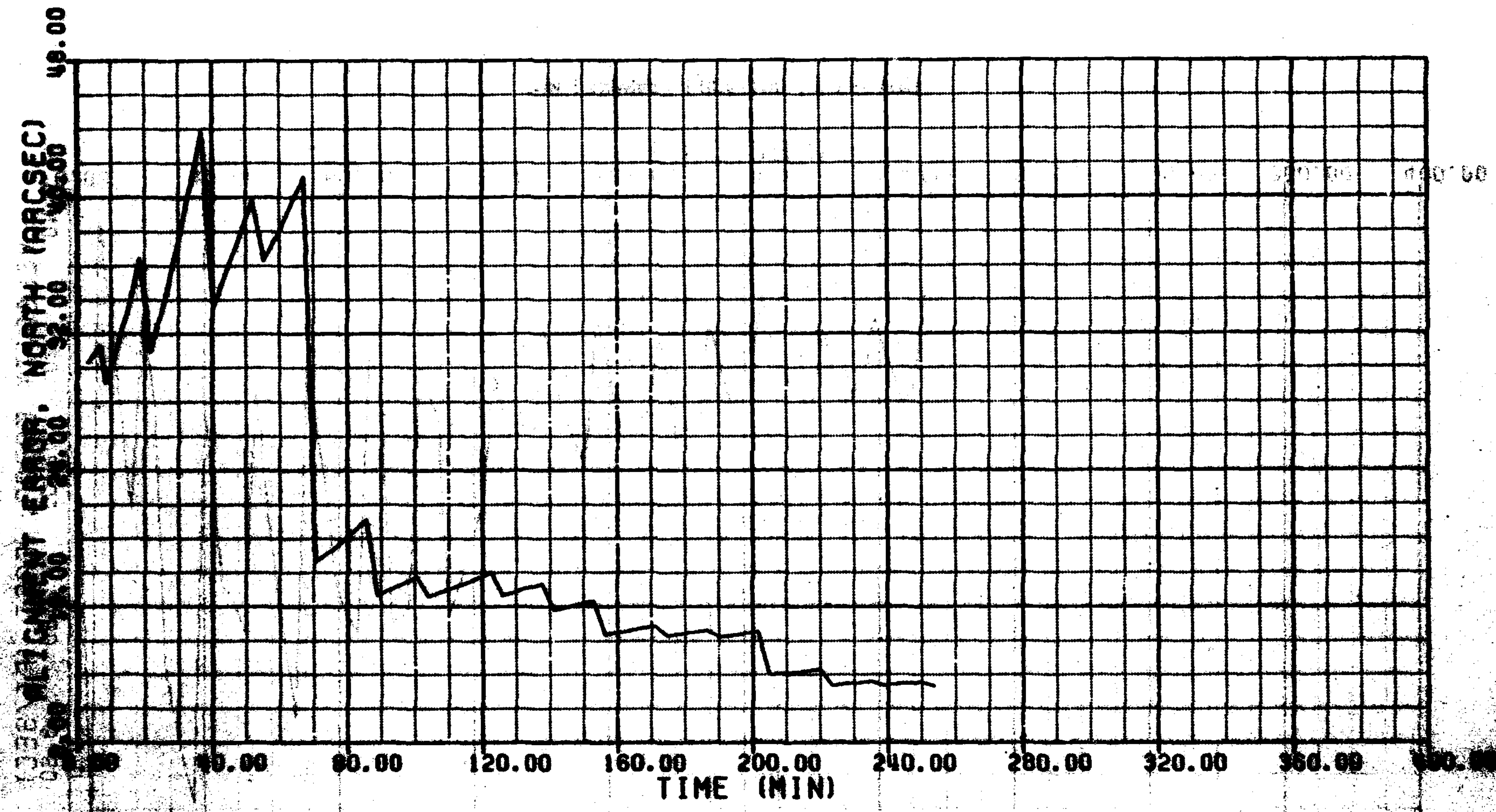

10M LANDMARK LOCATION UNCERTAINTY

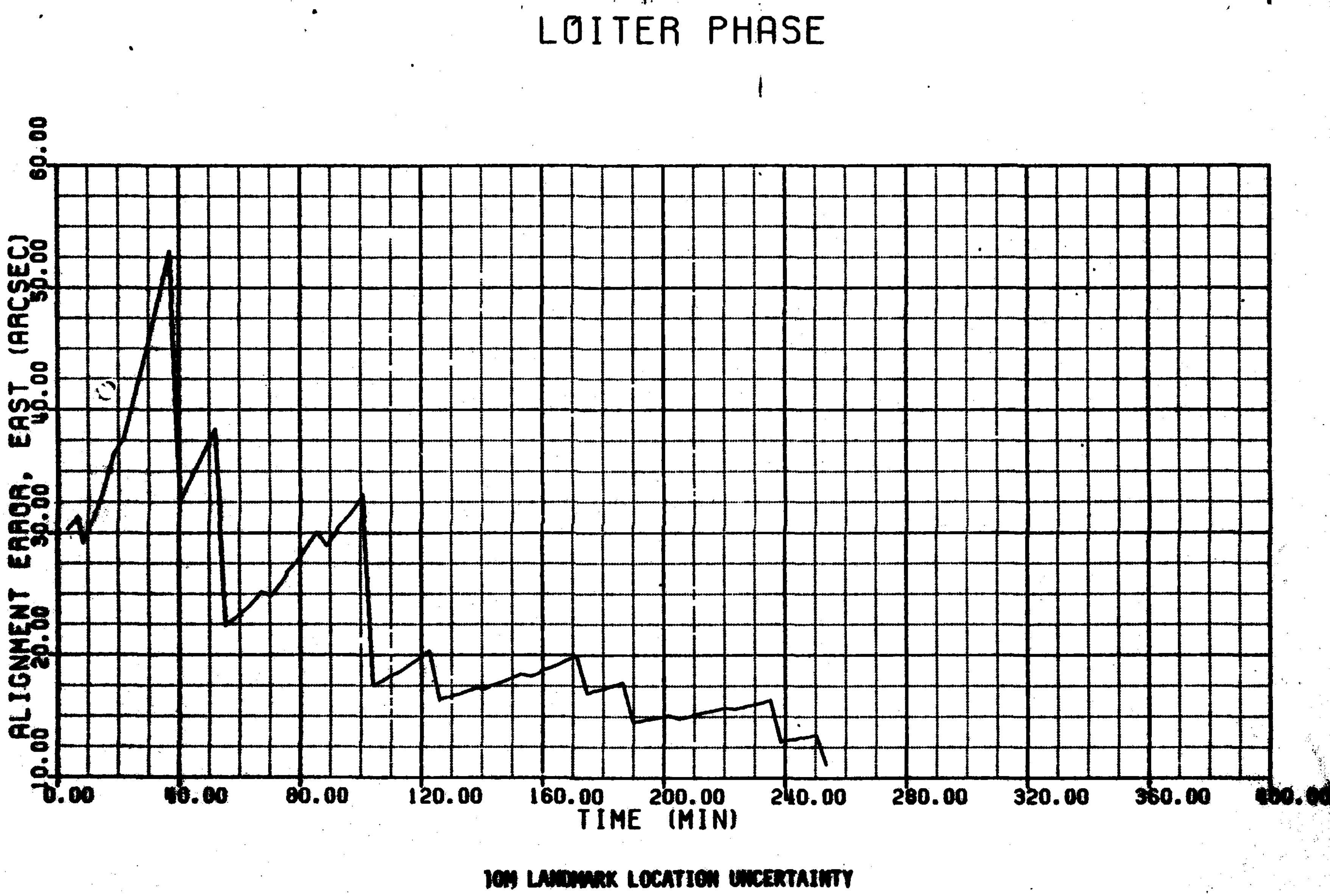
LØITER PHASE
ALIGNMENT ERROR, EAST (ARCSEC)
10.00
20.00
30.00
40.00
50.00
60.00
0.00
40.00
80.00
120.00
160.00
200.00
240.00
280.00
320.00
360.00
400.00
TIME (MIN)
10M LANDMARK LOCATION UNCERTAINTY

LME

8